RECENT MEASUREMENTS ON THE DUOPLASMATRON SOURCE

L. W. Oleksiuk*
Brookhaven National Laboratory

At Brookhaven interest has been expressed in determining the phase space densities for the conventional duoplasmatron ion source beam as well as studying the effects of extracting the duoplasmatron ion beam from an expanded plasma.

It was hoped that measurements of the beam brightness in the ion source extraction region would indicate the maximum attainable beam that could be injected into the linac and that by varying the plasma surface from which the beam is extracted some insight could be gained into the factors controlling ion source brightness.

Figure 1 shows a typical brightness profile for the BNL conventional (Mark I) duoplasmatron beam after acceleration to 750 kV. The measurements were performed by A. Van Steenbergen using a 4-slit method. It can be seen that the filling of four-dimensional transverse phase space is poor, and much of the linac acceptance is populated only by the tail of the brightness profile. The brightness "B_{MI}" could theoretically put in about 1000 mA in the present linac acceptance if all the transverse phase space were filled at this brightness.

Emittance measurements were performed on the conventional (Mark I) duoplasmatron as shown schematically in Fig. 2. Measurements were also performed using photocopying paper. The slit width of 0.010 inches produced beam images on the fluorescent screen, and these were photographed and measured to yield emittance values for the beam. Current measurements were performed by collecting current from the slit plate and from the current transformer. Corrections were made for secondary electron emission, these corrections yielding an uncertainty of $\pm$ 20% in the current measurements. Slit images for a 25 kV 200 mA (40 microsecond pulse width) beam are shown in Fig. 3, and the resulting phase space plot is shown in Fig. 4.

Preliminary measurements (see Fig. 5) for a range of extracted currents from the Mark I duoplasmatron from 30 mA to 400 mA indicate that the brightness of the Mark I, as measured by our techniques is

---

*Now at the University of Toronto, Toronto, Ontario, Canada.

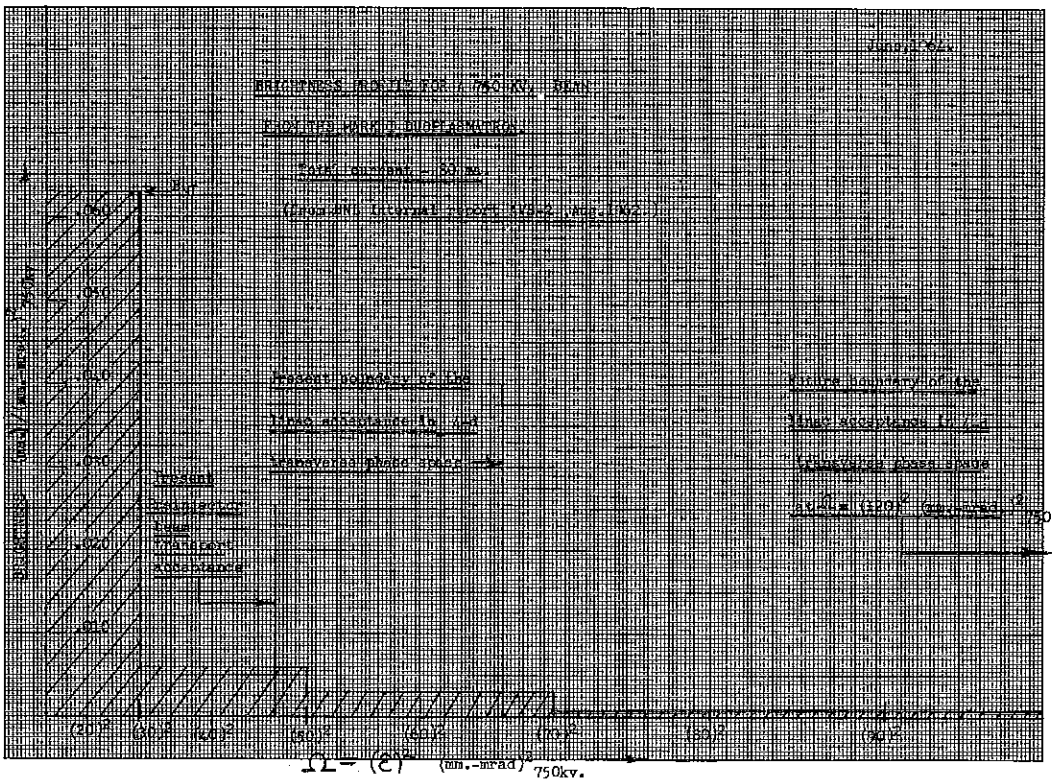

Fig. 1

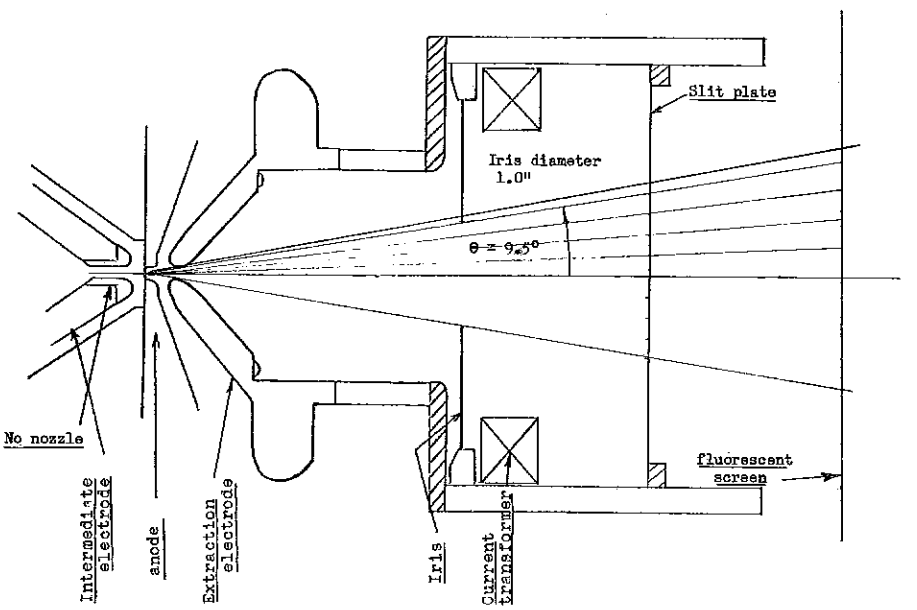

Fig. 2 Mark I duoplasmatron beam study geometry.

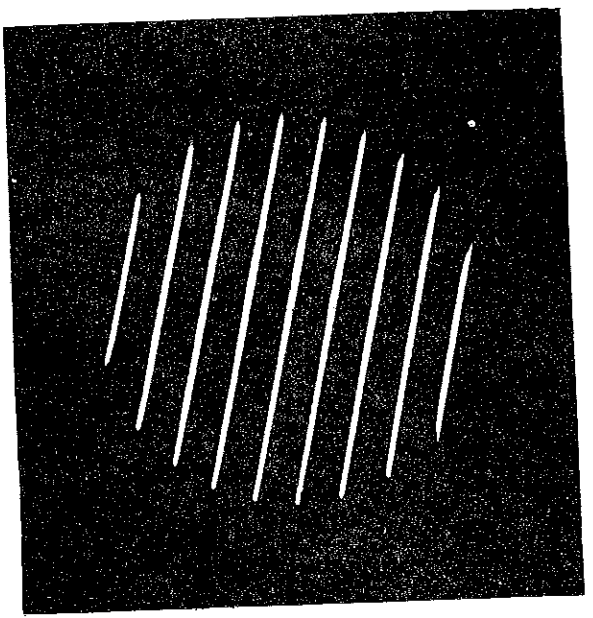

Fig. 3 Mark I duoplasmatrom beam: slit images for a 200 mA. beam.

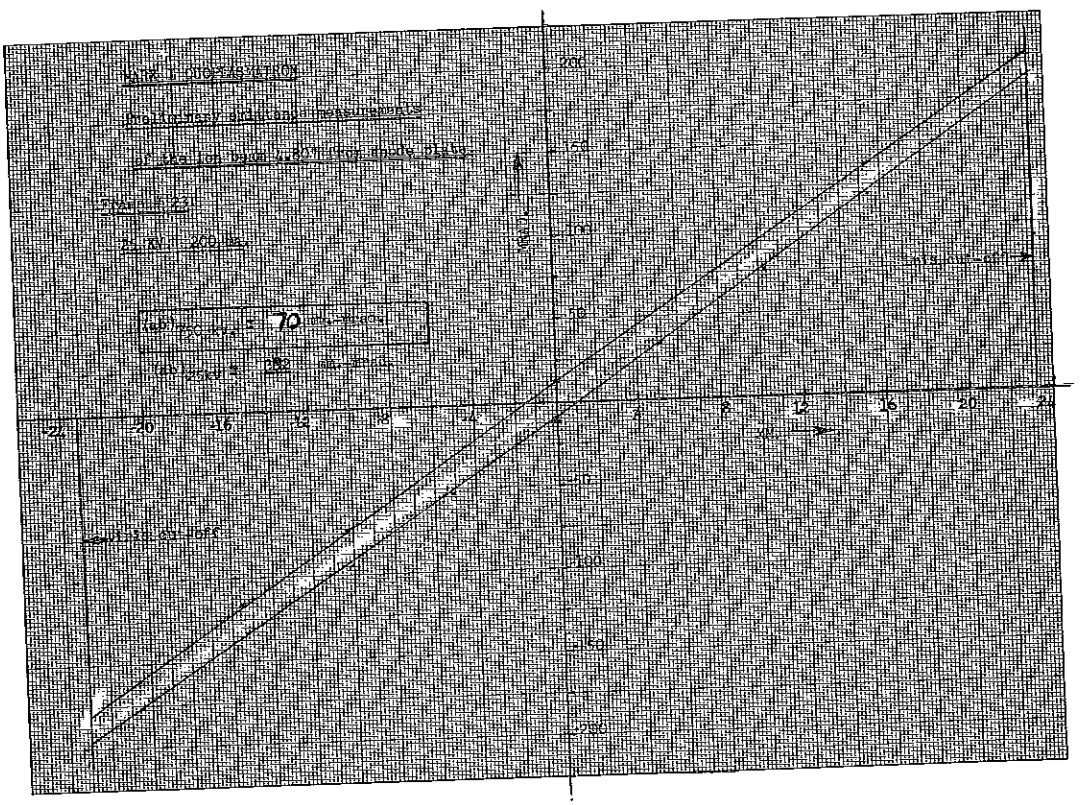

Fig. 4

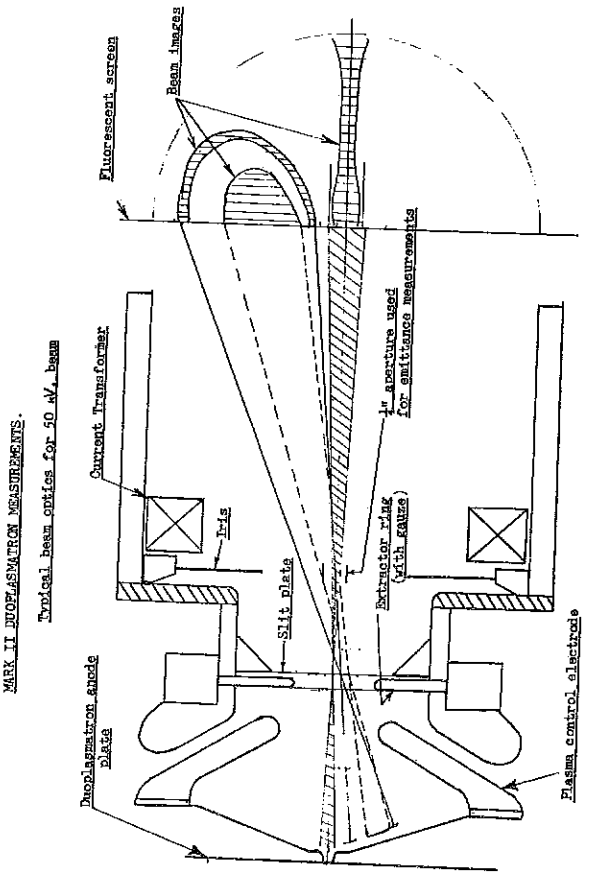

Fig. 6 Mark II duoplasmatron beam extraction geometry using the plasma expansion cup.

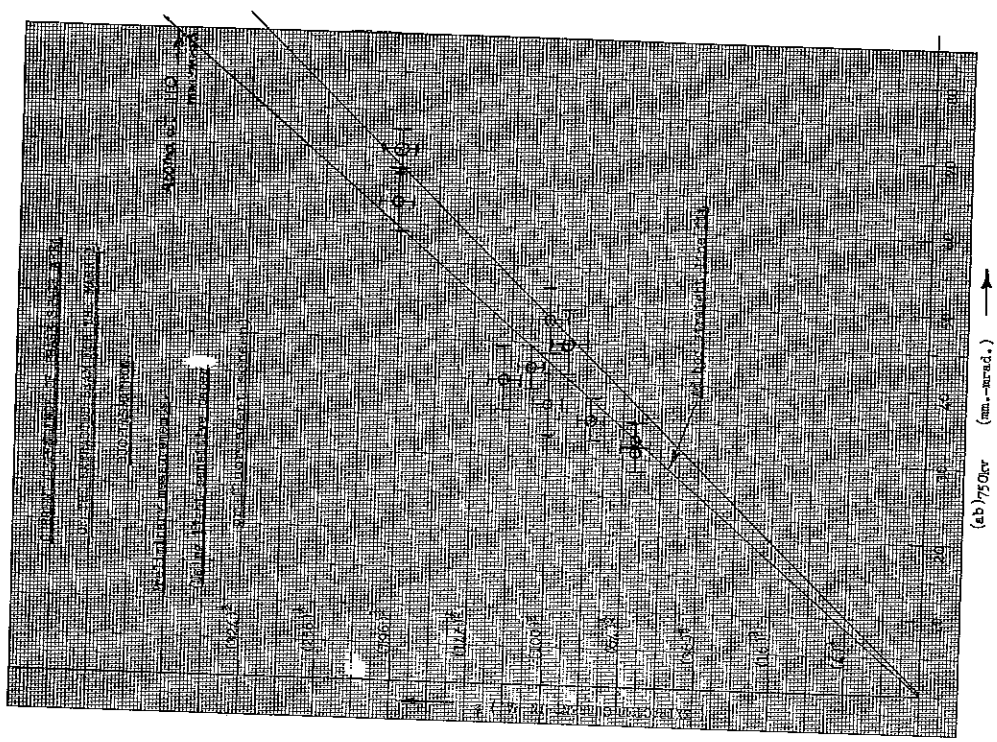

Fig. 5

between 0.04 and 0.06 mA/(mm-mrad)^2 750 kV which corresponds approximately to the region B_{MI} in Fig. 1. Since the uncertainties in defining the cut-off point on the brightness profile are large for this kind of measurement, it can be assumed that the measurements described here represent only the highly dense portion of the brightness profile.

The duoplasmatron extraction region was modified to incorporate an area for the expansion of the arc plasma through the anode aperture. This modification has been shown to be potentially capable of giving larger extracted beams of high brightness from a hot cathode arc discharge. The first model of this method of beam extraction at Brookhaven was the Mark II duoplasmatron, consisting of a Mark I ion source with a modified extraction geometry shown in Fig. 6. The beam optics for a 50 kV beam are also shown, indicating the existence of a beam cross-over just upstream from the iris position. The plasma control electrode was biased approximately 20 - 30 volts positive from the anode plate to prevent the plasma from expanding too close to this electrode. This bias had a significant effect on the intensity of extracted beam and in some modes of operation it could increase the extracted beam intensity by a factor of 3 over the beam intensity without bias. The extraction electrode had a fine tungsten wire gauze across its aperture to increase the focusing at the extractor electrode.

A set of emittance measurements were performed for the Mark II extractor geometry using slits placed near the extractor ring and 1.25 inches from the end of the Faraday cup. By narrowing the intermediate electrode channel to 0.10 inches diameter it was found possible to expand the anode aperture to 0.060 inches and get large extracted beams of the order 600-700 mA.

A typical emittance measurement is shown in Fig. 7 for a 60 kV - 710 mA beam extracted from the Mark II setup. Evidence for the existence of two phase space areas is shown in which the smaller area has probably the higher current density. The ion source was pulsing for a 40 microsecond pulse width and a 55 A discharge current for this measurement.

A summary of recent emittance measurements for the duoplasmatron type of ion source is given in Fig. 8. It can be seen that in general higher extracted currents with better brightness qualities can be obtained with the plasma expansion mode of extraction. It is expected that future trends for high accelerator beam intensities will be satisfied by means of careful attention to the ion extraction mechanism in ion source plasmas.

VAN STEENBERGEN: More in terms of a remark, it seems possible to change the magnitude of the plasma cup and get the same plasma density for a lower discharge current.

OLEKSIUK: That is right. I think the density is really dependent on discharge current. I believe that discharge current tells you how many neutrals you have relative to ionized particles in the plasma and this is perhaps where the strong dependence arises. If you are trying to control an ion density, I believe that this is the place to do it. The control of the plasma area I think will be perhaps a control on the aperture of the anode. We did get larger extracted currents, of course, using larger apertures, but the increase in brightness appears to come from the discharge current.

VAN STEENBERGEN: I remember Solnyshkov's results whereby he used 150 A discharge current for typically a 10-cm diameter plasma cup. He got equivalent results at least in emittance when he used, say 50 A with a 3-cm cup. It was as though the plasma density in both those cases was similar but he did not expand the plasma as far in the latter case.

OLEKSIUK: Yes, that sounds reasonable. In fact this may be the other way of doing it, that is, keeping the plasma expansion down to a certain finite degree.

VAN STEENBERGEN: Yes. This, of course, might limit the total current. You might not get 700 mA then.

OLEKSIUK: This would be for the same brightness figures. The brightness figures would not change radically--that is a possibility. We used only the one extraction geometry at this stage and, of course, there is a lot more work to be done that way.

MORGAN: On the 700 mA emittance work at 50 kV, I believe you say you used only 600 to 900 V bias on the target. Did you actually check this current calorimetrically. With a beam like this, this field would probably be insufficient for containing the electrons.

OLEKSIUK: The two readings we had were the current transformer and the Faraday cup. No calorimetric readings were obtained. We see what is hitting the iris and what is being collected in the cup and what the current transformer reads. We are biased for secondaries and we have a small area that the back-streaming electrons see anyway to get out. So it seemed that we were fairly safe in the current measurements.

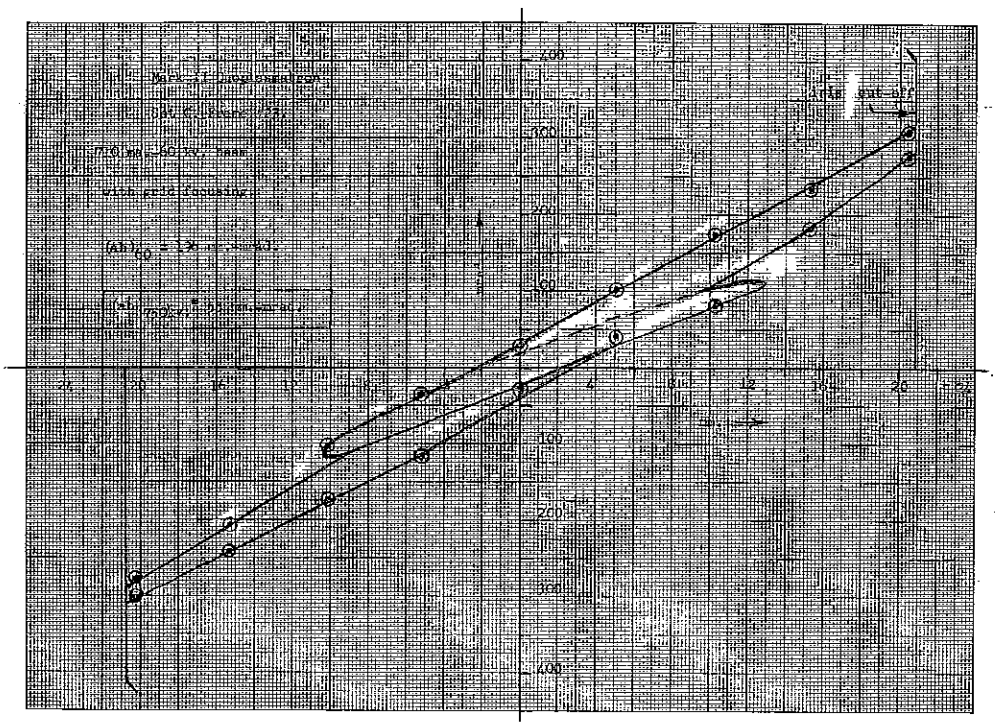

Fig. 7 Emittance of a 710 mA beam extracted from the Mark II configuration.

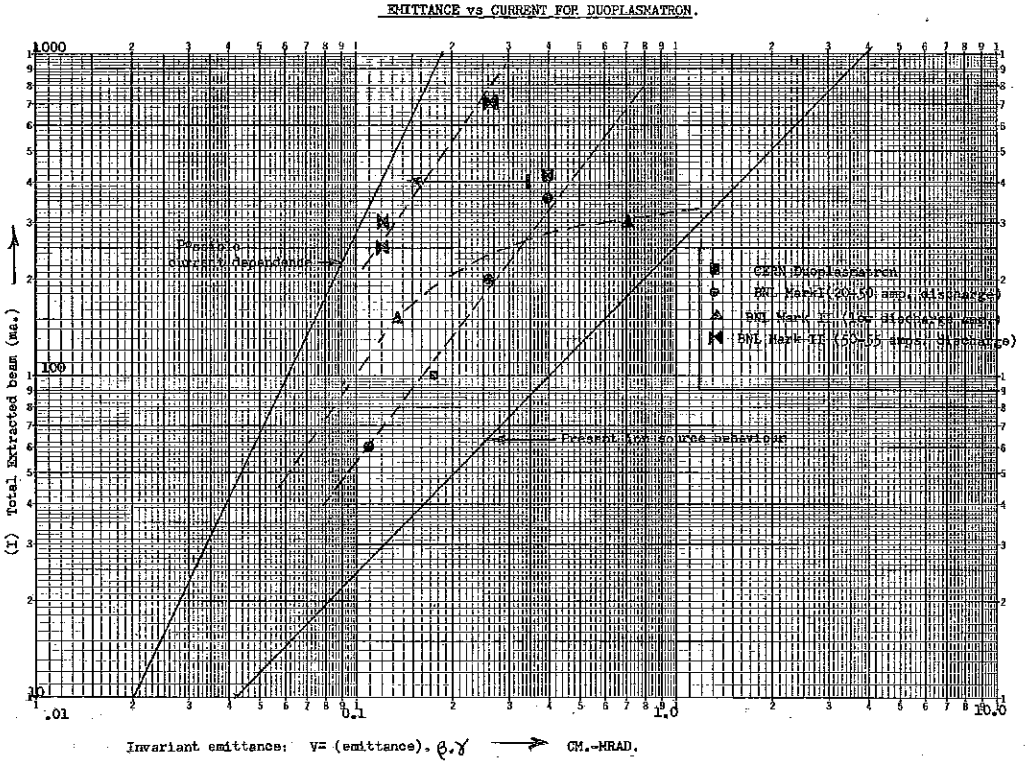

Fig. 8 Recent beam emittance values for the duoplasmatron type ion source.

MORGAN: Were the 700 mils through the iris or was that the total current, including the loss on the iris?

OLEKSIUK: The 700 mils were through the iris. There were possibly about 100 mils cutting in on the iris itself. So we measured the collected slit current and checked it with the transformer.

WROE: I just wanted to check on variation of emittance with arc current. Were you saying toward the end that the emittance you measure went down as the arc current went up?

OLEKSIUK: Yes.

WROE: This seems the wrong way around if you attribute the emittance to an ion temperature.

OLEKSIUK: Well, in fact, we do not know what the temperature does. One may be just changing ion density. Of course, I don't know how the plasma would see this. But, in fact, just looking qualitatively at the way this bright spot appears, I think we are introducing some sort of a new area in the plasma from the high discharge and this dense area is perhaps contributing to the large effects we are seeing in the brightness. Extraction from this new bright area may be giving us the high brightness numbers.

LAPOSTOLLE: You tested your source with and without grids. Could you say what you think is best?

OLEKSIUK: The grids tended to dilute the beam emittance a little bit. The emittance numbers were perhaps 20% higher for the same current extracted using the grids.

LAPOSTOLLE: Is it one or two grids?

OLEKSIUK: It is one grid. The grid changed the optics a bit as was expected. The other effect was that with the grid I could extract higher currents. That is, without grid I would be limited to perhaps 350 to 400 mA. Then by putting in the grid I could go up to 700 or 710 mA of beam under the same ion source conditions. So I think the grid is contributing secondaries which are neutralizing space charge, or something to this effect. It does have a good effect on the extraction.

VAN STEENBERGEN: It is interesting to note that at HVEC indications have been obtained that the various shapes in the emittance diagram

would be related to two kinds of beam shapes or beam profiles. The high intensity central core would come from a lower density plasma at the periphery of the plasma boundary and the rather wider beam of lower intensity, which constitutes the lower density filled distorted shape in the emittance diagram , would come from the central part. Thus there seem to be indications of an inhomogeneous density distribution at the plasma boundary. I don't know how this would tie in with the observation of a preponderance of heavy ions in the distorted shapes. Possibly beams from a lower density region with a lower plasma temperature might show a different proton percentage.

OLEKSIUK: I should really mention ion source oscillations; we get evidence of about a 10-12 Mc oscillation in the extracted beam and I believe this is due to ion sound-wave oscillations; one can estimate the frequency using the parameters in the discharge and get reasonable agreement with this range. I found it possible for the oscillation to disappear, due mainly to change in the aperture of the anode plate, that is, for large anode plate apertures the oscillation completely disappeared.

ION SOURCE AND COLUMN PERFORMANCE AT ORNL*

G. G. Kelley and O. B. Morgan
Oak Ridge National Laboratory

Most of the experimental work in controlled fusion in Oak Ridge is based on the trapping of high energy molecular ions in a magnetic "bottle" by dissociation of the ions in the bottle. For the past six years our group has been concerned with the development of injectors for these experiments. Large dc currents are needed and large current densities are desirable. Since we are not interested in short pulse performance and do not have to match emittance shape to an accelerator, our approach has been different from that of the people making preinjectors. We have not been measuring emittance but have concerned ourselves with passing a beam through the smallest possible channel in specific geometries. Our beams are pulsed on and off, but generally we are not concerned with the first 100 μsec after turn-on or turn-off. On the other hand, we have the problem of dissipation of very large amounts of power at high power densities.

Two power supplies and two test stands have been used for our studies. One test location is in a small laboratory. It has available up to 100 kV at 3 amp. Here we have made source studies and have done magnetic deflection beam analysis. The other test facility is in a large open area and is coupled to a 600 kV, 1 amp supply. At this site we have tested accelerator tubes and made studies of beam profile and of targets.

We have been using the duoplasmatron of von Ardenne. We started with what was practically a Chinese copy of a source described in his books, but we could not get sufficient heat transfer from the tungsten anode insert to the anode to permit operation at high dc arc currents. A current of about 5 amp was the most that could be maintained reliably for long periods. After we found that we could get good performance with nonmagnetic anodes, we changed to solid copper. A solid molybdenum should work somewhat better, but it is less convenient to use. One other change had to be made to permit operation at steady arc currents greater than 10 amp. The tip of the intermediate electrode needs to be cooled very well to prevent heating beyond the curie temperature. A water-cooled copper block is brazed to this electrode just beyond the tip. Figure 1 is

---

*Research sponsored by the U. S. Atomic Energy Commission under contract with the Union Carbide Corporation.

a cross-sectional view of one of our present sources. We are using filaments of a type designed by C. D. Moak of the Physics Division of ORNL. They are made from 40 mil tantalum wire covered with a platinum gauze and wrapped in a bi-filar spiral. Care is taken to see that no part of the finished filament is directly on the axis of the assembly. The filaments are then dipped in a barium strontium carbonate solution, the standard cathode dip used in tube manufacture. They require no activation procedure but should be outgassed in a separate system to prevent dirtying the source. Operating current is about 20 amp. These filaments have a life in the hundreds of hours when they are kept away from the high energy electrons which stream back through the anode aperture from the accelerating gap.

The methods we have used for determining the mass ratios in the plasma from the source will be described later. Our main interest has been in the production of molecular ions. When a source is run with a small spacing between intermediate electrode and anode--about 1/16 of an inch--and if the source is run gas starved, i.e., at sufficient arc voltage and at low enough source pressure that the desired output current is insensitive to variations in arc voltage, then the H_2^+ ion component is at least 60% up to 100 mA and at least 95 mA of H_2^+ has been obtained at correspondingly higher total currents. The proton yield can be increased by increasing the intermediate electrode to anode spacing to at least 1/4 inch, and by the use of high electron densities--by reduced anode aperture size and increased arc current for a given output. A relative proton yield of 90% has been obtained at moderate current, and proton yield seems to be even more favored at higher currents. Triatomic ions are produced by operating at high gas pressures and low arc voltage. A maximum of 37 mA of H_3^+ has been produced.

The plasma streaming through the anode aperture in the source consists of rather energetic electrons--up to 100 eV--and considerably lower energy ions. The ions have a directed energy of the order of about typically 8 V. When a strong electric field is created in the region beyond the aperture, the electrons are repelled and the ions accelerated. There results a plasma-beam boundary which forms at such a place that the space charge of the ion beam shields the plasma surface from the extracting field. Since the current density of ions in the anode aperture may be as high as 100 amp/sq cm (it is kept high to make the gas efficiency of the source high--typically greater than 90%) and since the maximum current density that can be supported with physically realizable extracting fields is under about 2 amp/sq cm, the plasma will expand into the region below the aperture. For a long time we thought that the arrangement using the highest possible field and correspondingly the smallest amount of expansion was most desirable. Recently we have

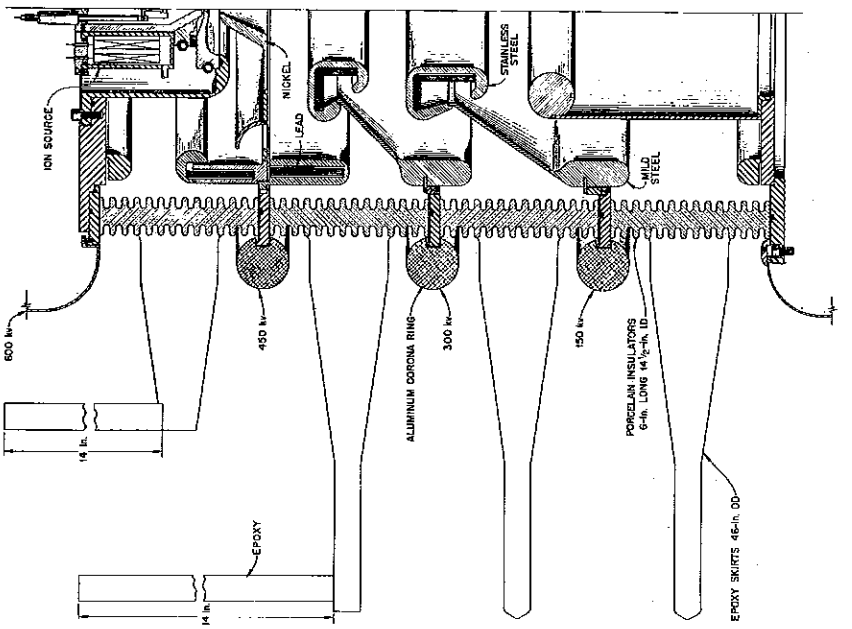

FIG. 2 600 KV ACCELERATOR TUBE

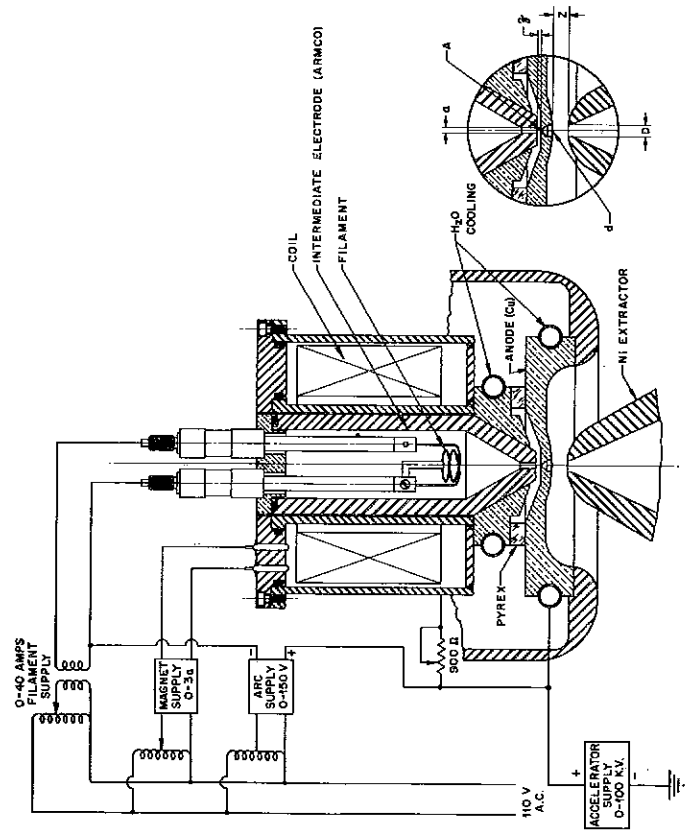

FIG. 1 MODIFIED DUOPLASMATRON ION SOURCE

been experimenting with large cup arrangements found to give better beam quality by the Leningrad group and others.* This arrangement has the further advantage of more reliable voltage breakdown characteristics.

The maximum current that can be obtained with a given maximum allowable divergence of the beam after extracting depends only on the extraction voltage. Since the current density for space-charge limited current is given, for an infinite plane beam, and for a parallel cylindrical beam using Pierce geometry, by the expression

$$j = \frac{5.44 \times 10^{-8} \phi^{3/2}}{M^{1/2} z^2}$$

where M is the mass number, j is in amp/sq cm, ϕ is in volts, and z is the electrode spacing in centimeters, the total current depends only on ϕ for a given ratio of spacing to beam diameter. We have found that this expression predicts the maximum current density even when the electrode shape is far from that which would be expected to produce a parallel beam according to the derivation of Pierce. (To get good agreement, however, it is necessary to make an empirical correction which consists of increasing the value of z by the radius of the aperture in the accelerating electrode.) For a spacing of twice the radius of the beam which seems to be a reasonable choice, the maximum current is given by $I = 19\ V^{3/2}$ where I is in mA and V is tens of kV for protons. The maximum current then which can be obtained in a beam of moderate divergence at 150 kV is slightly over 1 amp.

A current of 500 mA has been extracted from a source on the small test stand at 100 kV. A current of 400 mA was extracted from this source continuously for a period of four hours.

Our 600 kV supply has a 170 mA bleeder with taps at 150 kV, 300 kV, and 450 kV. We extract from the source plasma at 150 kV and accelerate the beam in three more 150 kV high-gradient, close-spaced steps. An ion from the source is accelerated to the full voltage in approximately 12 inches. Figure 2 is a cross-sectional view of the accelerator tube. There

---

*A. I. Solnyshkov et al., "Current Injector for a Strong Focused Linac," Proceedings of the Dubna Conference (1963). See M. D. Gabovich, Review Article, "Extraction of Ions from Plasma Ion Sources and Primary Formation of Ion Beams," Instruments and Experimental Techniques, No. 2, pp. 195-206 (March-April, 1963). See also N. B. Brooks et al., "Production of Low Divergence Positive Ion Beams of High Intensity," Rev. Sci. Instr. 35, 894 (July 1964).

are four alumina insulators six inches high by fourteen inches ID. These are fastened to stainless steel rings by the vinyl seal technique. The rings provide electrical connection and alignment. Viton O-rings are used between the metal pieces. Skirts of unfilled epoxy molded to the insulator sections provide a large external breakdown path. Some of these skirts have been in use for over two years with no trouble due to breakdown through the interface between epoxy and ceramic. The electrodes are designed to keep the metal surface area having a strong field at a minimum. We made tests which showed that voltage cleanup problems become much greater when the linear dimension of the surface at high field is large compared to the electrode spacing. A solenoid focusing magnet is provided just below the accelerator tube to converge the beam. It is capable of operation at 2.4×10^5 amp turns and has six-inch diameter throat.

The site of the development of this tube is shown in Fig. 3 and Fig. 4. The beam is passed into a long cylindrical tank where probe studies and visual observation can be made. By means of an extension on the bottom of this tank the beam can be allowed to travel about 17 feet before striking a target. A profile measurement at a number of points along the beam gave an extrapolated value of 2.9 inches for the diameter of the beam in the lens at a total beam current of 180 mA. This measurement was made quite some time ago. We believe now that with large source cups we can make the beam considerably smaller. Large beam currents can be mass analyzed by this test facility by making use of the different focal lengths of the magnetic lens for the different mass components. These can be focused successively through a small aperture and the power on a target beyond measured calorimetrically. There is an essentially complete self-neutralization of the space charge of the beam by electron trapping. The beam profile shows no space charge spreading down to the lowest operating pressure which can be obtained in the system--2×10^{-6} mm Hg. We found, however, that the beam cannot be passed through a crossover in the region below the lens without being seriously disrupted. When a beam component is focused in the observation tank, it appears to get brighter as it gets smaller down to a diameter of about 1 cm and then becomes less bright but continues to converge to a sharp point. Nothing is seen of the beam below this point. When the beam is allowed to fall on a target and the lens strength is increased, the spot size becomes smaller and smaller and more and more intense down to no more than a pin point. With a further increase in lens strength, the spot disappears. We intend to study this phenomenon in greater detail.

We have operated this accelerator at a total power supply drain of 330 mA. At the same time we were able to account calorimetrically for about 300 mA. We do not know what became of the other 30 mA. It did not flow to any of the electrodes in the tube. These currents were

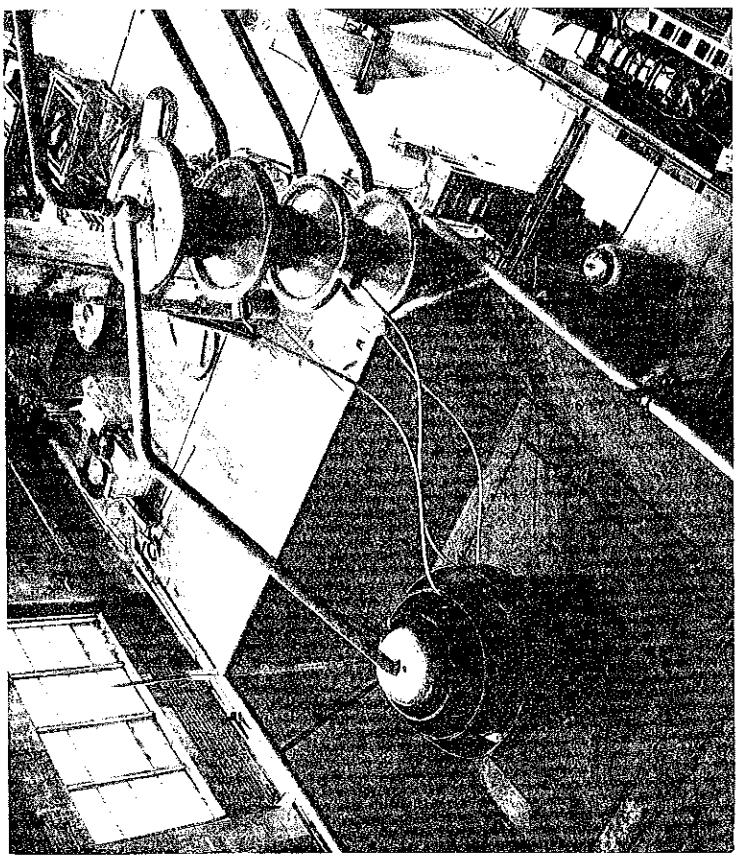

FIG. 4 TOP VIEW OF ACCELERATOR TEST STAND

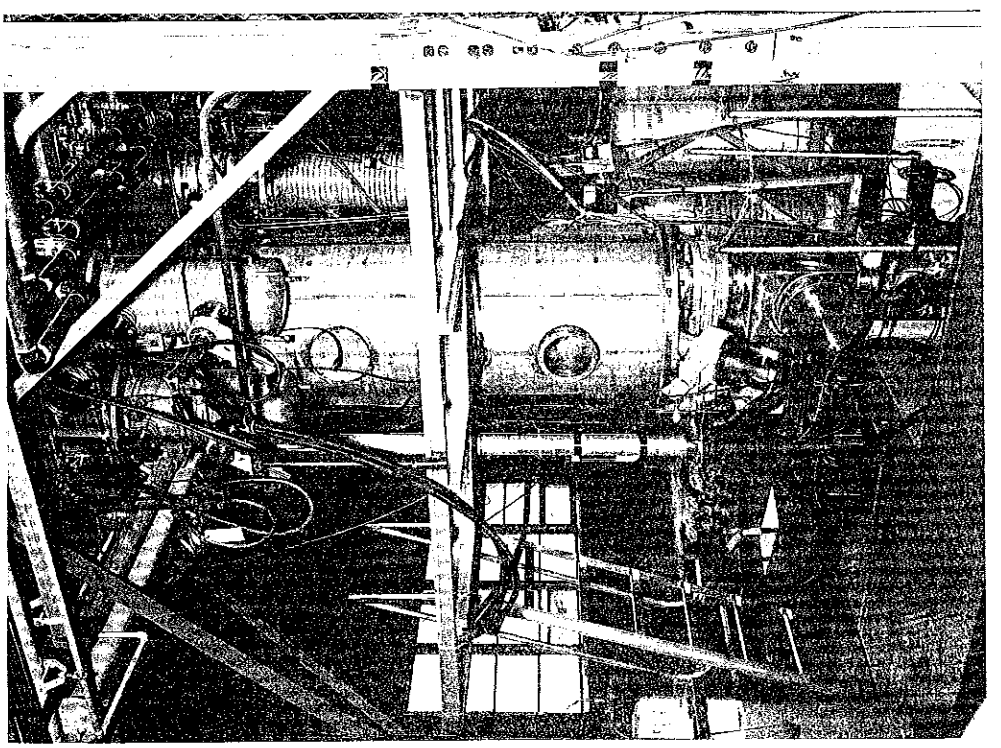

FIG. 3 VACUUM CHAMBER FOR ACCELERATOR TEST STAND

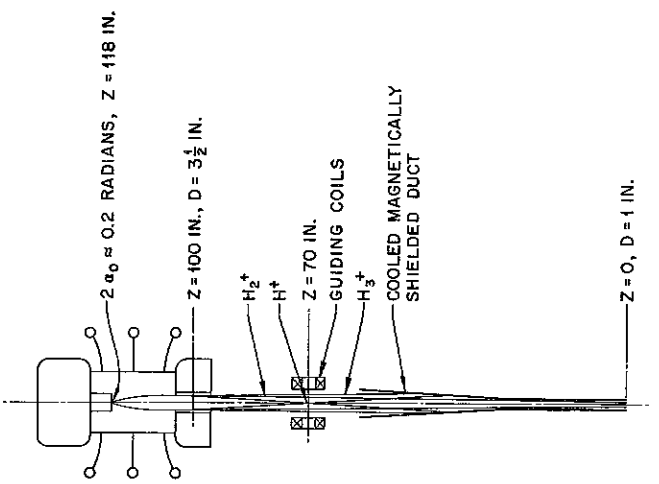

FIG. 6 DCX-2 INJECTION SYSTEM

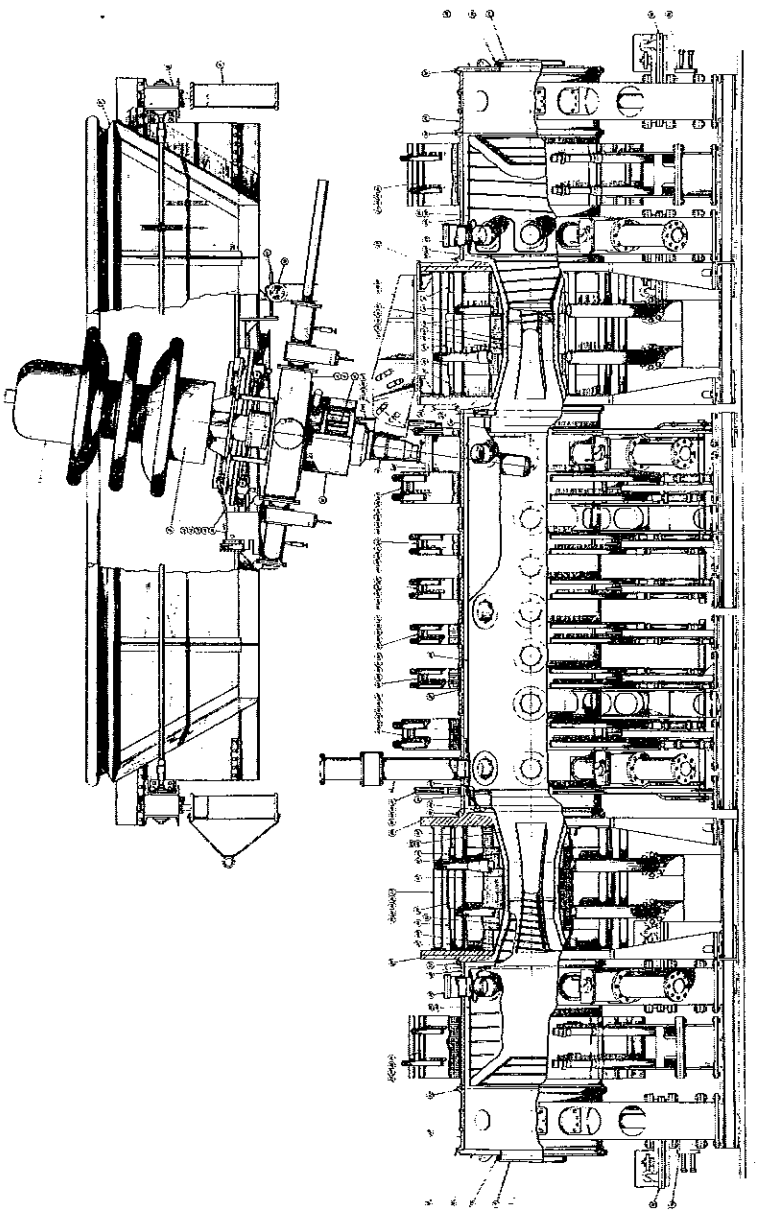

FIG. 5 CUTAWAY VIEW OF DCX-2

measured to be no larger than 1 mA. At the same time the power dissipated by the source anode was being monitored. An electron current of 0.5 mA at the full energy should have been detectable. No power difference was measured when the accelerating voltage was turned on or off.

The beam can be switched on and off by an electronic switching device in the source-arc supply. This switch is operated through a crater lamp-photomultiplier light beam link between ground and the 600 kV level. The beam can be turned on and off in less than 2 μsec.

The instantaneous beam current is transmitted from the 600 kV level to ground through a FM radio link. The system uses two commercial FM receivers having AFC, with slight modification. The arrangement has excellent linearity and low drift and has a time resolution of about 13 msec.

We have found, as have others, that an accel-decel arrangement can be used to permit neutralization of an ion beam. To be successful the arrangement must provide an electron-repelling field only in a small region around the beam. The exit electrode should be at ground potential and the beam beyond should not be able to "see" other potentials. We have neutralized a 50 mA, 70 kV beam after the beam had passed through an Einzel lens. A potential of - 3 kV, with aperture sizes of 1 to 1.5 inches, was enough to prevent electron loss from the beam.

Figure 5 shows a cutaway view of DCX-2, the largest of the experimental devices at Oak Ridge. In this device 600 keV H_2^+ ions are injected through a magnetically shielded channel into a uniform 12 kilogauss field. This field increases to 39 kilogauss at points 81 inches either side of the midplane. Ions enter the field 9 inches from the longitudinal axis at such an angle that they have a helical trajectory passing from a point near one magnetic mirror to slightly beyond a corresponding point near the other mirror. The orbit diameter is 10.3 inches. These ions reflect and return to the injector after having traveled a distance of the order of 100 meters. During their flight some of them are dissociated either by background gas and plasma or by a vacuum arc run between electrodes at opposite ends of the machine. The protons resulting circulate between reflection points and precess at each reflection, but some of them are deposited in the field in such a way that they do not return to the injector in spite of this precession. The mechanical and magnetic design of the injection channel is quite difficult. It consists of a hyperco cylinder with overlaid windings which compensate externally for the effect of the cylinder and also cancel the longitudinal component of magnetic field along the cylinder. The problems of design of the in-

jection duct make a small channel very desirable. The value chosen was 1-5/8 inches. Figure 6 is a schematic view of the beam path. Steering magnetic fields are provided in the pumping chamber just below the lens to compensate for small misalignments and for the effect of the stray magnetic field. This field is reduced along the beam path by the use of ferromagnetic materials in the electrodes and in other hardware wherever possible. It probably is the effect of the small residual field which has prevented injection of more than 50 mA of H_2^+ into DCX-2 in spite of the fact that, as has been said above, 95 mA have been passed through an identical structure in the test stand. The losses probably will be reduced by repair of the 600 kV supply which has been producing an abnormally large voltage ripple.

WROE: Could you just say quickly what type of resistors you used for grading the column?

KELLEY: I don't know the brand. They are just very many wire-wound resistors in an oil-filled column.

FEATHERSTONE: I was interested in your 1 A continuous 600 kV supply. Is it possible to keep the stored energy in the capacities fairly low, or do you worry about damage to electrodes in the column when a spark occurs?

KELLEY: Well, we worried about it until we found in practice that it did not cause us trouble. We have a 0.0125 μf condenser and then a 14,000 Ω series resistor between the condenser and the output, which consists of the isolation transformer capacity which I think mounts up to about 700 $\mu\mu$f.

THE PLA POLARIZED PROTON SOURCE

J. M. Dickson
Rutherford High Energy Laboratory

History

The design work on the polarized source was started in 1957. It was developed into a functioning source by 1959 and was first operated on the PLA in February 1961. The time during which a polarized beam has been available for nuclear physics experiments now totals 4670 hours, comprising 500 hours in 1961, 1500 in 1962, 1725 in 1963 and 945 in the first six months of 1964. The operational reliability of the source has been such that the percentage fault time of the P. L. A. has been only marginally lower with a polarized beam compared with thatof the normal unpolarized beam.

Development

Engineering development of the source has been a continuing process during its life and has been aimed at eliminating weaknesses in the original design, notably, lack of sufficient cooling, unreliability of control mechanisms between ground and the 500 kV platform, and alignment difficulties. The original ionizer was inefficient, gave an annoying inequality of "spin-up" and "spin-down" polarizations and intensities, and produced a beam which was not parallel to the axis of the injector. Two successive redesigns of the ionizer eliminated the polarization inequality and provided electrical steering of the beam. The ionizer now used is shown in Fig. 1. It has an ionization efficiency of about 10^{-3}, as used, but by modifying the extraction electrode and the ion mirror a factor 5 improvement might be achieved. The ionizer is followed by two pairs of deflector electrodes similar to the X, Y plates of an oscilloscope.

Surrounding the ionizer there are three pairs of coils arranged in the general form of Helmholtz coils. These are used to produce a low field (3 to 10 0e) in the ionization region to orient the polarized atomic beam in the desired direction. This system is very convenient to use and very flexible, in that any desired direction of proton polarization can be produced and the direction can be precisely reversed by reversing the current in one or two of these pairs of coils. For horizontal transverse polarization the Helmholtz coils need not be used since the sextupole magnet of the atomic beam system was designed to give a stray dipole field at the ionizer and the sextupole polarity can be reversed.

The atomic beam intensity has been increased by a factor of 1.5 by a new collimator in the dissociator. This collimator consists of a large number ($\sim$1000) fine bore pyrex tubes of uniform cross section (length $\sim$1 mm, bore $\sim$0.1 mm). It is similar in concept to the original collimator but the individual tubes are more uniform in size and the assembly technique produced much better alignment of the tubes.

Polarization and Intensity

The accelerated beam of protons, measured at the output end of tank 3, has normally a polarization of 0.40 and a mean intensity of 2×10^8 protons/sec (at 1% duty cycle). The polarization and intensity cannot be measured at any other point along the accelerator. This leads to some slight difficulty during operation of the accelerator and in locating some faults. The total beam current from the injector is about 20 times the proton current and the polarization cannot be measured at low energy. However, the rf and other parameters of the PLA are now well enough monitored to overcome nearly all these difficulties.

There is now rather good instrumentation for measuring the polarization and intensity of the output beam (the mean energy can also be measured to good accuracy). The polarization is measured by degrading the beam energy to 15 MeV (mean) and scattering the protons at 45° by a 2 MeV thick carbon target into four scintillation counters placed up, down, left and right of the proton beam. The degrader and target are mounted on a wheel rotating at 2.5 revs./sec. Variation of the number of degrader-target pairs from 2 up to 10 allows sampling of from one proton pulse in ten up to alternate pulses. In general two 50 MeV and two 30 MeV degrader-target pairs have been mounted, so that on changing machine energy from 50 MeV to 30 MeV the only change required is an adjustment to the gating circuits to ensure that counts from the appropriate target are registered. A signal from the rotating wheel is used to trigger the accelerator timing system and ensures synchronization of the target wheel and the proton pulses. Elastically scattered protons from the carbon target are selected by discriminators in the counting system. More details of this apparatus are given in the 1962 and 1963 PLA Progress Reports.

This system enables one to measure the transverse (vertical and horizontal) components of the beam polarization continuously. During a typical experiment, running for several hundred hours, the measured beam polarization varied by only $\pm$ 0.01 (standard deviation) per counting cycle, each of which had a statistical counting error of $\pm$ 0.002. At the same time the horizontal component of the polarization varied between - 0.008 and + 0.003 $\pm$ 0.002 and averaged - 0.002.

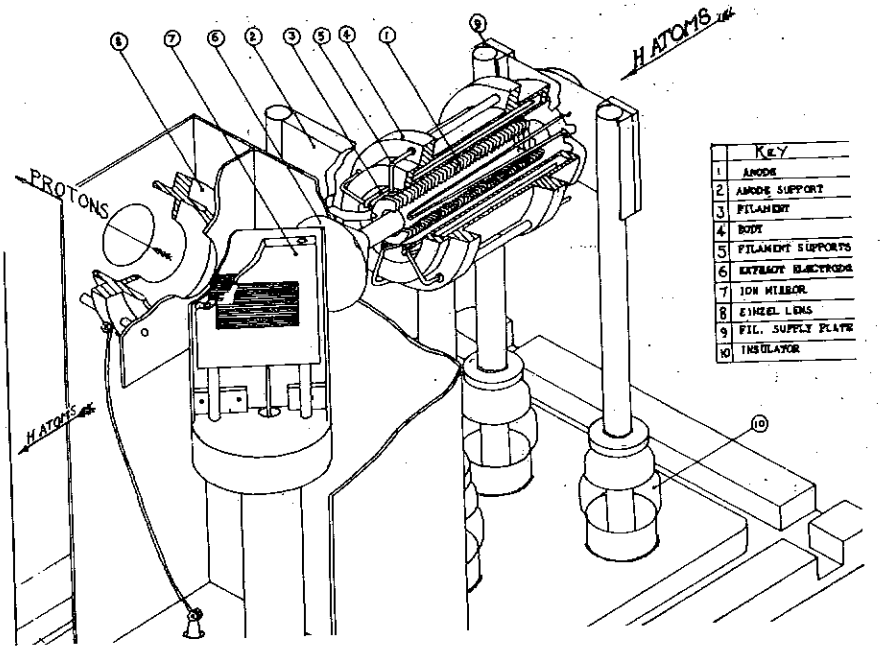

Fig. 1. Ionizer

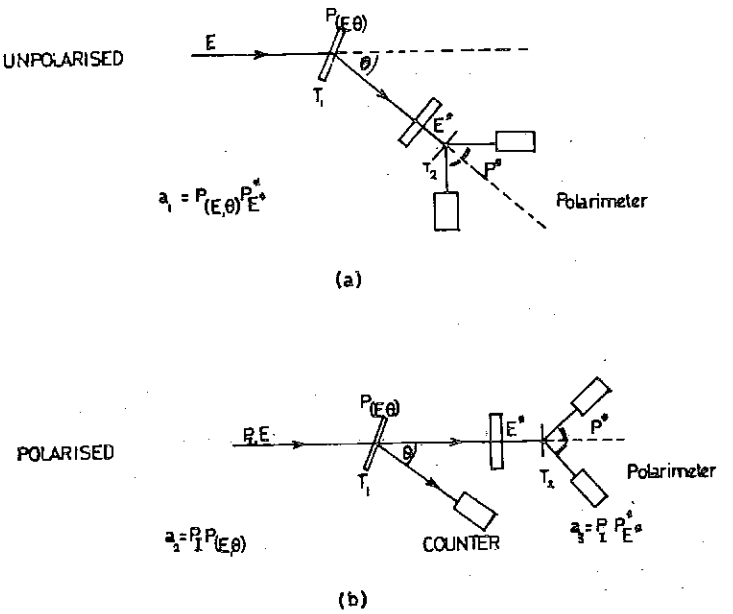

Fig. 2. Scattering Geometry for the Measurement of the Carbon Polarimeter Analysing Power.

The beam intensity is measured in an ion chamber filled with 1 atmosphere argon + 10% methane mixture. Mean proton currents down to 10^4 protons/sec can be measured using a dc amplifier and peak pulse currents of 10^7 protons/sec can be detected in a pulse amplifier.

Absolute Calibration of Polarization

The polarimeter described above could be calibrated from data available in the literature for (p-C) polarization at about 15 MeV but it was thought desirable that an absolute calibration measurement should be performed. The apparatus for this calibration is shown schematically in Fig. 2. From the three asymmetries measured with a polarized and an unpolarized beam the polarization of the beam is found from the relation

$$P^2 = a_2 a_3 / a_1 .$$

From the asymmetry a' measured by the continuous polarimeter its analyzing power $P' = a'/P$ can be found, $P' = 0.562 \pm 0.006$ at 50 MeV. The analyzing power, however, is a function of the mean proton energy incident on the polarimeter target so a correction factor had to be calculated from the results of a subsidiary experiment to enable one to measure the beam polarization for energies other than that used during the calibration. The absolute value of the beam polarization can be measured to an accuracy of ± 0.005 (standard deviation).

To obtain a beam with zero polarization it has been found necessary not just to switch off the sextupole magnet of the PPS, but to degauss the magnet by reversing the current several times while decreasing it. Otherwise residual polarizations of 0.01 may be observed.

Future Modifications

Since the statistical accuracy of polarization measurements depends on P^2, it is always desirable to increase the beam polarization. The present source has a theoretical maximum polarization of 0.50 so not much improvement can be expected. However, by using the adiabatic passage "spin-flip" technique first described by Abragam and Winter and so successfully exploited by the Saclay cyclotron group a factor of two improvement can be achieved. The necessary modifications to the source are now being proposed for installation later this year.

If the atomic beam, after selection of the $J = +\frac{1}{2}$ states in the sextupole magnet, is passed through an rf field in a low magnetic field,

which varies slowly through resonance, the $I = +\frac{1}{2}$ state can be completely converted into a $I = -\frac{1}{2}$ state. If the beam is then ionized in a strong magnetic field (~1000 0e), a theoretical proton polarization of 1.0 can be achieved. Since ionization in a strong field is more efficient, the proton current will also be increased. It is expected that a polarization of 0.80 at an intensity of about 10^9 protons/sec will be obtained.

One disadvantage of the modified source will be that the present Helmholtz coil system cannot be used. The polarization direction will be vertical initially, but it can be rotated in the transverse plane by a solenoid, located in the 500 kV terminal. To obtain longitudinal polarization a crossed electric and magnetic field spin rotator will have to be installed.

Scheduling of experimental time on the PLA is handicapped by the fact that the unpolarized beam intensity obtainable from the PPS is lower than most experimenters require, and changing over to the normal source requires at least a 24-hour shutdown. It is desirable, therefore, to combine in the same vacuum system the PPS and a proton source of a few mA peak current.

Acknowledgements

D. A. G. Broad has been responsible for the recent development work on the polarized source. He has been assisted by R. C. Carter and A. G. D. Payne in the laboratory and the engineering has been the responsibility of K. McAinsh and J. A. Taylor.

MARTIN, J. H.: What was the pulsing rate of the machine?

DICKSON: It is 50 pulses per second and the pulse length is 200 μs.

FEATHERSTONE: Are you using the high frequency rf transition at about 1400 Mc or are you using the low frequency?

DICKSON: We are using the low frequency transition at about 10 G and 8 Mc/s which gives a transition from state 1 to state 3 by the adiabatic passage method.

ION SOURCE WORK AT ANL

D. H. Nordby
Argonne National Laboratory

I. Column

In the pursuit of higher beam currents with lower emittance a 500 kV test facility has been constructed. It has been built in such a way that various columns and ion sources can be tried with ease. Figure 1 shows the layout of the development room. Figure 2 shows a column that is presently being tested. It is a 15-inch long constant acceleration type column which is planned for the first section of a future 750 kV column (see Fig. 3). The column section is designed to run at about 250 kV, but as yet has only reached 175 kV.

II. Ion Source

This source shown in Fig. 4 was designed to be small enough to fit in a re-entrant column with an inside diameter of 10 inches. This requirement was met by using formvar-coated copper tubing in the magnet and a small diameter insulator. We use an oxide-coated cathode as has been used in the ZGS preaccelerator for the past two years. The expansion cup has been wound with formvar-coated copper tubing to give us another tuning parameter. The arc modulator is made in two sections so that the filament and intermediate anode voltage can be varied with respect to the anode independently. The modulator is transistorized and has a current capability of 30 A from the intermediate anode to anode. Source parameters are shown in Table I.

We have gotten over 600 mA with this source on a test stand.

III. Results

The column and ion source combination has been run at 575 mA and 120 kV. Crude emittance measurements were made which seem to indicate a beam quality improvement of a factor of 8-10 with a beam intensity increase of a factor of four over our present 750 kV preaccelerator. We expect to make more accurate measurements at various beam conditions later this month.

TABLE I

SOURCE PARAMETERS

Filament Current	15.5 A
Filament Voltage	5.9 V
Magnet Current	130.0 A
Extraction Voltage	20.0 kV
Focus Voltage	40.0 kV
Filament - Anode Voltage	200.0 V
Intermediate Anode - Anode Voltage	70.0 V
Filament - Intermediate Anode Current	12.0 A
Intermediate Anode - Anode Current	24.0 A
Source Press	0.2 Torr
Beam Current	400.0 mA
Acceleration Voltage	130.0 kV
Aperture	Nickel with Copper Tungsten Insert

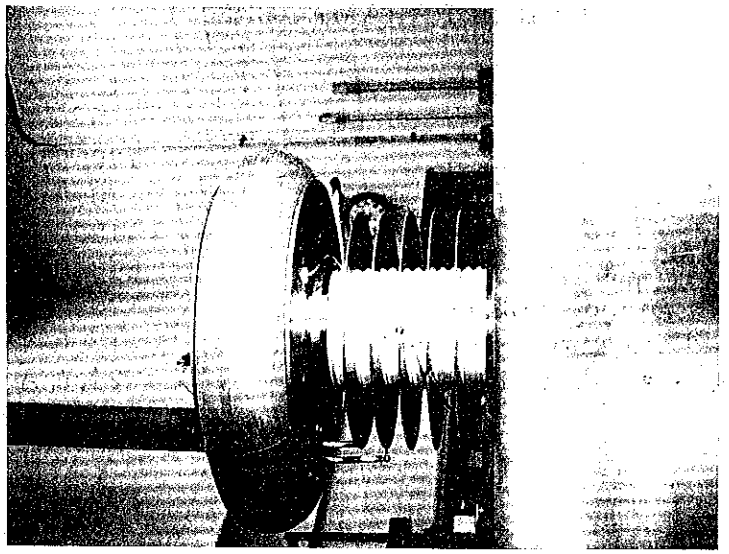

FIG. 2

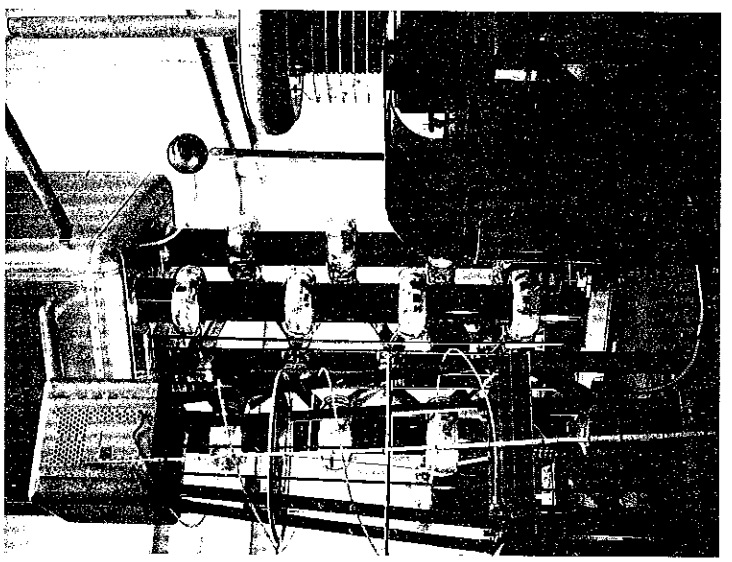

FIG. 1

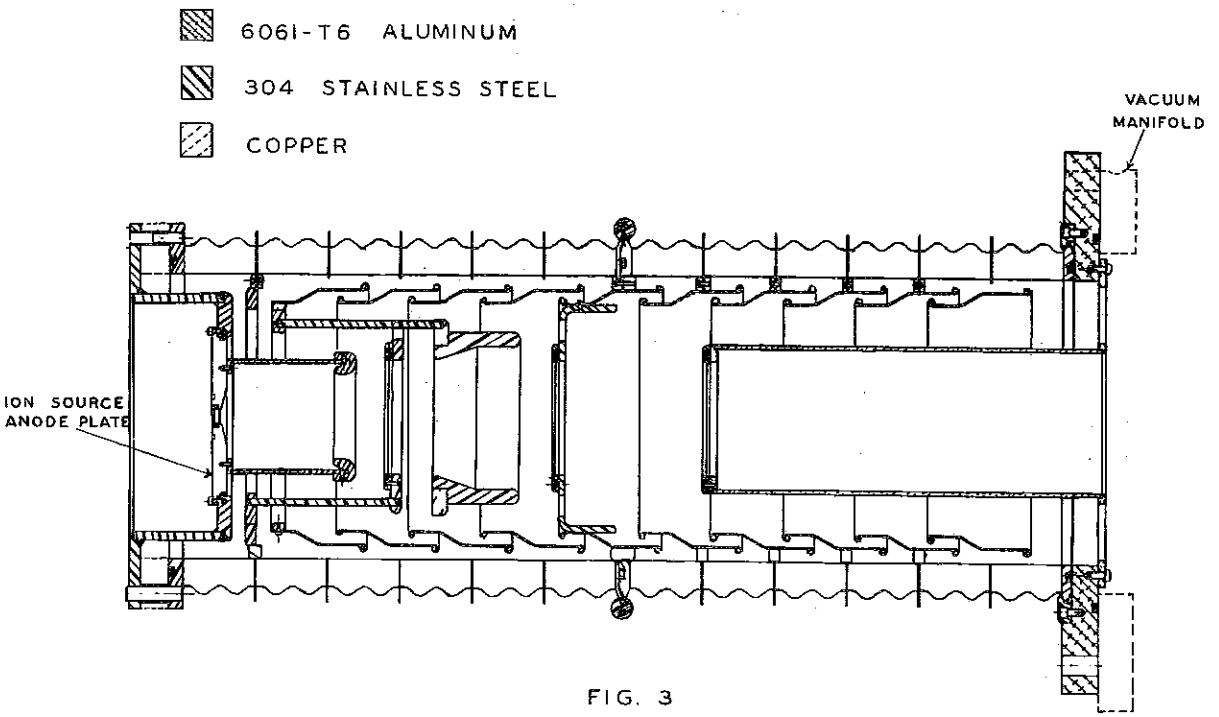
6061-T6 ALUMINUM
304 STAINLESS STEEL
COPPER
VACUUM MANIFOLD
ION SOURCE ANODE PLATE

FIG. 3

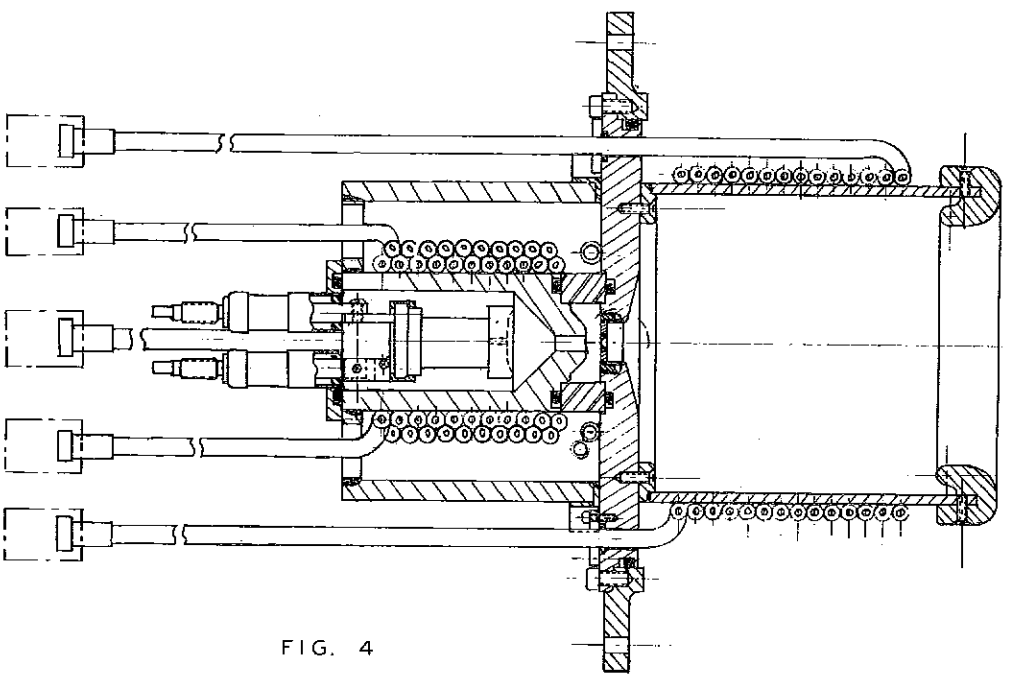

FIG. 4

AN EXTENDED RF ION SOURCE WITH SMALL PHASE SPACE EMITTANCE AREA

Rolland Perry
Argonne National Laboratory

Several types of ion sources have been designed for use on particle accelerators, and considerable effort has been devoted to attaining large beam currents. Somewhat less work has been done in the direction of reducing the beam divergence or of minimizing the effects of space charge. Since the latter effects are greatest in the region of low beam velocity, and since the emittance properties are established at the source, the present work is aimed at making some improvements in these two respects, without sacrificing intensity.

Historically, the first concepts were stimulated by a discussion of an electron gun for an electron microscope by A. V. Crewe, and the results are applicable to electrons as well as ions, except in different methods of production. Moreover, while the present design is based on the use of an rf excitation of a plasma, one might possibly adapt other methods of plasma production and extraction to achieve similar results.

The general arrangement of the source is simply that of a hollow donut-shaped cavity excited by an rf power source as shown in Fig. 1. Ions are extracted from the cavity by means of a dc field applied across a diameter between A and C, and the ions must traverse a narrow channel or slit arrangement which restricts their divergence angle. Since the slit extends all the way around the circular length of the donut, the area of extraction may be large even though the width w is made small, thus permitting almost arbitrarily large beam extraction.

The beam exit direction may be oriented at any arbitrary angle , which may be chosen to be compatible with some focusing and accelerating system.

First we look at the case of $\varphi = \pi/2$ in which case the central rays from all points around the circumference of the circular slit are emitted parallel to the axis of symmetry. The noncentral rays will have maximum divergence angle

$$\Delta\varphi = \frac{w}{\ell}$$

where ℓ is the length of the extraction channel. The area in phase space is

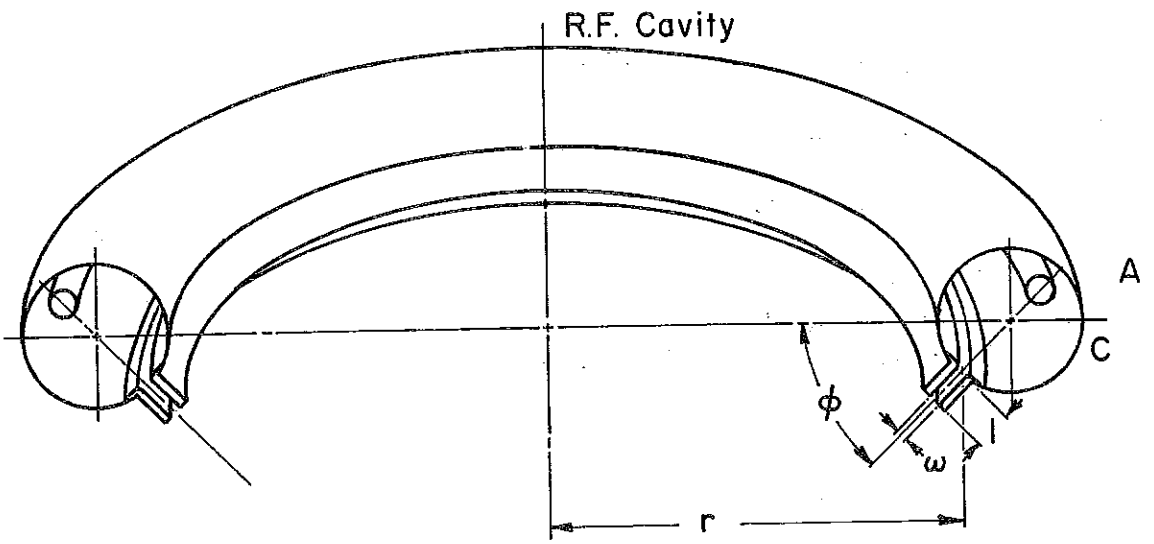

FIG. 1

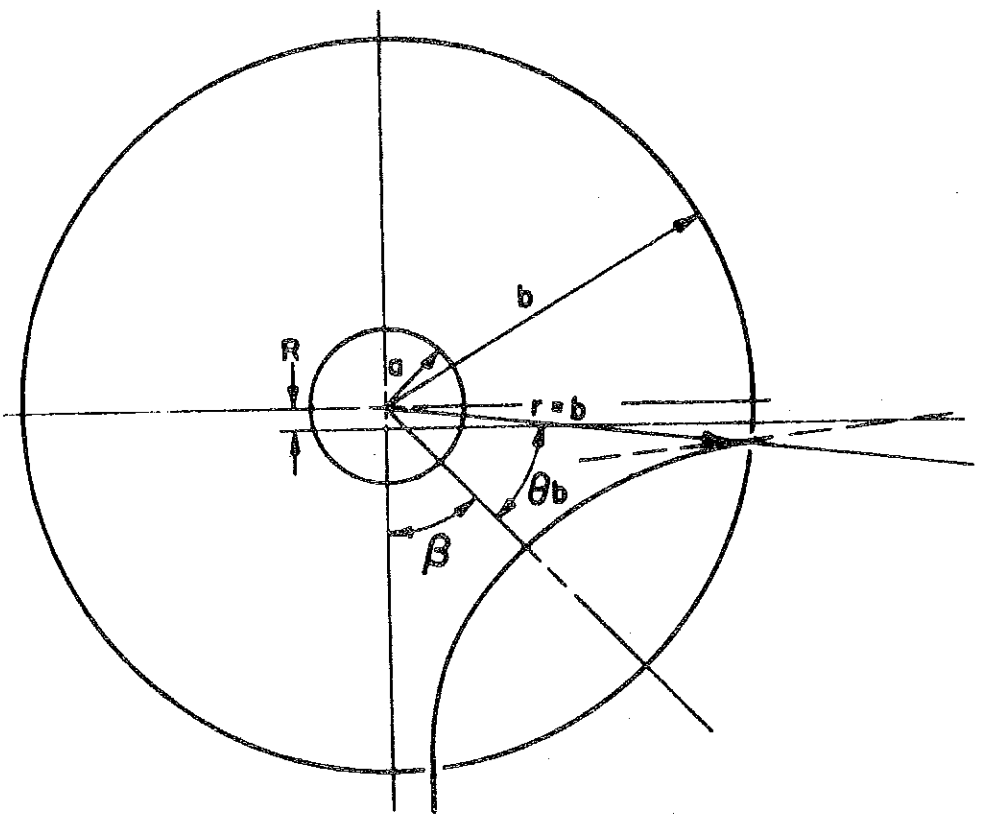

FIG. 2

$$A_x' \equiv r\alpha\pi = r\Delta\varphi\pi \quad .$$

Let $w = 0.010''$, $\ell = 1''$, $r = 7.5$ cm. Then

$$A_x = r\,\Delta\varphi\,\pi = 7.5 \times 0.01\pi = 75\pi \text{ cm mrad}$$

at an extraction voltage of 20 or 30 kV which is typical for an rf source. This becomes about 12.5π cm mrad at 750 keV or 15π cm mrad at 500 keV. The extraction area for this condition is

$$S = 2\pi\, r\, w$$

$$= 2\pi \times 7.5 \times 0.025$$

$$= 1.18 \text{ cm}^2.$$

Compare these numbers with the corresponding values for rf sources of the CERN type, where

$$A_x \simeq 20\pi \text{ cm mrad at 500 keV}$$

$$S \simeq \pi (0.2)^2 = 0.125 \text{ cm}^2.$$

Now the geometry of accelerating tubes may not be compatible with a beam diameter as large as 15 cm, so the diameter may be chosen to satisfy this limitation. Likewise one may wish to inject into the accelerating tube at some arbitrary focusing angle. This may be done either by choosing the angle to meet the requirements, or, if this is not otherwise compatible, by injecting into a spherical condenser cavity and deflecting it by means of the electrostatic field in the cavity to form a hollow beam of arbitrary diameter and convergence angle.

The requirements for accomplishing this are as follows: The central ray from the slit must enter the spherical cavity at $r = b$ tangent to a hyperbolic path shown in Fig. 2 and described by the relation

$$\frac{1}{r} = \frac{\sqrt{\left(V_a \frac{ab}{b-a}\right)^2 + 4R^2 V_e + \left(V_a \frac{a}{b-a}\right)^2} \cos\theta - V_a \frac{ab}{b-a}}{2R^2 \left[V_e + V_a \frac{a}{b-a}\right]}$$

This is a solution of the equations of motion for a particle of mass m and charge e moving in a central force field:

$$m\left[\ddot{r} - r\dot{\theta}^2\right] = \frac{Q\,e}{r^2}$$

$$m\left[2\dot{r}\dot{\theta} + r\ddot{\theta}\right] = 0 \quad .$$

The quantities in the trajectory equation are as follows:

a = radius of inner sphere

b = radius of condenser cavity

R = distance from center of sphere to asymptotic line toward which the hyperbola tends at infinity

V_a = potential on inner sphere

V_e = extraction voltage which corresponds to the kinetic energy the particle must have as it enters the chamber, i.e.,

$$e\,V_e = \frac{1}{2}\,m\,U_i^2 + \int_{\infty}^{b} \frac{Q\,e}{r^2}\,dr = e\,V_i - e\,V_b; \quad V_b \equiv V_a\,\frac{a}{b-a} \quad .$$

The asymptotes are defined by

$$\tan\beta = \frac{2\,R\left[V_e + V_a\,\frac{a}{b-a}\right]}{V_a\,\frac{ab}{b-a}} \quad .$$

There are two benefits to be expected from using a hollow cylindrical or conical beam, viz

1. Since space-charge effects are more nearly the same for all particles due to the $\frac{1}{r}$ dependence, the distortion of the phase space figure due to space charge will be minimized, and

2. Since all particles traversing an axially symmetric lens will see essentially the same field configuration, lens aberrations should be minimized, thus reducing growth of phase space area from this cause.

A number of problems need to be examined in connection with the rf source as described. Figure 3 shows a conceptual design for such a source together with a spherical condenser lens system. The rf cavity would be driven in the TM_{010} mode from a wave guide coupling through

an iris into the cavity. For a cavity diameter of about 4 cm the frequency would be about 5000-6000 Mc/sec. Peak power requirements would be a few hundred watts.

CURTIS: With respect to your concern about violating Liouville's theorem, should I understand from your numbers that density in the region of phase space occupied by the particles has increased in the deflected beam over what it was in the converging ring of beam?

PERRY: One is concentrating the beam into a smaller diameter in the deflected beam. One might expect from Liouville's theorem that the divergence angle would actually go up in the process. The divergence angle does go up but it apparently does not increase in proportion to the reduction of beam radius according to my simple calculations which I am pretty sure are questionable.

LAPOSTOLLE: That worries me, and I also have some doubts about your estimated emittance. It is clear that, having a narrow slit, you can reduce very much the angle of divergence in the direction perpendicular to the slit. But in the direction parallel to the slit the emittance can be very large. The two directions cannot be considered independently in your bending system and I think that this could explain the apparent disagreement with Liouville's theorem.

PERRY: The extraction field has no component in the parallel direction, so the component of velocity in this direction is only the thermal component, which would be small in comparison.

LAPOSTOLLE: But there is no focusing in this direction from your deflecting system.

CURTIS: There would actually be divergence in this direction from the deflecting system.

PERRY: Yes, this is true. I cannot vouch for anything at present in terms of actual magnitude of emittance.

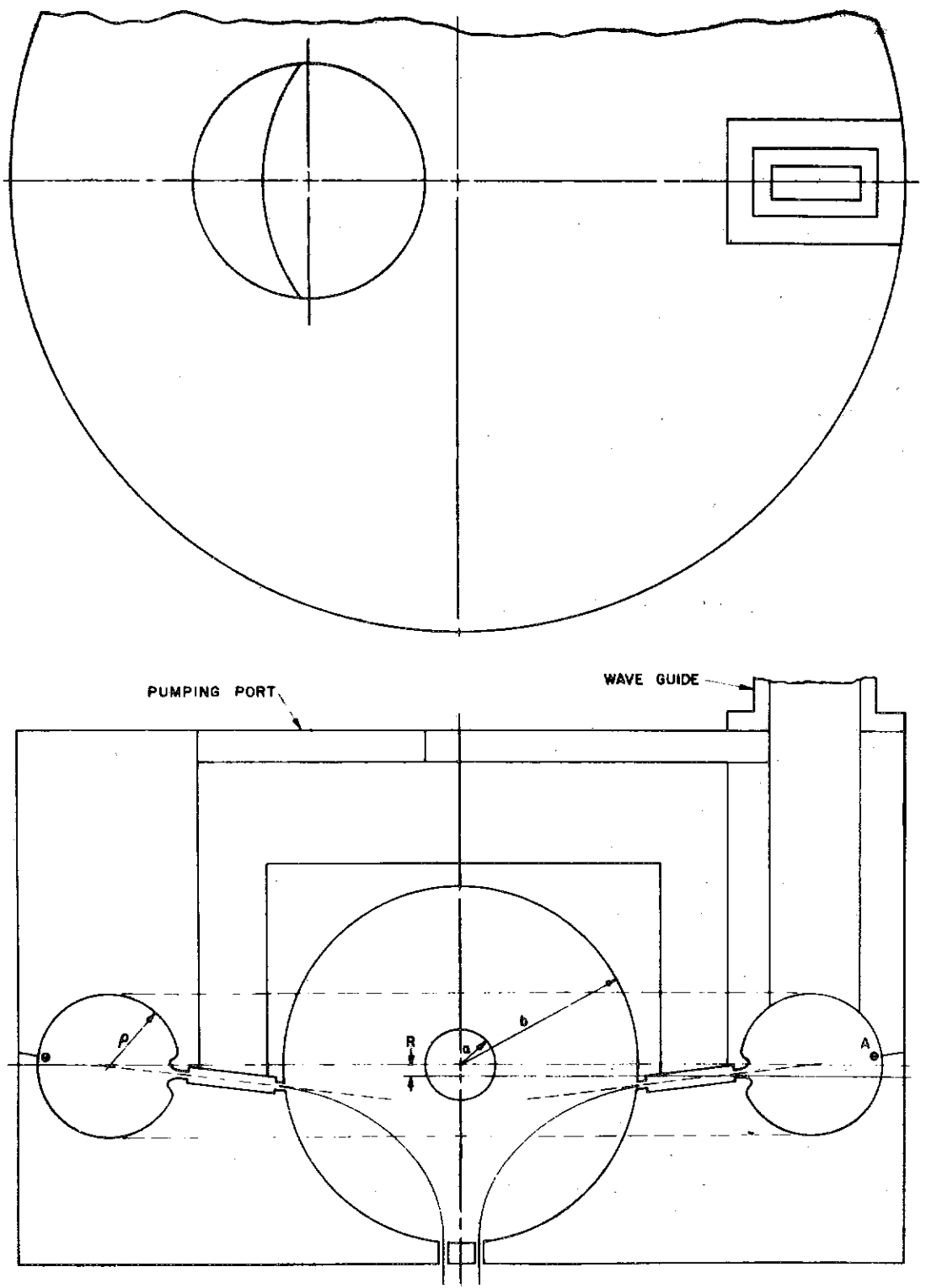

FIG. 3 EXTENDED RF ION SOURCE

A NEW APPROACH TO PREINJECTORS

H. Wroe
Rutherford High Energy Laboratory

1. Introduction

It has been realized for some time that the conventional preinjector, consisting of an ion source and focusing electrodes followed by a long accelerating column, could be simplified. If the vacuum breakdown problems could be overcome, then acceleration to the final energy in one step, across a single gap, has many advantages. Focusing could be done at earth potential thus reducing the quantity of equipment which has to be operated on the high voltage platform. The beam would be accelerated rapidly thus minimizing the effects of space charge.

Some work on the principle of single gap acceleration is described below.

2. A Single Gap Acceleration Experiment

An obvious first step is to arrange a pair of electrodes in a vacuum vessel and have a conventional ion source in the high voltage electrode. As a quick preliminary experiment, the apparatus illustrated in Fig. 1 was set up. In this case a standard rf source was operated at earth potential and the beam was accelerated to a negative potential across a single gap. This circumvented the need for the high voltage electrode. The latter contained a collector cup with a transverse magnetic field for secondary electron suppression, the only measure of beam current being a resistor on the low voltage side of the energy storage capacitor, as shown.

With no beam present the "pressure effect" was observed when a voltage was applied to the gap. The steady loading currents of several hundred μA which occurred at 3×10^{-5} Torr dropped to a negligible value at a pressure of about 5×10^{-4} Torr.

A beam current of about 40 mA (pulse length 1 ms) was accelerated to - 220 kV without breakdown of the gap at a pressure of 10^{-3} Torr in hydrogen. These values were the maximum available from the various power supplies at the time.

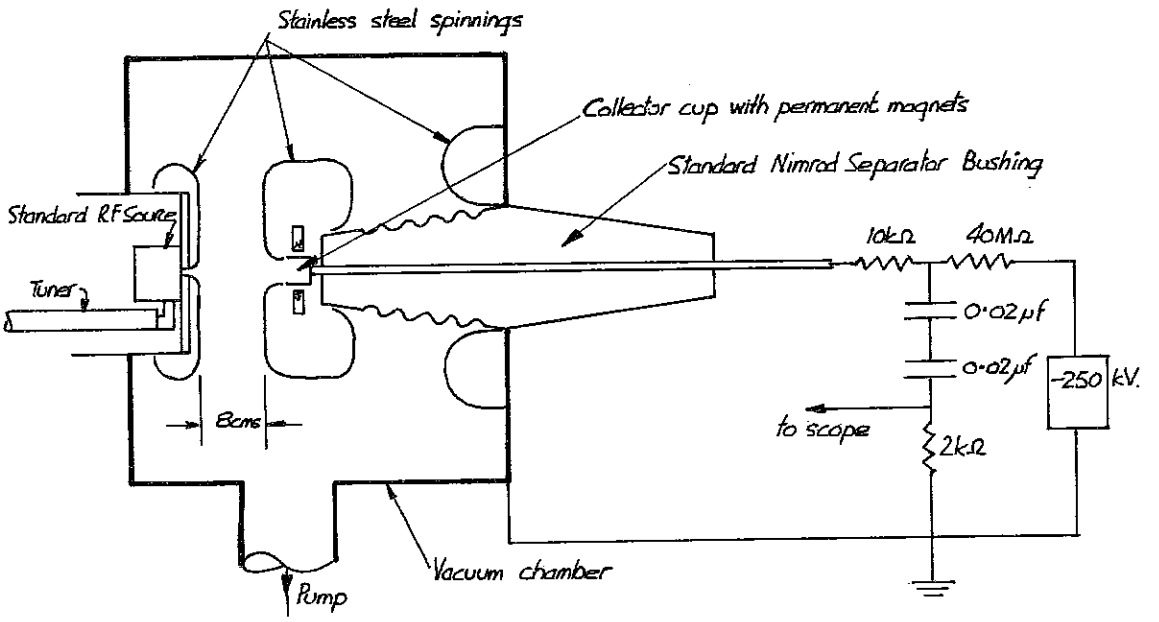

Not to scale

FIG. 1 Diagram of single gap experiment

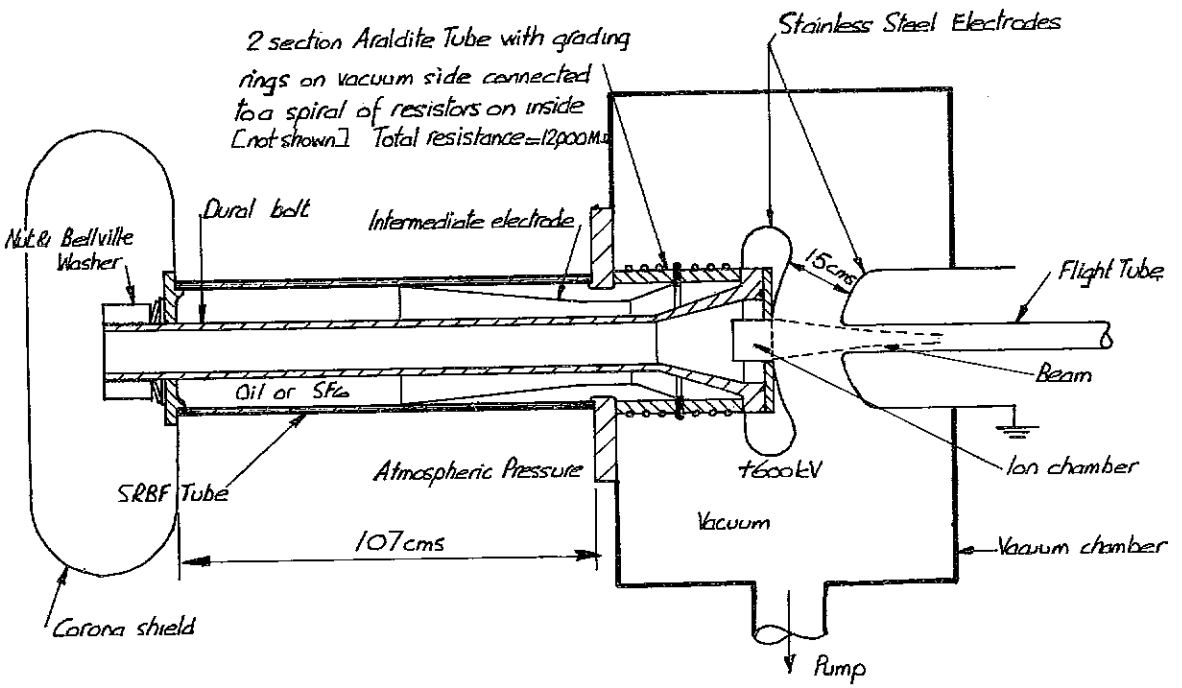

FIG. 2 Scaled-up Ion Source with 600 kV Lead-in Bushing

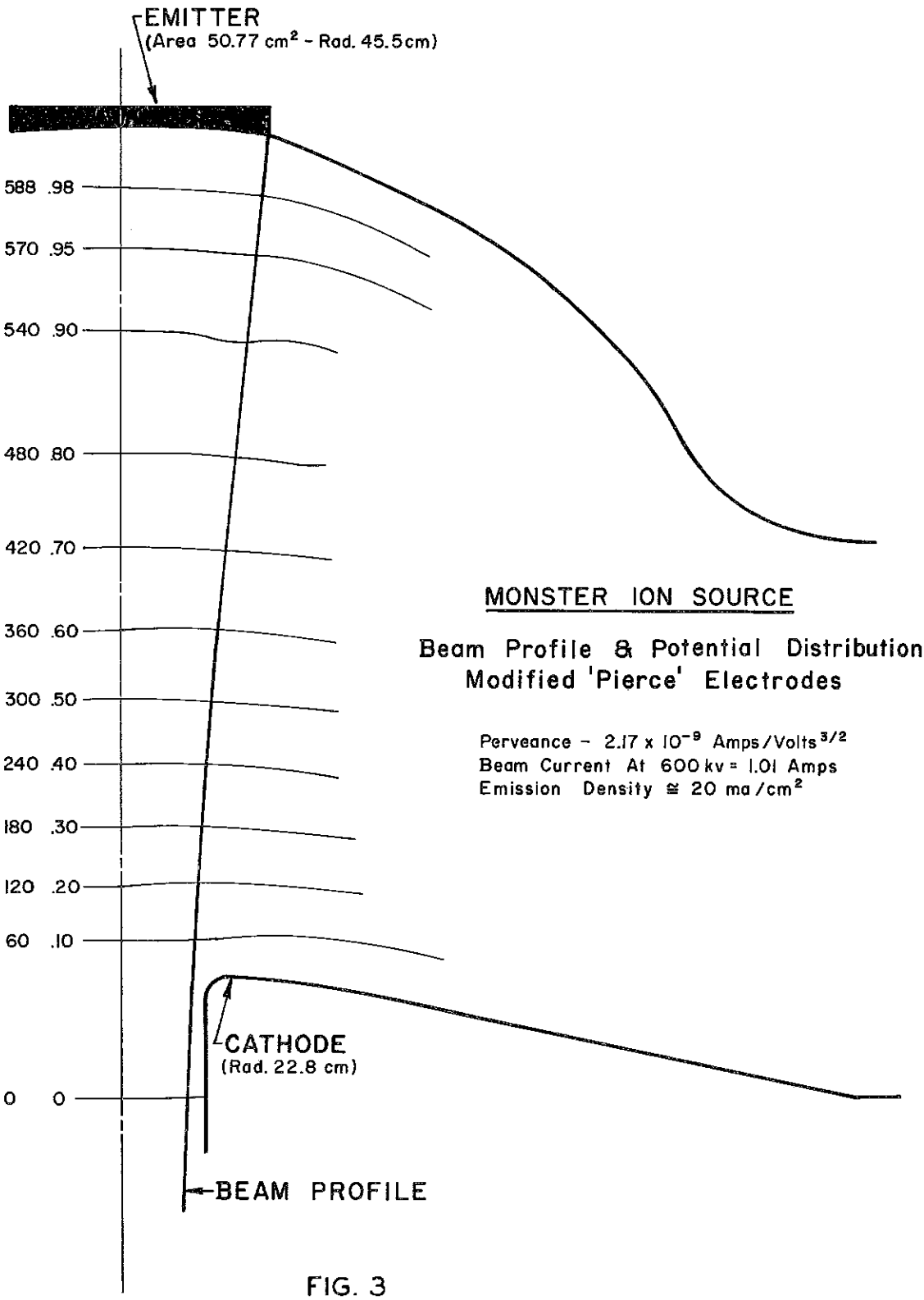
EMITTER
(Area 50.77 cm² - Rad. 45.5cm)
588 .98
570 .95
540 .90
480 .80
420 .70
360 .60
300 .50
240 .40
180 .30
120 .20
60 .10
0 0
CATHODE
(Rad. 22.8 cm)
BEAM PROFILE
MONSTER ION SOURCE
Beam Profile & Potential Distribution
Modified 'Pierce' Electrodes
Perveance - 2.17 x 10⁻⁹ Amps/Volts^3/2
Beam Current At 600 kv = 1.01 Amps
Emission Density ≅ 20 ma/cm²

FIG. 3

3. A Scaled Up Ion Source

The "pressure effect" makes it feasible to operate some sort of ion chamber and an accelerating gap at the same pressure, thus avoiding the canal or orifice needed in conventional sources to limit gas flow. The ions could be extracted over a large area at low current density from a discharge operating in the pressure range 10^{-3} - 10^{-4} Torr.

Work is proceeding on a device utilizing this principle as shown in Fig. 2.

A discharge chamber is housed in the end of a lead-in bushing. It has a gridded aperture 8 cm in diameter through which the ions are extracted. The extraction voltage corresponds to the accelerating voltage of a conventional preinjector, 600 kV in this case. The electrodes of the single gap have surfaces which are parts of concentric spheres. The radii of the anode and cathode are 30 cm and 15 cm respectively. With an ion emitting aperture of 8 cm diameter, assuming spherical space-charge flow and ignoring the hole in the cathode, the perveance is 3.6×10^{-9} $A/V^{3/2}$ for protons. Thus at 600 kV the space-charge limited proton current would be 1.7 A, requiring an emission current density at the plasma boundary of 30 mA/cm^2. The optics in the accelerating gap is illustrated in Fig. 3.

Two possible low pressure discharges are being examined as plasma sources--a Penning type and a discharge using an electrostatic electron trap.[1]

The design of the lead-in bushing is a major technological problem. The design shown in Fig. 2 consists of four parts, a mounting flange, an epoxy resin cylinder about 30 cm long and 34 cm diameter projecting into the vacuum chamber, a bakelite tube 107 cm long and the same diameter, and finally a strong tubular tie bolt down the center to hold the assembly together and give access for electrical leads to the ion chamber. The space between the bolt and the tubes is filled with transformer oil (and possibly compressed SF_6 at a later date). The surface of the epoxy resin tube is electrically graded by means of 8 metal rings on the outside (i.e. the vacuum side) connected through the epoxy resin to a spiral of resistors on the inside (i.e. immersed in oil). The total resistance is 12,000 M . The outside of the bakelite tube (i.e. in air at atmospheric pressure) may also be graded. An intermediate electrode is incorporated into the bushing as shown to make the radial potential distribution more uniform in the gap between the bolt and mounting flange.

Acknowledgements

The author wishes to acknowledge the valuable assistance of Mr. R. G. Fowler, Mr. D. G. Moneypenny and Mr. S. C. Sutherland and Mr. J. Ellis in the above work.

VAN STEENBERGEN: In your figure you show an H.V. electrode aperture about equal to the beam diameter at that location. The rectilinear beam is of course a zero emittance approximation, which is not true in practice. A certain fraction of the beam will end up outside the beam periphery determined with the "Pierce" approach. As a consequence, one would expect secondary electron production on the H.V. electrode when the aperture diameter is close to the theoretical beam diameter.

WROE: Yes.

CURTIS: What was the distance across the gap? If the gradient is high enough, that angular divergence due to thermal motion would not be very large, would it?

WROE: It shouldn't be. The gap is 23 cm and the beam radius 4 cm.

MORGAN: A comment. As you know we normally extracted at 150 kV from a duoplasmatron ion source. We have also extracted at 300 kV with a 1-cm gap. This is for either a 50% duty cycle or dc operation. There are other possible complications, but there is no indication of it being advantageous to operate in an increased pressure range. In fact a lower pressure range of $\sim 3 \times 10^{-6}$ torr is better for stability in our case.

WROE: Well there is a feeling these days in the vacuum breakdown field that you can divide the phenomena into two parts: short gaps where the fields are high and gaps several centimeters long where the mean fields are quite low. The pressure effect is observed in the long gap case.

HUBBARD: How do you supply the power to the ion source?

WROE: Down the tube--the bolt that holds the whole thing together is hollow. The idea is to use such a simple ion chamber that few supplies will be necessary. However, if you put a duoplasmatron in there with many supplies needed, there will be some difficulty. However, there is a 2-1/2-inch hole down the bolt which holds the assembly together.

HUBBARD: But then you have to have it up at high voltage in the back end? You need a platform just like a conventional machine?

WROE: Oh sure, you need a platform.

KELLEY: you say a PIG source, for example, looks like a good thing. I was wondering, in making your ions in the ion source, how are you sure that you have an essentially zero energy cathode. You said everything was calculated for zero initial velocities.

WROE: Yes it is. That is what the computer program assumes, though it won't be true in practice. The ions will have initial velocities. But the initial energy is quite small compared to the total potential of the gap.

VAN STEENBERGEN: I am interested in hearing the pressure effect mentioned here in connection with voltage breakdown. This came up some time ago when the pressure in the linac was being discussed. I wonder if it could be useful in a linac to improve the maximum attainable gradient, say by running the linac at a pressure of 10^{-4} mm Hg instead of 10^{-6} mm Hg.

WROE: Well, I won't be sure about that. This phenomenon seems to manifest itself in the case of long gaps at low pressure. I am not sure this has been observed in impulse or rf breakdown--just dc. The theory of this is nowhere near as advanced as the short gap case. There are some quite acceptable theories in the short gap case of breakdown where the mean fields are high and you can invoke some sort of field emission at the cathode to start the thing off. The mean fields here, across these gaps, are nowhere anywhere big enough for that. In the old days one of the earliest theories was that you have a particle interchange; an electron or negative ion is emitted here, crosses the gap, and liberates an ion which comes back and a chain reaction is set up. The effect of putting gas in as far as I understand it is just that you might get an occasional charge exchange event or scattering which interferes with this particle interchange. There are also micro discharges which you probably know about. If you observe the current through this gap, even though it is not breaking down, you see bursts of current. These micro discharges are also suppressed while working in this pressure range. I think there is no doubt that it occurs for the dc case.

NORDBY: I would be afraid in linacs at 10^{-4} mm Hg that your mean free path goes down pretty fast.

WROE: Well, it is true that it will be close to the gap dimensions. You are working in a rather critical position, if you put the pressure up too

high, you come onto the low pressure side of the Paschen curve. You have to try to ride this rather tricky edge between the two.

NORDBY: I think you are all right at 23 cm, but in a couple hundred-foot tank things might be bad.

WROE: Yes, that is true.

FEATHERSTONE: We do observe in the Minnesota tanks that sparking becomes a problem when we get much above 10^{-5} torr.

BLEWETT: I guess this suppression of breakdown by gas pressures is observed mostly in dc separators. I believe the gas that is conventionally used is nitrogen. Are you sure this is true of hydrogen?

WROE: I talked to the Bevatron people and they use argon and they do not think it would make much difference what gas was used. Fundamentally, if the idea of charge exchange is correct, I don't really see why it should make much difference.

CURTIS: I think there is some information on that from the people at Ion Physics Corporation, who have used various gasses in their dc gaps, and they observed the improvement with all of these. They do not really prefer one gas over another, particularly, I think.

OLEKSIUK: Did you mention what you expected the sheath thickness to be?

WROE: It is just given by this formula. This is a very simple calculation for the one-dimensional case.

OLEKSIUK: This is just the Debye length that people talk about?

WROE: No, it would depend on the voltage you apply between the plasma and the cathode, you see.

PREACCELERATOR COLUMN DESIGN

C. D. Curtis and G. M. Lee
Midwestern Universities Research Association

I. REQUIREMENTS

There are three principal requirements that we should like to meet in the design of a high current accelerating system. The first is that the undesirable effects of space-charge forces within the beam on beam emittance be removed or rendered insignificant. One practical approach to accomplish this is to use a beam from the source which is initially large in diameter to reduce the self-forces and which can be accelerated very quickly to reduce the time for the forces to act. Another approach is to use a Pierce-type field geometry to balance out the self-forces. Both approaches lead to a high field gradient in the accelerating gap or column. A second requirement is for reliability of operation against breakdown. Because of the premium placed on high field strength capability here, we wish, if possible, to design the overall system so that the chance of breakdown due to conditions external to the accelerating gap is small. Our principal concern then is the voltage-holding properties within the column. The third requirement is for ion source accessibility. Under the assumption that servicing of the ion source is a major cause of down time on a preaccelerator, it is important to provide for fast access and change capability. In particular, on an experimental facility where frequent changes may be needed, this is important. The use of two preinjectors with one on standby can be considered, of course, to give increased reliability in the case of accelerator operation.

II. ELECTRODE DESIGN

To provide for a large diameter beam we have chosen to use the scheme of a plasma expansion cup attached to a conventional duoplasmatron source, following the example of Solnyskov[1] and others. We propose that the extraction grid be the first electrode of the high gradient acceleration region. The beam will thus be accelerated quickly without the delay required in passing first through a focusing lens. The hope is that one can control the focal properties of the beam to some extent for any given current intensity by simultaneous adjustment of the plasma density and the extraction voltage. Use of a fine mesh grid to shape the boundary would be a welcome addition, if successful. A properly concave plasma surface will render the beam

initially converging. The source position is shown in Fig. 1. The exact configuration of the source cup and extraction grid are subject to experimental change.

Unless one uses an accelerating field of the appropriate shape to counteract the space-charge forces, there will be some divergence of the beam. We can obtain some idea of the dependence on beam size and field gradient by assuming a uniform accelerating field. If one further assumes a cylindrical beam of radius R and of uniform charge density, which remains uniform across the beam diameter, one can derive an expression for the divergence of the ion beam after acceleration through some potential drop. This is given approximately for a particle at the edge of the beam by

$$\theta = \frac{I}{ER}\sqrt{\frac{m}{-2eV}}\ln\frac{V}{V_o}$$

for a long beam with neglect of end effects. The beam here is assumed parallel as it crosses the surface of potential V_o relative to the source. For a given final potential V one notes the divergence angle to be proportional to beam current I and inversely proportional to beam radius and to field strength E. For constant gradient and variable V there is a maximum θ for $\ln V/V_o = 2$. As an example we may consider a beam of 4 cm radius accelerated through a column or gap of 30 cm length. If the initial potential of the parallel beam is $V_o = -50$ kV and the final potential V is-500 kV, the angle θ becomes 6×10^{-3} radians. If V is changed to - 1000 kV, θ becomes 2.6×10^{-3} radians. This divergence is comparable with the spreading which results from thermal motion of the ions at the source but does not play the same role in determining beam emittance.

When a short high gradient accelerating column is considered, one is led to wonder if a single-gap two-electrode accelerator is feasible. If the field in such a gap were converging, it would tend to offset the beam divergence due to space-charge forces, to the diverging aperture lens at the gap exit and to the absence of focusing electrodes between source and gap entrance. A simple converging field geometry, not of the Pierce type, is given by concentric spherical electrodes as shown in Fig. 2.

The optics of the system is given by the formulas in the figure where f is the focal length of the exit aperture lens and F is the distance of focus from this aperture for a beam, which, starting from rest, is accelerated radially between the spheres. The drawing is for the special

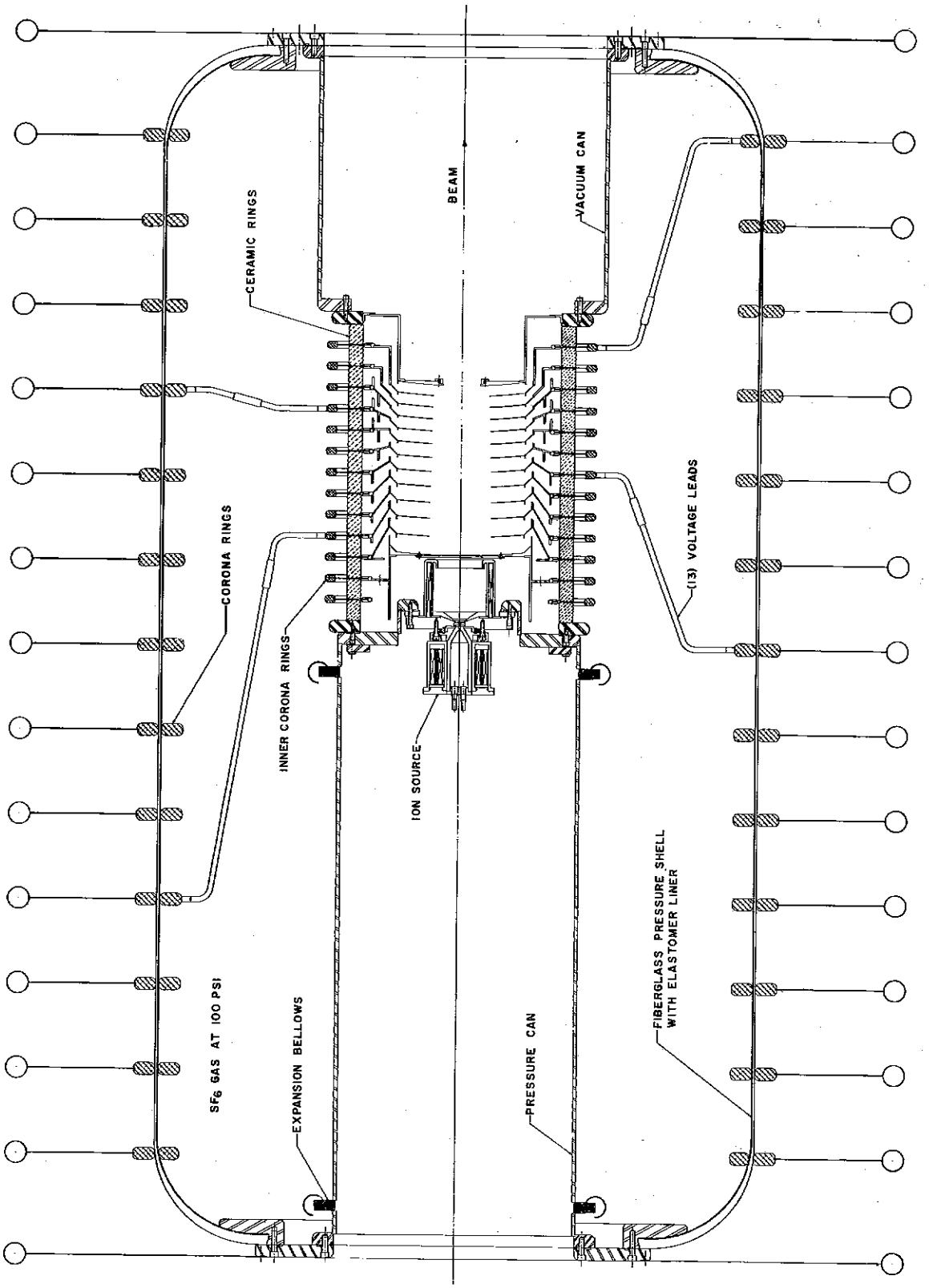
CERAMIC RINGS
BEAM
VACUUM CAN
CORONA RINGS
INNER CORONA RINGS
ION SOURCE
(13) VOLTAGE LEADS
SF_6 GAS AT 100 PSI
EXPANSION BELLOWS
PRESSURE CAN
FIBERGLASS PRESSURE SHELL
WITH ELASTOMER LINER

FIG 1

case of the sphere radii having the ratio of 4/3, which renders the beam parallel beyond the exit.

Aside from the question of adequate voltage insulation between the electrodes in vacuum, there is the problem of insulation at the boundary between vacuum and external pressure. One approach is to take the beam out through a grounded tube which passes through a high voltage bushing support for the high potential sphere. Another approach is to distort the electrode shapes to give a spherical field in the beam region when the grounded electrode is bent back to surround the high voltage electrode as shown in Fig. 2. The shapes given there were determined in an electrolytic tank and give closely the required field shape. A similar geometry, except for cylindrical electrodes, is used successfully as an electron gun[2] on the MURA 50 MeV accelerator. In this arrangement, the source leads enter through a high voltage bushing which supports the high voltage electrode.

Of prime concern in such a two-electrode system for the 500 to 1000 kV range is the large area of the electrodes in vacuum. Through the "area effect", one can expect to hold less voltage for large than for small area. For small gaps between stainless steel electrodes withstanding of the order of 100 kV, the breakdown voltage varies with area[3] approximately as $\frac{V}{V'} = \left(\frac{A'}{A}\right)^{0.15}$.

A way to reduce the electrode area required is to use a multi-electrode design, the usual practice, to aid in distributions of the potential across the gap. If one does this but keeps the re-entrant electrode shape suggested by Fig. 2, one obtains a design shown, in principle, in Fig. 3. The electrode area exposed to the total voltage difference is now greatly reduced, although the area of each electrode is still quite large. The "total voltage effect", however, whereby the breakdown voltage above 100 kV is approximately proportional to square root of electrode separation, is not now so severe. The voltage is divided across the several gaps of Fig. 3 by an external voltage divider (not shown). A further benefit resulting from use of the intermediate electrodes should be a reduction in x-ray intensity. It is clear that there exists good shielding of the ceramic rings from the beam.

There are certain problems of mechanical design associated with the sketch of Fig. 3. In addition, access to the ion source is limited, allowing removal of no more than the filament holder through the high voltage bushing. A large diameter access channel would be possible by this route only by use of ceramic rings of quite large diameter.

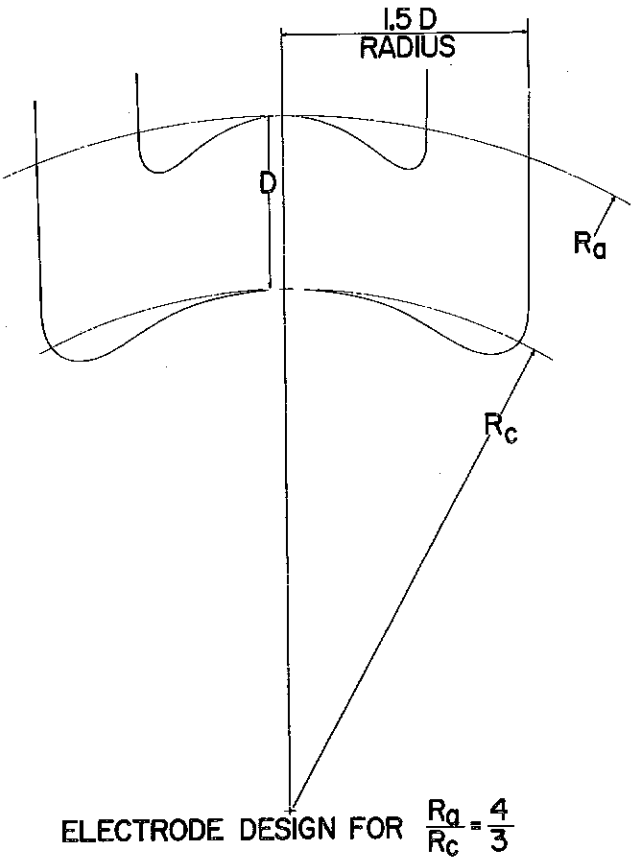

$$\frac{1}{F} = \frac{1}{R_c} + \frac{1}{f}$$

$$\frac{1}{f} = \frac{\Delta E}{4V} = -\frac{R_a/R_c}{4(R_a - R_c)}$$

$$\frac{1}{F} = \frac{3R_a/R_c - 4}{4(R_a - R_c)}$$

FIG 2

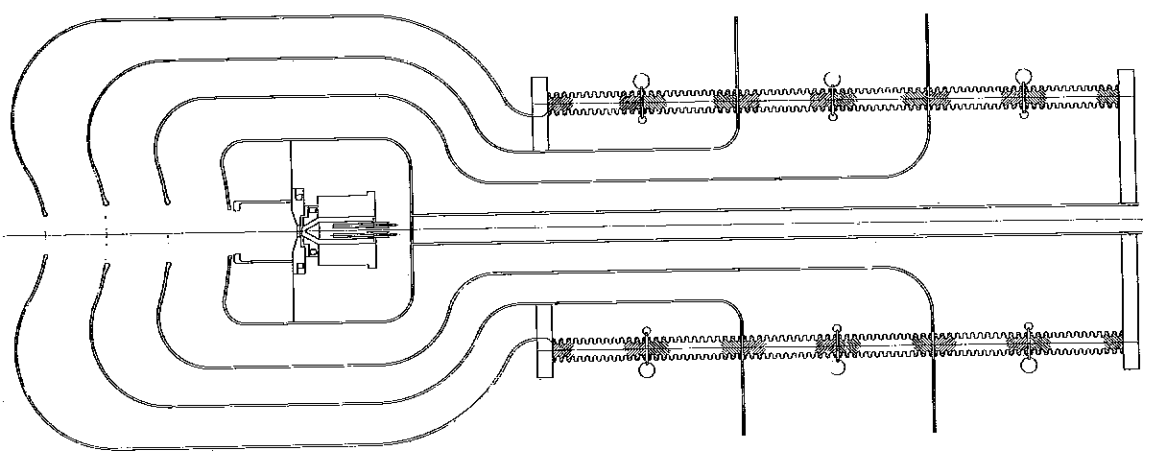

FIG 3

In the interest of achieving a high gradient column with good accessibility to the ion source as well as to the exit beam, we considered it prudent for the present to use a multi-electrode design with a more nearly conventional arrangement of the ceramic insulators. This is the design of Fig. 1, which still retains a converging field with the optics of Fig. 2. The accelerating gap is 30 cm long. The thin spherical electrodes have supports which flare out to a longer ceramic column of 21-inch length having 14 sections. A variable extraction voltage is applied across the first two sections while the other sections have an equal voltage difference across them.

The required field was achieved in an electrolytic tank by John Spooner with only the top and bottom spherical electrodes in place together with the z-shaped portions of the other eleven electrodes. This meant that the remaining electrodes of spherical shape could be placed along already existing equipotential surfaces. One can thereby hope that with accurate placement, the thin electrode edges will not be prone to voltage breakdown and will offer only a small perturbation in the field distribution due to finite electrode thickness. The thickness planned is 1/16 inch.

If the exit aperture in the last electrode is covered by a grid, the beam optics will, of course, be changed. The exit lens action is removed and an otherwise parallel beam will converge, except for space-charge effects, toward a minimum at the center of the spheres.

The electrode material having the best voltage holding properties in the 100 kV range that has come to our attention is a titanium alloy, Ti-7 Al-4 Mo. Furthermore, since it has a thermal coefficient of expansion which closely matches that of the ceramic rings, it becomes a good ring spacer material. Certain voltage tests which we have carried out on 304 stainless steel indicate that this also may be suitable. These included tests of a 0.9 cm gap between the end of a thin-walled right circular cylinder of 10-inch diameter and a plane. A cylinder of 1/16-inch wall held dc voltages well beyond 100 kV without breakdown when the gap was paralleled with a 0.02 μf capacitor. In the column a voltage gradient of 75 kV per gap, where the minimum spacing is 1 cm, would give over 900 kV for the total accelerating voltage.

The ceramic rings are 16 inches outer diameter. Each ring is 1-inch thick by 1-15/32 inches high and is recessed at the ends as may be seen in Fig. 1. This is to take advantage of any improvement in ability to hold voltage, as observed by others[4] when the cathode end is recessed. The rings will be vinyl sealed together.

In assembly the electrodes will be inserted into the column through the high voltage end. A jigging arrangement will permit accurate positioning of each spherical electrode with its attached z-shaped portion before it is connected to its conical support.

III. PRESSURIZED SHELL ASSEMBLY

In order to diminish the possibility of voltage breakdown outside the accelerator column, we decided to enclose the column in a pressurized atmosphere. A practical way to do this is to use a filament-wound fiberglass vessel as shown in Fig. 1. Such items are commercially made in a variety of sizes for rocket motor cases and chemical tanks. The vessel we plan to use is wound onto end flanges that were machined here at MURA. The wall thickness is 1/8 inch with an additional 1/16-inch butyl rubber liner to seal the fiberglass for SF_6 up to 100 lbs/in^2. The rubber can be made semiconductive to allow accumulated charge on the wall to drain off. The vessel is 42 inches inside diameter and 84 inches long.

There is a 17-inch diameter access channel to the source, which remains at atmospheric pressure. Bellows in this tube allow for some stretching of the pressurized tank. The column is under compression when evacuated and approximately neutral when up to air. Source changes are thus possible without the need to disturb tank pressure.

Each column electrode is connected to external corona rings on the fiberglass shell. A resistor string, not shown, divides the voltage here. The resistors can readily be changed if one should wish to alter the field distribution within the column. The position of the column within the tank can be changed, of course, from that shown by changing the electrode leads and the relative lengths of the source and beam exit channels.

Should one wish to test other electrode configurations, the tank should be capable of accommodating designs which vary greatly in electrode and insulator structure from that described here.

KELLEY: It looks as though there are several places in that design, first of all where electrons can be trapped from the magnetic field that you use for shaping the plasma surface. And I think you might get pigging trouble in those regions. Have you tested this?

CURTIS: No, this design has not been tested. The magnetic field indicated in the region of the cup may be undesirable and perhaps unnecessary.

KELLEY: We don't find it necessary to have a labyrinth sort of arrangement with a many bounce path between column and the beam. It seems that just barely shadowing is all that is necessary.

CURTIS: We wondered if this was really necessary and thought that the design might be a bit conservative in this respect.

KELLEY: Did I understand that your thin sheets now along equipotentials were there so that when you have the beam you will still force equipotentials at those places? Otherwise you don't need any electrode surface there.

CURTIS: One should not need any electrodes, except that they do reduce the area of the total gap and may therefore aid the voltage-holding ability. They also should reduce the x-ray level. We may actually remove them, depending on what experience tells us.

VAN STEENBERGEN: Does it make much difference in equipotential distribution outside, say, the beam region, if the high intensity beam is present or not? Are the electrodes at the correct place with beam?

CURTIS: They are in the correct place without beam as designed. It doesn't make a lot of difference whether the beam is present or not. This, of course, depends on the magnitude of beam current. For a 200 mA beam of 4 cm radius, the potential at the center of the beam increases by a few hundred volts. One can compare this with a voltage gradient of approximately 20 kV/cm for a total voltage of 600 kV to determine the displacement of the equipotential surfaces. Now it is possible, by varying the voltage on these electrodes to push the potential surfaces around quite freely. So I think it may be possible to adjust the voltage distribution externally and adequately correct any trouble resulting from displacement of the potential surfaces by the beam.

PRIEST: Lamb was saying that he had done exactly what you are saying and we have done it too. We vary the potential on these electrodes and get very good beam control and then having found out what the potential distribution is we then redesign the thing so that it doesn't need this variation. There is one comment I would like to make. It may be applicable in this case, I am not sure. In electron guns which are at all sophisticated where we really want to get a clean beam and the minimum amount of interception at the anode and so forth, we find we have to pay very special attention to the geometry at the edge of the cathode. And the thing we call the focus electrode, which is the element that does the field shaping, which surrounds the cathode and normally is at the same potential, has to be put in exactly the right place. I mean within a mil

or so or you get into trouble. We found that we have to pay very good attention to this, and a trick we found we can play to overcome the effect of poor tolerances or misalignment is to insulate this electrode so that in the case of electrons we can put a little negative voltage on it, maybe 20 or 30 V. This does wonders to clean up the beam and I suppose if you put a positive voltage on this in your case it might do the same.

CURTIS: Is this again with a Pierce-type geometry?

PRIEST: Yes, I have seen several of these drawn here in the course of the day.

CURTIS: We also found that similar electrode biasing in a Pierce electron gun we once built was quite effective.

MARTIN, J. H.: In regard to breakdown, how much better is this titanium alloy than some good stainless steels?

CURTIS: Of course, different people who make measurements on the same materials do not always obtain the same results. Comparison measurements were made by Ion Physics Corporation people. At the same time that they reached 80 kV across a 1 mm gap for buff-polished Ti alloy electrodes of 20 cm^2 area, they could hold only 60 kV for 304 stainless steel. They achieved, I believe, 110 kV for optically polished Ti alloy.

WROE: I am thoroughly convinced that there is this difference between long and short gaps and I wouldn't consider extrapolating that result into a long gap for instance. I mean that this difference in materials may not apply either.

CURTIS: Yes, I am quite aware of that. We may be just as well off with stainless as with titanium alloy for long gaps. These short gap figures are just the only comparative information I have. There are, of course, several relatively high field short interelectrode gaps in the column design which I have described.

REFERENCES

1. A. J. Solnyshkov et al., Proceedings of the International Conference on High Energy Accelerators, Dubna (Atomizdat, Moscow, 1964), p. 507.

2. C. D. Curtis et al., Rev. Sci. Instr. 35, 1447 (1964).

3. A. S. Denholm, F. J. McCoy, and C. N. Coenroods, Proceedings of the Symposium on Electrostatic Energy Conversion (Power Information Center, Philadelphia, April, 1963), p. 3-1.

4. Thomas J. Holce, 1962 Transactions of the Ninth National Vacuum Symposium of the American Vacuum Society (The Macmillan Co., New York, 1962), p. 376.

THOUGHTS ON MODE DISTRIBUTION IN RF MANIFOLDS

F. Voelker
Lawrence Radiation Laboratory

I first reported on this idea of an rf manifold at the Yale meeting. I want to add to these ideas some further work we have done regarding the mode structure of an rf manifold system. For the benefit of those who are not familiar with it, I will describe such a system. If we have a long linear accelerator cavity which we want to excite, we parallel it with a transmission line or wave guide. At the ends we short circuit the transmission line so that there are an integral number of half-wave lengths along its length at the operating frequency of the linac. This defines a number of E_{max} points along the length of the transmission line. It is permissible to connect to these E_{max} points, but all other points are forbidden.

Now the linac may be divided up into N parts, and let each section be connected to an adjacent E_{max} point on the transmission line so that there are n half-wave lengths between load points. Thus the whole system is $nN\ \lambda_g/2$ in length.

We have let the section of linac be a π-mode rf cavity. See Fig. 1. This figure shows the $\omega - \beta\ell$ diagram for such a cavity and the equivalent circuit for one of the resonances. L_m, C_m, G_m and M_m are the circuit parameters defined at the input loop to the cavity.

Since the cavity must be coupled to the transmission line (or rf manifold), we will arrange the length such that the value of M_m is tuned out and the parallel circuit appears at the E_{max} or load point. This is a very tight coupling to the manifold. The next several modes to the desired one are so close in frequency to ω_o that the value of M_m is effectively tuned out for these also.

We have let these values of

$$Y_{L,m} = G_m (1 + j\, 2\, \delta_m\, Q_m) \quad \text{where} \quad \delta_m \equiv 1 - \frac{\omega^2}{\omega_m^2} .$$

Now we represent the rf manifold in this way.

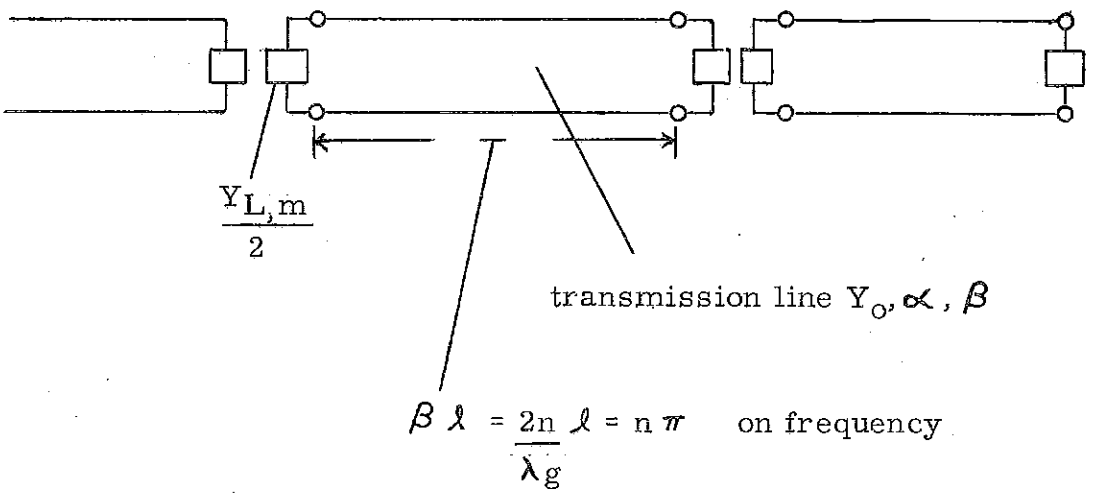

The loaded manifold is now a loaded transmission line, and we will let it have the parameters α_L, β_L, and it has a characteristic admittance Y_{o_L}. The equation governing the values of α_L, β_L as a function of α and β is the following.

$$\cosh \nu_L \ell \equiv \cosh \nu\ell + \frac{Y_L}{2\,Y_o} \sinh \nu\ell,$$

where $\nu_L = \alpha_L + j\,\beta_L$ and $\nu = \alpha + j\,\beta$. These lead to the equations

$$\cosh \alpha_L \ell \cdot \cos \beta_L \ell = \cosh \alpha\ell \cdot \cos \beta\ell + \frac{G_m}{2\,Y_o} \left[\sinh \alpha\ell \cdot \cos \beta\ell - 2\,Q_m\,\delta_m \cosh \alpha\ell \cdot \sin \beta\ell \right]$$

$$\sinh \alpha_L \ell \cdot \sin \beta_L \ell = \sinh \alpha\ell \cdot \sin \beta\ell + \frac{G_m}{2\,Y_o} \left[\cosh \alpha\ell \cdot \sin \beta\ell + 2\,Q_m\,\delta_m \sinh \alpha\ell \cdot \cos \beta\ell \right]$$

In order for the transmission line to have the properties we want for a manifold, we let the following be true.

$\alpha\ell << 1$ so that $\cosh \alpha\ell \cong 1$ and $\sinh \alpha\ell \cong \alpha\ell$.

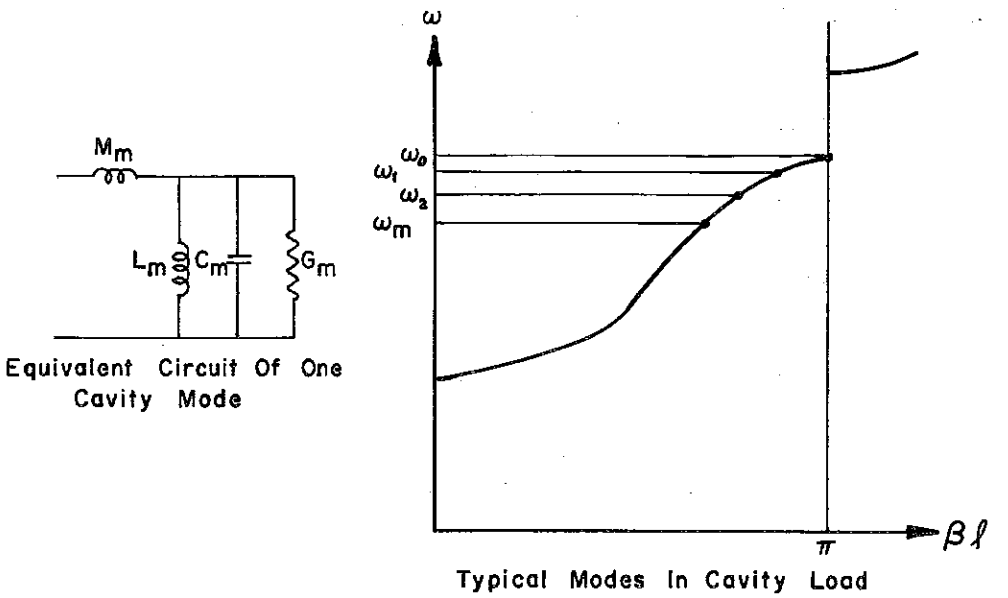
Mm
Lm
Cm
Gm
Equivalent Circuit Of One Cavity Mode
ω
ω0
ω1
ω2
ωm
π
βℓ
Typical Modes In Cavity Load

FIG. 1

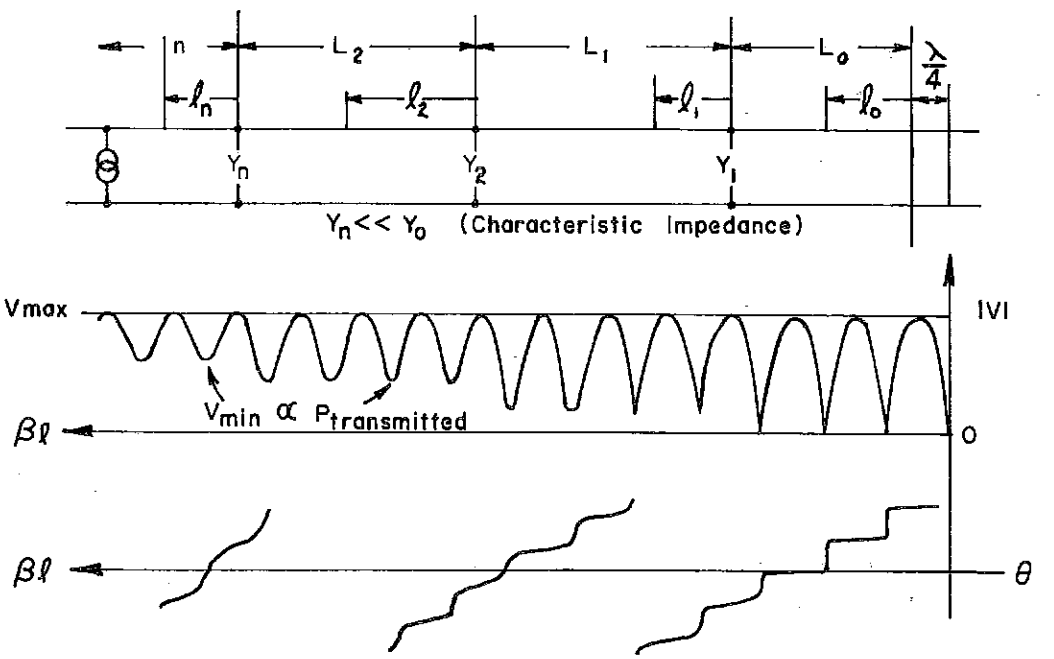
n
L2
L1
L0
λ/4
ℓn
ℓ2
ℓ1
ℓ0
Yn
Y2
Y1
Yn<< Y0 (Characteristic Impedance)
Vmax
|V|
Vmin ∝ Ptransmitted
βℓ
0
βℓ
θ

FIG. 2

Also we require that $\beta = n\pi(1 + \delta_o)$ where δ_o is a small quantity. Then

$$\sin\beta \cong \pm \delta_o n\pi$$

$$\cos\beta \cong \pm \left[1 - \frac{1}{2}(\delta_o n\pi)^2\right] .$$

The above equations then reduce to

$$\cosh \alpha_L \ell \cdot \cos \beta_L \ell = \left[1 - \frac{(\delta_o n\pi)^2}{2}\right] \left\{1 + \frac{G_m}{2Y_o} \cdot \alpha\ell\right\} - \delta_o n\pi \left\{\frac{G_m}{2Y_o} \; 2\delta_m Q_m\right\}$$

$$\sinh \alpha_L \ell \cdot \sin \beta_L \ell = \delta_o n\pi \left\{\alpha\ell + \frac{G_m}{2Y_o}\right\} + \left[1 - \frac{(\delta_o n\pi)^2}{2}\right] 2\delta_m Q_m \frac{G_m}{2Y_o} .$$

Solving these equations simultaneously will give values for α_L and β_L, the propagation coefficients for the loaded manifold.

I have not solved them. There are two cases of interest, that are easy to solve.

Let $\omega = \omega_o$ so that $\delta_o = 0$. Then the two equations become

$$\cosh \alpha_L \ell \cdot \cos \beta_L \ell \cong 1 + \frac{G_o}{2Y_o} \alpha\ell$$

$$\sinh \alpha_L \ell \cdot \sin \beta_L \ell \cong 0 .$$

The solutions are $\beta_L \ell = n\pi$ and $\alpha_L \ell \cong \sqrt{\frac{G_o}{Y_o} \alpha\ell}$.

Since $\beta_L \ell = n\pi$, the voltage at each E_{max} point differs from that at each other in phase by zero or π, and in amplitude by a factor

$$e^{\sqrt{\frac{G_o}{Y_o}\alpha\ell}\,M}$$

If $\frac{G_o}{Y_o}$ is a small number which we desire for other reasons and if the α of the transmission line is low which we naturally try to achieve, then the amplitudes are very nearly the same unless we allow the value of ℓ to be too large. Another way of putting this is that if we have a preconceived value that is acceptable,

$$e^{\sqrt{\frac{G_o}{Y_o}\alpha\ell}\,N}$$

will be limited to some value.

A generator can be introduced at any E_{max} point on the manifold, but the nearer the generator is to the loads the smaller the argument above will be, and the more tightly coupled the loads will be to the generator. If more than one generator is added, they are effectively in parallel (making sure that the sign of the phase is correct), and, if they act as current generators, will share the load depending on their drive. Figure 2 shows a section of a manifold with several loads and one generator.

I might explain that since the E_{max} are all locked together, and since $P_{transmitted} = \frac{V_{max}\, V_{min}}{2\, Z_o}$, then the value of V_{min} is proportional to the power transmitted at a given point on the manifold. If there is a plane of symmetry or end wall that no power flows past, $V_{min} = 0$, and V_{min} grows larger as one moves past each load point.

In practice each cavity will have its phase servoed to a reference line from the same master oscillator that drives the amplifiers. Then if the cavities do not wander too far from their correct resonant frequency, each cavity will have its fields locked in phase and in amplitude to each other cavity. If the cavities are not quite at resonance, the amplifiers must supply the reactive energy necessary to keep the cavities in phase. They will be able to do this because

1) the various load cavities should tend to average out the reactive energy required, and

2) in order to overdrive the linac in order to obtain fast rise time, the amplifiers must have considerable surplus of energy available, which can go to supply reactive energy.

An amplitude servo will be required to increase the drive so that beam loading can be supplied by the amplifier tubes. Probably it will be desirable to servo the phase of the drive line to the phase of the anode line, to minimize the losses in the amplifier tubes.

The immediate worry one has when one first sees this scheme is, "what about the other modes"? By going back to these original equations and looking at what happens near $\omega = \omega_o$ or $\delta_m = \delta_o$, the equations become

$$\cos \beta_L \ell \cong 1 - \frac{(\delta_o n \pi)^2}{2} \left[1 + \frac{2}{n\pi} \frac{G_o Q_o}{Y_o} \right]$$

$$\alpha_L \ell \cdot \sin \beta_L \ell \cong \delta_o n \pi \left[\alpha \ell + \frac{G_o}{Y_o} + \frac{2}{n\pi} \frac{G_o Q_o}{Y_o} \right] .$$

The solutions to these equations are

$$\beta_L \ell \cong \delta_o n \pi \left[1 + \frac{2}{n\pi} \frac{G_o Q_o}{Y_o} \right]^{1/2}$$

$$\alpha_L \ell \cong \alpha \ell + \frac{G_o}{Y_o} + \frac{2}{n\pi} \frac{G_o Q_o}{Y_o} .$$

See Fig. 3. Note the slope of the $\omega - \beta\ell$ curve and that there is a stop band adjacent to ω_1, the next cavity mode.

Analogous to the modes along the $\omega - \beta\ell$ curve for the π cavity (see Fig. 1), there will be modes along this $\omega - \beta\ell$ curve if the value Nn is too large. The limits of the frequency where this first permissible point can be found will vary between

$$\frac{1}{nN} < \delta_A < \frac{1}{nN \left[1 + \frac{2}{n\pi} \frac{Q_o G_o}{Y_o} \right]^{1/2}} \quad ; \quad \delta_A = \frac{\omega_A - \omega_o}{\omega_A}$$

depending where it falls on the $\omega - \beta\ell$ curve.

Next consider a long cavity in the π mode. Panofsky's formula says that the mode next to the operating frequency is given by $\delta_I = \frac{\lambda^2}{8 M^2 \ell_o^2}$ where $\ell_o = \beta_{particle} \frac{\lambda}{2}$. The total length

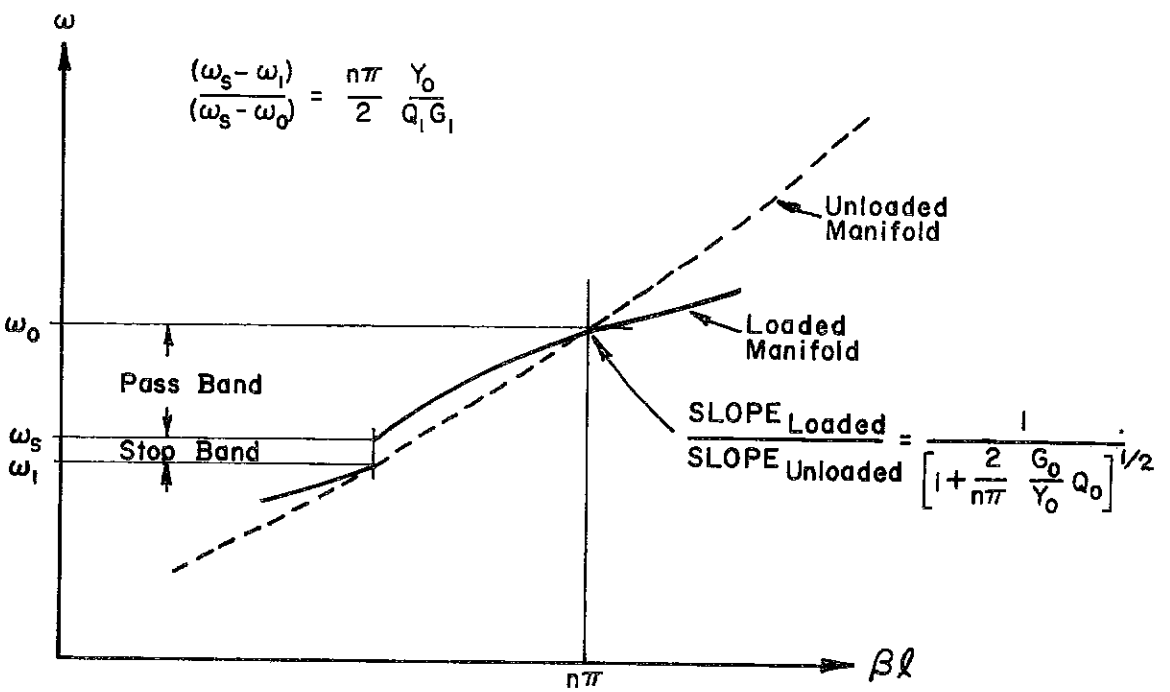
ω
$\frac{(\omega_s-\omega_1)}{(\omega_s-\omega_0)} = \frac{n\pi}{2}\frac{Y_0}{Q_1 G_1}$
Unloaded Manifold
Loaded Manifold
ω_0
Pass Band
ω_s
Stop Band
ω_1
$\frac{\text{SLOPE}_{\text{Loaded}}}{\text{SLOPE}_{\text{Unloaded}}} = \frac{1}{\left[1+\frac{2}{n\pi}\frac{G_0}{Y_0}Q_0\right]^{1/2}}$
$n\pi$
$\beta\ell$

FIG. 3

$\ell_T = M\ell_c$ and also equals $nN\frac{\lambda_g}{2}$, so that it can be written as $\delta_I = \frac{1}{2n^2N^2}\frac{\lambda^2}{\lambda_g^2}$. If the manifold is a coaxial line as it might well be at 200 Mc, then $\frac{\lambda}{\lambda_g} = 1$, and $\delta_I = \frac{1}{2n^2N^2}$. This is to be compared with δ_A which varies as the first power of nN.

Also note that if N = 1, it gives the value of ω_1 in Fig. 3.

RF PHASE AND AMPLITUDE CONTROL*

Robert A. Jameson
Los Alamos Scientific Laboratory, University of California
Los Alamos, New Mexico

Basic Specifications

From beam dynamics

Phase - Average tank phase, measured over a period of ~10 μsec, to remain within a $\pm 2^{\circ}$ square well around the reference phase.

Since the short-term phase instabilities will include random effects, the above specification must be redefined as a mean deviation such that a random phase jitter of Gaussian distribution remains in the $\pm 2^{\circ}$ square well some percentage of the time:

Percent of Time Within Square Well	σ
99%	0.8°
95%	1.0°
90%	1.2°

Amplitude - $\pm$ 2%

From power amplifier

The HPA (Coaxitron) has transit time phase shifts of the order of 2.5°/1% change in plate voltage. This indicates the necessity for amplitude control to less than 0.5%, if operating open loop.

The transit time problem is further complicated by the necessity of increasing of power output to match increasing beam loading as the beam is turned on. The effects of various load configurations on the amplifier are being studied to determine how great this effect is.

General Layout -- Figure 1

Comments

1. After initial setup, tanks n and n' are ganged together with sensing from one tank.

*Work performed under the auspices of the U. S. Atomic Energy Commission.

2. Both fast and slow phase shifters may be required, depending on range available from fast shifter. Survey of existing mechanical, ferroelectric and varactor phase shifters indicate fast phase control must be done at power levels like 10 watts CW or less.

Quotations have been received for development work on ferroelectric shifters capable of handling 100 W CW (1700 W at 6% duty), shifting $\pm 10^{o}$ in 1-2 μsec. This is already a development task--shifters capable of handling higher power levels would require major development.

Basic Control Loops - Block Diagrams--Figure 2

1. Coupling Effects

a. Major coupling from IPA and HPA plate voltage changes to phase of Coaxitron output, as mentioned earlier. Effect is nonlinear, given approximately by:

$$\text{Transit time, cathode to plate} \quad \frac{3\,dcg + dgp}{5.93 \times 10^{7}\sqrt{\frac{V_{po}}{10}}} \text{ sec.}$$

where dcg and dgp are cathode-to-grid and grid-plate distances in centimeters, and $\frac{V_{po}}{10} = V_p \text{ min} = V_g \text{ max.}$

b. Second-order couplings between amplitude and phase in tank. More on this later.

2. Other Nonlinearities

a. Phase comparator output proportional to the sine of the phase error.

b. Nonlinear phase shifter characteristics.

c. Tank behavior nonlinear for large signals.

3. The effect of beam loading on the loop must be included.

4. Basic Frequency Stability Requirements

It is interesting to note what frequency stability is required of a standard in order that the short-term stability of the standard itself does not introduce phase disturbances which exceed the specified tolerances. Assume that the characteristic time constant in the transfer function from the reference phase to the tank phase

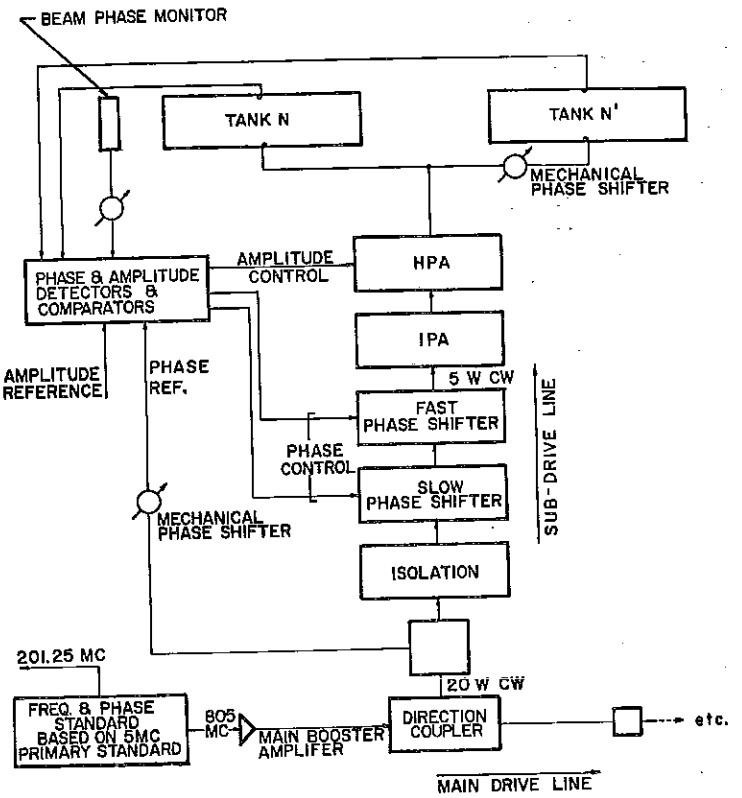

FIG. 1 **GENERAL LAYOUT**

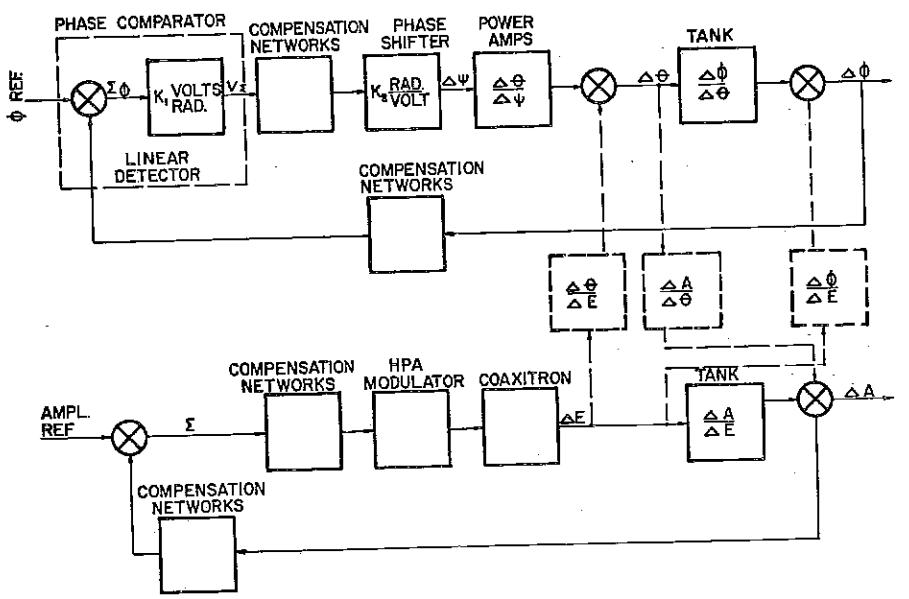

FIG. 2 **BASIC CONTROL LOOPS — BLOCK DIAGRAMS**

is that of the tank--in the order of 10 μsec. We are thus interested in phase perturbations that occur at rates of ~16 kc or less. The relation for frequency uncertainty due to a short-term phase instability is

$$\frac{\Delta f}{f} = \frac{\Delta\theta}{2\pi N}$$

where $\frac{\Delta\theta}{2\pi}$ = phase stability, proportional to noise-to-signal ratio

N = number of periods used for measurement

$$\frac{\Delta f}{f} = \frac{2^{o}}{360^{o} \times 800 \times 10^{6} \times 10^{-5}} = 7 \times 10^{-7} \text{ for 10 } \mu\text{sec measurement at 800 Mc.}$$

$$= \frac{7 \times 10^{-7}}{100} = 5 \times 10^{-9} \text{ for 10 } \mu\text{sec measurement at 5 Mc.}$$

Thus the primary frequency source which will provide the reference and drive signals must be very precise--in fact somewhat better than any source advertised at this date.

5. Measurement Techniques

The state-of-the-art nature of the stability requirements and some of the hardware promise difficulties in obtaining accurate and repeatable measurements.

Transfer Functions--Phase Loop

1. Phase Comparator

The simplest comparators use the rf signals directly, without converting to intermediate frequencies, etc. Because of their simplicity and reliability, this type is being considered in the early studies.

The comparator might thus be a quadrature mixer whose two outputs are linearly detected and differenced to form the error signal:

$$V_E = \pm k\sqrt{2}\ E_2 \sin \epsilon_\varphi$$

where k = detector efficiencies
E_1 = unknown signal
E_2 = reference signal
$E_1 \gg E_2$

$$\cong \pm k\sqrt{2}\ E_2\, \epsilon_\varphi \quad \text{for } \epsilon_\varphi \ll 1 .$$

2. Phase Shifter

At this time, it is proposed to use a varactor controlled phase shifter. Indications from industry are that these devices will soon be available at the desired power levels (~10 W CW), with phase shift ranges of greater than $\pm 90^{\circ}$. The phase shift vs. bias voltage characteristic is nonlinear, tending to saturate at the high end. A linear approximation may be used for small phase swings.

3. Power Amps

The chain is treated as a single resonant cavity, with the envelope responses characterized by an exponential rise to a step input; e.g.

$$\frac{\text{Output Amplitude}}{\text{Input Amplitude}} = \frac{\alpha}{s+\alpha}$$

$$\frac{\text{Output Phase}}{\text{Input Phase}} = \frac{\alpha}{s+\alpha} .$$

The phase transfer function is good for small signals only, becoming an inverse tangent function in the time domain for large signals, which introduces a nonlinearity.

4. Tank[1]

The tank transfer functions are derived from the transient analysis of a lumped parameter equivalent circuit for the accelerator cavity:

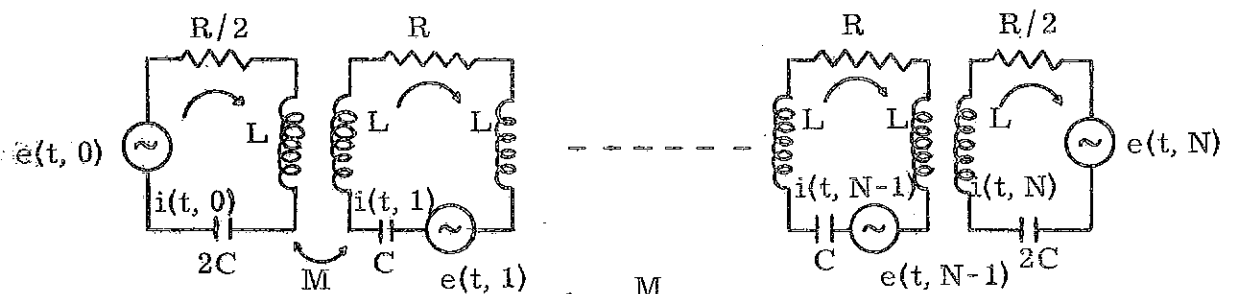

$$k = \frac{M}{L}$$

$$\omega_o = 1/\sqrt{2LC}$$

$$Q = 2\ \omega_o L/R$$

[1]These results are summarized from LASL Tech Memos P-11/RAJ-3 and P-11/RAJ-4.

The steady-state theory for this circuit has been developed by Nagle and Knapp--some results of this were given in Knapp's talk earlier.

The matrix equations for the circuit were written using Laplace transforms, transforming first with respect to time, and then, after using jump functions to express the repetitive nature of the cells, again with respect to the cell number. The solution of the homogeneous equation gives the characteristic equation and the n dependence. The inhomogeneous equation is then solved using an orthogonality relation based on the n dependence. The complete solution for the current in any cell is:

$$I(s,n) = \sum_{d=0}^{N} \sum_{q=0}^{N} \frac{2 \cos \frac{\pi n q}{N} \cos \frac{\pi d q}{N} W_1(q)\, s\, E(s,d)}{N\left(1+k\cos\frac{\pi q}{N}\right)\left[s^2 + \frac{\omega_o}{Q\left(1+k\cos\frac{\pi q}{N}\right)} s + \frac{\omega_o^2}{\left(1+k\cos\frac{\pi q}{N}\right)}\right]}$$

where d = index on rf drive, e.g. E (s, d) is a drive in the d^{th} cell
q = mode number
n = cell number
E (s, d) = drive term normalized by 1/2 L

$$W_1(q) = \frac{1}{\delta_{n,o} + \delta_{n,N} + 1} .$$

The transfer function with respect to a particular drive is

$$\frac{I(s,n)}{E(s,d)} = G(s,n,d) =$$

$$= \sum_{q=o}^{N} \frac{2 \cos \frac{\pi n q}{N} \cos \frac{\pi d q}{N} W_1(q)\, s}{N\left(1 + k \cos \frac{\pi q}{N}\right)\left[s^2 + \frac{\omega_o}{Q\left(1 + k \cos \frac{\pi q}{N}\right)} s + \frac{\omega_o^2}{1 + k \cos \frac{\pi q}{N}}\right]}$$

For example, the time response to a single sinusoidal drive in the d^{th} cell started at t = 0:

$$e(t,d) = u(t) \sin \omega t)$$

$$i(t,n) \cong \sum_{q=0}^{N} K_q \left[\sin(\omega t + \Phi_\omega) + e^{-\alpha_q t} \sin(\omega_q t + \Phi_{\omega_q})\right]$$

where

$$K_q = \frac{2\omega\,(|\text{Magnitude of drive}|)\,W_1(q)\cos\frac{\pi d q}{N}\cos\frac{\pi n q}{N}}{N\left(\left[\omega^2\left(1+k\cos\frac{\pi q}{N}\right)-\omega_o^2\right]^2+\left[\frac{\omega_o\omega}{Q}\right]^2\right)^{1/2}}$$

$$\Phi_\omega = \tan^{-1}\frac{-Q\left[\omega^2\left(1+k\cos\frac{\pi q}{N}\right)-\omega_o^2\right]}{\omega_o\,\omega}$$

$$\Phi_{\omega_q} = \tan^{-1}\frac{\sqrt{4Q^2\left(1+k\cos\frac{\pi q}{N}\right)-1}\left[\omega^2\left(1+k\cos\frac{\pi q}{N}\right)-\omega_o^2\right]}{-\left[\omega^2\left(1+k\cos\frac{\pi q}{N}\right)+\omega_o^2\right]}$$

$$\alpha_q = \frac{\omega_o}{2Q\left(1+k\cos\frac{\pi q}{N}\right)}$$

$$\omega_q = \frac{\omega_o}{\left(1+k\cos\frac{\pi q}{N}\right)}\sqrt{\left(1+k\cos\frac{\pi q}{N}\right)-\frac{1}{4Q^2}}$$

and the approximation results from retaining only the first term of the expansion of the factor $\dfrac{1}{\sqrt{1-\frac{1}{4Q^2}\left(1+k\cos\frac{\pi q}{N}\right)}}$ which modified the transient part of the solution.

Discussion

1. The steady-state solution says that the steady-state current at any particular drive frequency is the sum of components from each mode. If the drive is at a mode resonant frequency, that component has its maximum amplitude and is in phase with the drive. The other components are present because of the losses in the system. They are driven far from resonance and thus have small amplitudes and are about 90^o out of phase with the drive.

2. The natural frequencies and damping factors are apparent as the transient terms. The initial amplitudes are very nearly the same as for the corresponding steady-state term, and the initial angles are almost 180^o out of phase with the steady-state angles. The amplitude and phase variations during the transient period both die out with the same time constants.

3. The cos (dq/N) and cos (nq/N) terms add 180° to the phase when they are negative. Note that a drive in an end cell excites all the modes, while a drive in the center (N even) cell excites only the even numbered modes. Placing drives at node points to suppress various modes can be used effectively to increase the apparent "mode separation."

Envelope Responses

The transfer functions of real interest are those of the amplitude and phase envelopes:

From Input Amplitude to Output Amplitude
From Input Amplitude to Output Phase
From Input Phase to Output Phase
From Input Phase to Output Amplitude .

We write the response to the desired drive (in this case amplitude or phase step changes in a sinusoidal drive) as follows:

$$i\,(t,n) = \sum_{q=0}^{N} \mathcal{I}m \left\{ \left[a_q\,(t)\, e^{i\phi_q(t)} \right] \; e^{i\omega t} \right\}$$

where $a_q(t)$ = amplitude envelope function
$\phi_q(t)$ = phase envelope function .

Examples, the time response to a sinusoidal drive started at t = 0, used before:

$$i\,(t,n) = \sum_{q=0}^{N} \mathcal{I}m \left\{ K_q\, e^{i\omega t} \left[e^{i\Phi_\omega} + e^{-\alpha_q t}\, e^{i\left[(\omega_q-\omega)t + \Phi_{\omega_q}\right]} \right] \right\} .$$

Two types of approximation to the response are considered:

a. The components of the response are taken as the driven mode component and an out-of-phase component. The latter is found by first assuming that each off-resonance component is exactly $\pm\ 90^{\circ}$ out of phase with the driven mode component at steady state. The amplitude is then taken to be the vector sum of these steady-state amplitudes, and called ΣK_q. The damping term is taken to be that of the driven mode α_N for π-mode drive. The beat frequency $\beta = \omega_q - \omega$ is taken to be that produced by the

nearest mode frequency to the drive frequency that is present in the tank.

b. Response of the driven mode component only. The steady-state amplitude of this component for π mode drive is K_N.

The results for the first approximation are listed below, for π - mode drive. Simplification to the second follows by letting $\Sigma K_q = 0$. The exact responses have been found using a computer program. The approximate responses have been superimposed on the exact in Figs. 3 - 10.

1. Response to pulse turn-on (Large amplitude step).

$$a(t) = \left\{\left[K_N (1 - e^{-\alpha_N t}) - \Sigma K_q\, e^{-\alpha_N t} \sin \beta t\right]^2 + \left[\Sigma K_q\, (1 - e^{-\alpha_N t} \cos \beta t)^2\right]\right\}^{1/2}$$

$$\phi(t) = \tan^{-1} \frac{-\Sigma K_q\, (1 - e^{-\alpha_N t} \cos \beta t)}{K_N (1 - e^{-\alpha_N t}) - \Sigma K_q\, e^{-\alpha_N t} \sin \beta t}$$

2. Response to small amplitude step = k from steady state; $k \ll 1$:

$$a(t) = \sqrt{K_N^2 + (\Sigma K_q)^2}\left[1 + k\left(\frac{K_N^2 (1 - e^{-\alpha_N t}) - K_N \Sigma K_q\, e^{-\alpha_N t} \sin \beta t + (\Sigma K_q)^2 (1 - e^{-\alpha_N t} \cos \beta t)}{K_N^2 + (\Sigma K_q)^2}\right)\right]$$

$$\phi(t) = -\frac{\Sigma K_q}{K_N}\left[1 + k\, e^{-\alpha_N t} (1 - \cos \beta t)\right] ; \quad \frac{\Sigma K_q}{K_N} \ll 1$$

Small signal transfer functions:

$$\frac{\Delta A(s)}{\Delta E(s)} = \frac{\alpha_N \sqrt{K_N^2 + (\Sigma K_q)^2}}{S + \alpha_N} - \frac{\Sigma K_q\, \beta S}{(S + \alpha_N)^2 + \beta^2}$$

$$\frac{\Delta \phi(s)}{\Delta E(s)} = -\frac{\Sigma K_q}{K_N}\left[\frac{\beta^2 S}{(S + \alpha_N)\left[(S + \alpha_N)^2 + \beta^2\right]}\right]$$

3. Response to step phase change of φ radius from steady state:

$$a(t) = \Big\{ K_N^2 \left[1 - 2\, e^{-\alpha_N t} (1 - \cos\varphi)(1 - e^{-\alpha_N t}) \right] + 2 K_N \Sigma Kq \left[(1 - \cos\varphi)\, e^{-\alpha_N t} (2\, e^{-\alpha_N t} - 1) \sin\beta t + \sin e^{-\alpha_N t} (1 - \cos\beta t) \right] + (\Sigma Kq)^2 \left[1 + 2\, e^{-\alpha_N t} (\sin\varphi \sin\beta t - (1 - \cos\varphi)\cos\beta t) + 2 (1 - \cos\varphi)\, e^{-2\alpha_N t} \right] \Big\}^{1/2}$$

$$\phi(t) = \tan^{-1} \frac{K_N \left[(1 - e^{-\alpha_N t}) \sin\varphi \right] - \Sigma Kq \left[\cos\varphi + e^{-\alpha_N t} ((1 - \cos\varphi)\cos\beta t + \sin\varphi \sin\beta t) \right]}{K_N \left[\cos\varphi + e^{-\alpha_N t} (1 - \cos\varphi) \right] + \Sigma Kq \left[\sin\varphi + e^{-\alpha_N t} ((1 - \cos\varphi)\sin\beta t - \sin\varphi \cos\beta t) \right]}$$

Small signal transfer functions:

$$\frac{\Delta A(S)}{\Delta\theta(S)} = \frac{K_N \Sigma Kq}{\sqrt{K_N^2 + (\Sigma Kq)^2}} \left[\frac{\beta^2 S}{(S + \alpha_N)\left[(S + \alpha_N)^2 + \beta^2 \right]} \right]$$

$$\frac{\Delta\phi(S)}{\Delta\theta(S)} = \frac{\alpha_N}{S + \alpha_N} - \frac{\Sigma Kq}{K_N} \frac{\beta S}{(S + \alpha_N)^2 + \beta^2}$$

KEANE: This is a very nice piece of work. One comment; you did not take into consideration the response for each particular mode. As a matter of fact for what I was talking about, the next mode would be the TM_{011}. Because of my weak coupling to that mode, I had very slight scalloping. To the mode where I had strong coupling, namely the TM_{012}, the scalloping was much more pronounced.

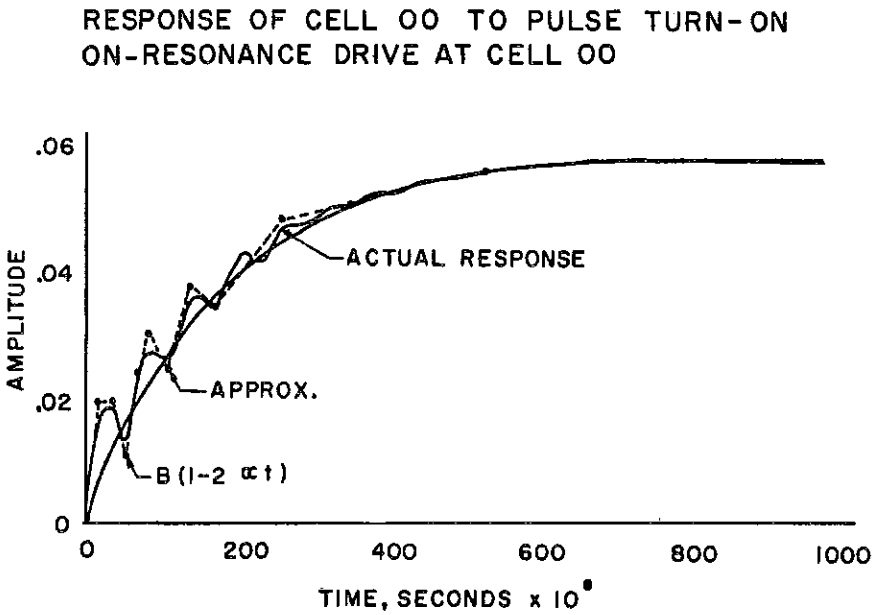
RESPONSE OF CELL 00 TO PULSE TURN-ON
ON-RESONANCE DRIVE AT CELL 00
.06
.04
.02
0
AMPLITUDE
ACTUAL RESPONSE
APPROX.
B(1-2 ∝t)
0
200
400
600
800
1000
TIME, SECONDS x 10⁶

FIG. 3

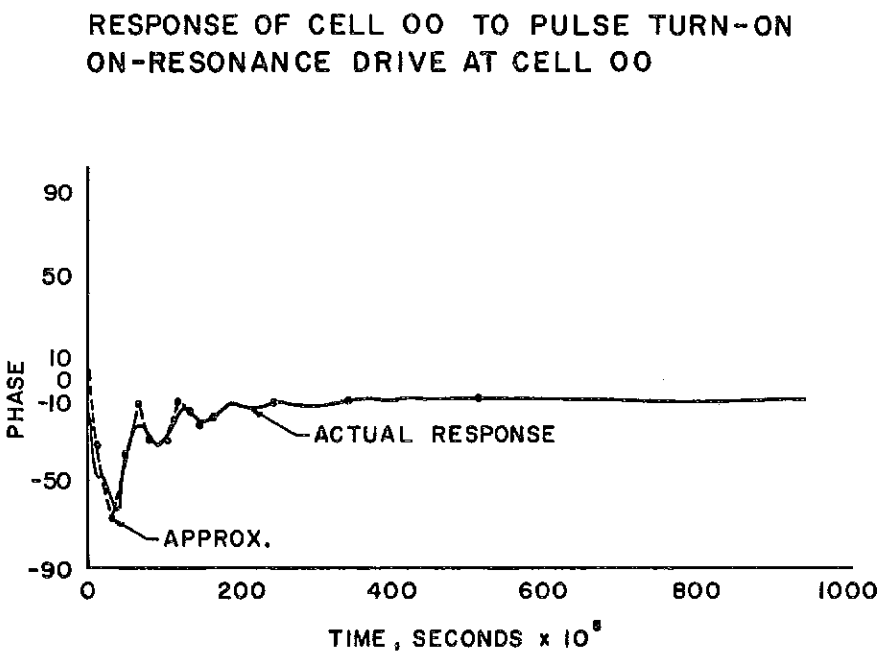
RESPONSE OF CELL 00 TO PULSE TURN-ON
ON-RESONANCE DRIVE AT CELL 00
90
50
10
0
-10
-50
-90
PHASE
ACTUAL RESPONSE
APPROX.
0
200
400
600
800
1000
TIME, SECONDS x 10⁶

FIG. 4

RESPONSE OF CELL 00 TO +2 PERCENT AMPLITUDE STEP APPLIED TO STEADY-STATE ON-RESONANCE DRIVE AT CELL 00

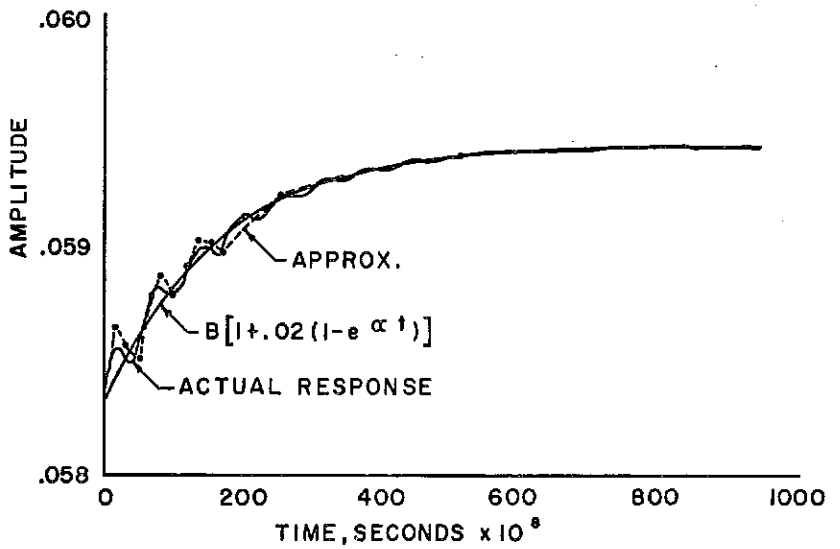

FIG. 5

RESPONSE OF CELL 00 TO +2 PERCENT AMPLITUDE STEP APPLIED TO STEADY-STATE ON-RESONANCE DRIVE AT CELL 00

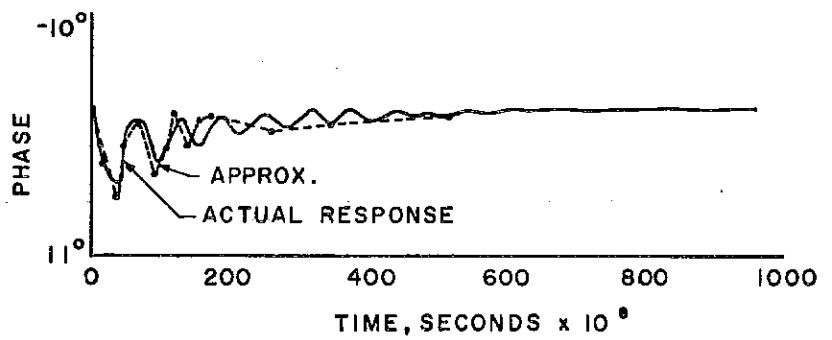

FIG. 6

RESPONSE OF CELL 00 TO 180° PHASE STEP APPLIED TO STEADY-STATE ON-RESONANCE DRIVE AT CELL 00

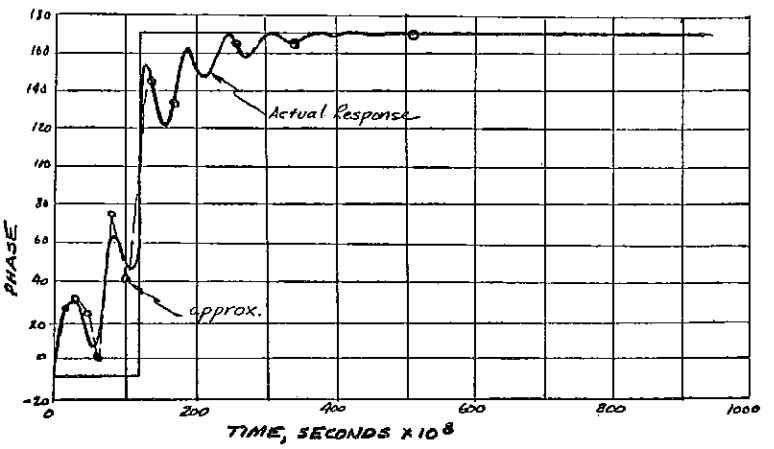

FIG. 7

RESPONSE OF CELL 00 TO 180° PHASE STEP APPLIED TO STEADY-STATE ON-RESONANCE DRIVE AT CELL 00

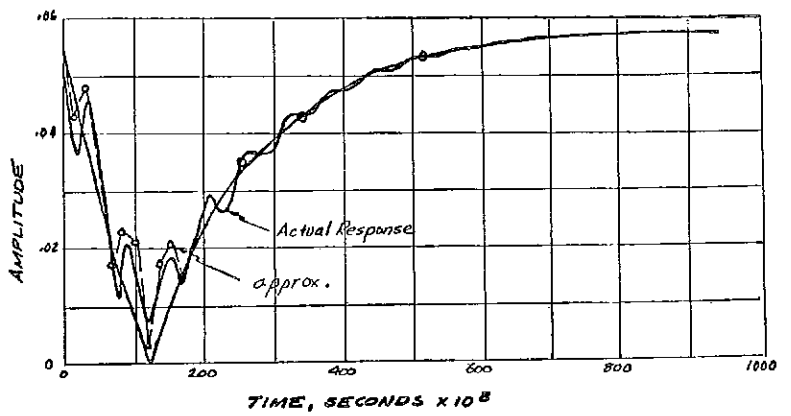

FIG. 8

RESPONSE OF CELL 00 TO +2 DEGREE
PHASE STEP APPLIED TO STEADY-STATE
ON-RESONANCE DRIVE AT CELL 00

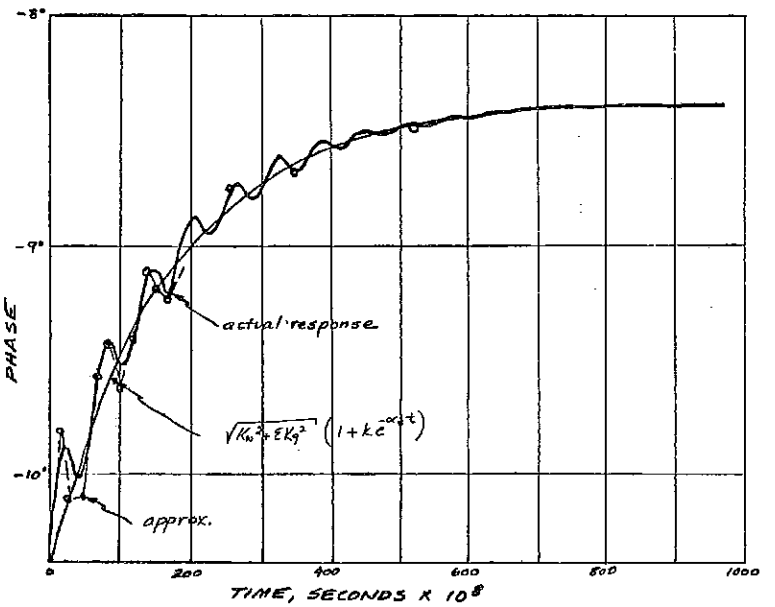

FIG. 9

RESPONSE OF CELL 00 TO +2 DEGREE
PHASE STEP APPLIED TO STEADY-STATE
ON-RESONANCE DRIVE AT CELL 00

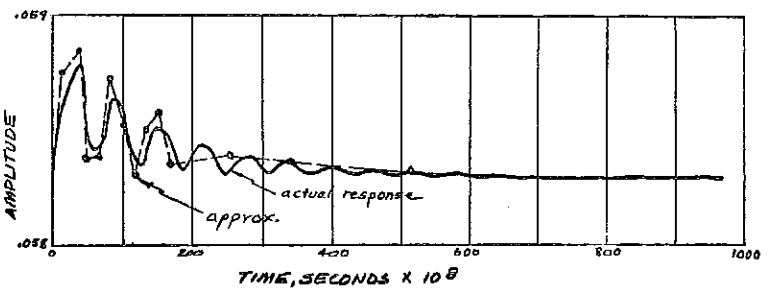

FIG. 10

JAMESON: That is not true. The answer for the current in any cell shows the dependence on the location of the drive, or drives, as well as the modal dependence. It shows that if you pick the right place to drive, the mode separation problem becomes easier. For instance, at the center you don't excite any of the odd number modes; you excite only the even number modes. So that helps you out by a factor two.

VOELKER: I want to mention our experience on the HILAC. We had two tanks coupled together with a coupling line and the scallop was directly related to the difference in frequency between the two cavities so that we used this as a rough tuning. When we took off the coupling line and began to drive from a separate amplifier, we found that we no longer had phase lock; we had as much as 10^{o} between the two tanks during the pulse. On some experiments the beam would go away during the early part of the pulse. In the last few months we have put in a phase servo with a veractor in a low level stage and have reduced the phase shift from about 10^{o} to 2^{o} .

JAMESON: You do have to take into account the fact that these other modes are there even though the effect is very small. Below is a picture of output from an 11-cell iris-loaded tank, which we drove at signal level frequencies. That is the input pulse on the upper left-hand corner. Then I used the sampling scope to look at the output of the tank in the various cells of the tank. This allows us to look at the rf directly and you can see the scallops that arise. This tank has a Q of 8300, a coupling of 2%, N was equal to 10 in the theory, and it was driven at the center. It shows quite well what the effect is. We also drove at the end of the same tank, and in the cells furthest away from the drive we observed, at the turn-off of the pulse, the pip where the energy actually goes up for an instant before it comes back down. Jim Leiss mentioned this yesterday.

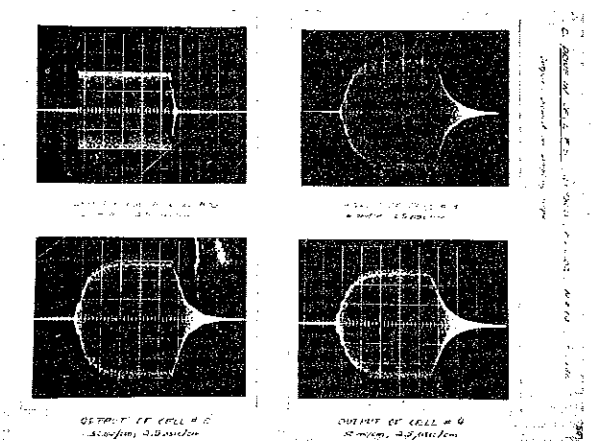

RECHARGING LARGE CAPACITOR BANKS

H. R. Shaylor
Brookhaven National Laboratory

The power bill for a large linac such as that proposed for the AGS conversion would be in the order of $100,000 per year. This is for an 0.6 msec pulse length and 30 pps, and an 8,000 hour year. It also assumes fairly high efficiency in the rf power stages. A typical "meson factory" would involve a power bill ten times as great.

A simple method of recharging a modulator condenser bank or storage line from zero volts to a given voltage would be to use a standard dc power supply and a series resistance to limit the current. Such a circuit would dissipate as much energy in the resistance as it supplied to the condenser bank, and the power bill would then be doubled.

Clearly then it is very worthwhile to design condenser recharging circuits with view to achieving a high recharge efficiency, any improvement of a few per cent or more will be significant.

The modulator energy storage system usually takes the form either of a delay line or a single capacitor bank. After considering the alternatives it was decided that the single capacitor bank is the most suitable alternative when (a) the pulse length was too long to permit the use of a pulse transformer, and (b) it was necessary to modulate the dc plate voltage on the rf amplifier in order to control the rf amplitude in the linac tank, (c) the rf power amplifier was some sort of triode with a dc plate voltage around 30 kV. The reasons for this choice will not be enumerated here. Further practical considerations show that the optimum choice of capacitor bank size is not one which stores twice the energy delivered to the load, although this is the smallest bank in terms of energy stored. A capacitor bank that droops about 10% during the discharge, and stores about five times the energy delivered to the load is a better choice.

Recharge Analysis

The basic circuit upon which the analysis has been made is shown in the circuit diagram:

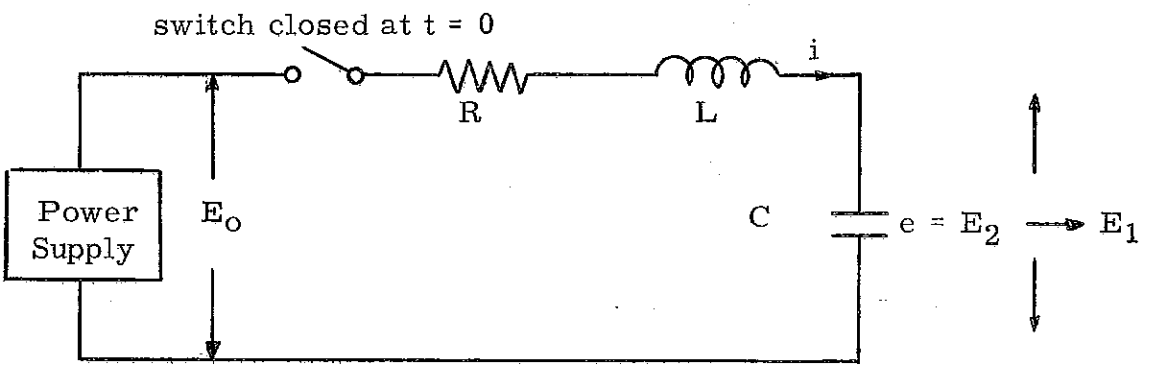

Circuit Diagram

The condenser is discharged by the load circuit (not shown) to voltage E_2. The recharge is effected by closing the switch at time t = 0. A variable current i flows and the condenser voltage e rises from E_2 at t = 0 to E_1 at t = T. At time T the current flow is interrupted either by opening the switch, or by some other means. The power supply voltage is E_o, and the energy dissipated in the circuit from time 0 to time T is U_R.

Arrangement of formula

In order to show that the analysis is dependent only upon the relative values of L, C and R, the results have been normalized. The capacitor current i becomes a dimensionless quantity

$$n_i = \frac{i}{(E_1 - E_2)} \frac{T}{C} ,$$

the capacitor voltage e becomes

$$n_e = \frac{e - E_2}{E_1 - E_2}$$

and the energy dissipated in the resistance U_R becomes

$$N_R = \frac{U_R}{(E_o - E_1)^2} \quad \frac{2}{C} \quad .$$

The efficiency of the recharging circuit can be obtaine directly from N_R since

$$\frac{\text{Energy dissipated}}{\text{Energy supplied to capacitor}} = N_R \frac{E_1 - E_2}{E_1 + E_2}$$

Thus for a capacitor with 10% voltage droop during discharge, an N_R value of 1 will give a 5% loss.

The circuit has been analyzed for the values of energy dissipated in R (N_R), the maximum capacitor voltage (N_C), the peak charging current (N_m), and the charging current at the end of the recharge period (N_T). The latter current is significant since it determines the rate of change of condenser voltage at switchoff, and hence the time tolerance requirements for a given voltage accuracy.

The analysis falls naturally into two cases, one when Q is greater than one-half, and the other when it is less. In the $Q > 1/2$ case, were it not for the power supply rectifiers, the capacitor voltage would be a damped periodic function of time; however, the decrease in capacitor voltage after the first peak is accompanied by a reversal of the charging current, and the rectifiers cut off at this point leaving the capacitor charged to the peak voltage. Thus, if the circuit is not interrupted by the switch, the recharge period will be one-half of the ringing period, the current at this time will be zero, and the capacitor voltage will be greater than (or in the limit equal to) the recharge voltage. The formula relating to the $Q > 1/2$ case assumes that the charge is terminated by current reversal at the end of the first half cycle, and shown in the first summary table.

SUMMARY

$$Q = \frac{1}{R}\sqrt{\frac{L}{C}} > \frac{1}{2}$$

$$\frac{\pi}{T} = \sqrt{\frac{1}{LC} - \frac{R^2}{4L^2}} \qquad P = \sqrt{\frac{4L}{R^2C} - 1} = \sqrt{4Q^2 - 1}$$

$$n_i = \frac{\pi}{N_c}\left(\frac{1}{P^2} + 1\right) e^{\frac{-\pi}{P}\frac{t}{T}} \sin\frac{\pi t}{T}$$

$$i = \frac{(E_1 - E_2)C}{T}\, n_i \qquad N_T \equiv 0$$

$$n_e = \frac{1}{N_c}\left(1 - e^{\frac{-\pi}{P}\frac{t}{T}}\left(\cos\frac{\pi t}{T} + \frac{1}{P}\sin\frac{\pi t}{T}\right)\right) = \frac{e - E_2}{E_1 - E_2}$$

$$N_c = \frac{E_1 - E_2}{E_o - E_2} = 1 + e^{\frac{-\pi}{P}}$$

$$N_R = \frac{1}{N_c^2}\left(1 - e^{\frac{-2\pi}{P}}\right)$$

$$U_R = \frac{(E_1 - E_2)^2 C}{2}\, N_R$$

Here P is a function of Q, and T is defined as half the natural periodicity of the circuit.

N_T, the value of n_i at time T is zero. N_c is the recharge voltage ratio. Both current and voltage are damped trigonometrical functions of time. N_R is a function of P (and hence Q) only.

In the $Q < 1/2$ case the capacitor voltage rises asymptotically towards the recharging voltage, so the recharge period is assumed to be terminated after time T by opening the switch. Thus there is a finite current flowing at time T and the final capacitor voltage is always less than the recharge voltage. The formula relating to the $Q < 1/2$ case is shown in the second summary table.

In this case the recharge period T is not uniquely determined by Q and C as in the $Q > 1/2$ case, so the period has to be specified. It has been normalized (somewhat arbitrarily) as the quantity $V = \frac{T}{RC}$. S is a function of Q, chosen so as to avoid the use of complex notation. The other symbols used are similar to the $Q > 1/2$ case. N_T may be found by putting $t = T$ in the n_i formula.

The current and voltage are exponential functions of time, and N_R is a function of Q and T.

Recharging Power Supply

A practical power supply would not deliver a smooth dc voltage as assumed in the analysis, but a rectified ac voltage. However, such a supply would be at least six phase and the ripple would be less than 15%, so results calculated for the dc case would be reasonably accurate.

The power supply would also have a finite internal impedance (generally inductive) and this impedance will, of course, add to any external resistance and inductance in the circuit.

The exact relationship of the power supply transformer leakage inductance and resistance to those values found as source impedance in a complete multiphase power supply is not clear, but it is probable that a resistance that would account for the supply dc regulation in series with the leakage inductance per rectifier phase would give the correct value of source impedance.

SUMMARY

$$Q = \frac{1}{R}\sqrt{\frac{L}{C}} < \frac{1}{2}$$

$$V = \frac{T}{RC} \qquad S = \sqrt{1 - \frac{4L}{R^2C}} = \sqrt{1 - 4Q^2}$$

$$n_i = \frac{V}{N_c S}\left(e^{\frac{-2V}{(1+S)T}t} - e^{\frac{-2V}{(1-S)T}t}\right)$$

$$i = \frac{(E_1 - E_2)C}{T} n_i$$

$$n_e = \frac{1}{N_c}\left[1 + \left(\frac{1}{S} - 1\right)\frac{e}{2}^{\frac{-2V}{(1-S)T}t} - \left(\frac{1}{S} + 1\right)\frac{e}{2}^{\frac{-2V}{(1+S)T}t}\right] = \frac{e - E_2}{E_1 - E_2}$$

$$N_c = \frac{E_1 - E_2}{E_o - E_2} = \left[1 + \left(\frac{1}{S} - 1\right)\frac{e}{2}^{\frac{-2V}{(1-S)}} - \left(\frac{1}{S} + 1\right)\frac{e}{2}^{\frac{-2V}{(1+S)}}\right]$$

$$N_R = \frac{1}{N_c^2 S^2}\left[(1 - S^2)\, e^{\frac{-4V}{(1-S^2)}} - (1 + S)\frac{e}{2}^{\frac{-4V}{(1+S)}} - (1 - S)\frac{e}{2}^{\frac{-4V}{(1-S)}} + S^2\right]$$

$$U_R = \frac{(E_1 - E_2)^2 C}{2} N_R$$

Evaluation of Results

Since the evaluation of formula by inspection is a difficult mental exercise, it was decided to program the Brookhaven computer to plot out the results. Copies of these results are shown in the next few diagrams.

Figure 1 shows the variation of current and voltage with time for Q values of 0.7 and 5. The Q = 5 case shows the current as a sine curve and the voltage as a cosine curve. The Q = 0.7 case shows heavily damped versions of the same curves. Figure 2 shows N_c, the recharge voltage ratio; N_m, the peak to average current ratio; and N_R, the loss factor; varying with Q for the $Q > 1/2$ case.

For the $Q < 1/2$ case, Figures 3, 4 and 5 show the variation of current with time. They show Q values of 0.5 and 0.12, and T/RC values of 0.5, 1 and 3. Note that the definition of T is quite different from that in the $Q > 1/2$ case, so the values of $\frac{t}{T}$ in the two cases have no correspondence. It will be seen that as the recharge period $\frac{T}{RC}$ is made shorter, the Q = 0.12 curve shapes approach the simple RC exponentials.

For the $Q < 1/2$ case the values of N_c, N_T, N_R and N_m are shown as functions of T/RC rather than Q, since the recharge period is the more significant parameter. Figure 6 shows N_c and N_T, and Figure 7 shows N_R and N_m.

It may be seen from the plots that the dissipation value N_R is always greater than one for $Q < 1/2$, and less than one for $Q > 1/2$. Two further points may be seen in the $Q > 1/2$ case; with increasing Q the dissipation decreases toward zero, and the maximum current during the recharge period I_m decreases toward $\pi/2$. This would seem to indicate that the highest attainable Q is the ideal situation. However, with high Q values the N_C ratio tends toward 2, and this leads to an unstable recharge voltage in that when the capacitor bank is discharged to an unusually low voltage (e.g. because of a partial breakdown) then the bank is recharged to a higher voltage than normal. In the extreme case consider a bank which normally has a 10% droop and would require a recharge voltage E_o of about 95% of the maximum capacitor voltage E_1. If such a circuit were discharged to zero voltage then the capacitor bank would theoretically recharge to 1.9 times the normal maximum voltage, which could be very dangerous.

A practical compromise would seem to be a circuit designed to give a Q a little above 0.5, say 0.75. This would give a dissipation value of 0.9, which means a power loss of 4.7% during the recharge of a 10% droop;

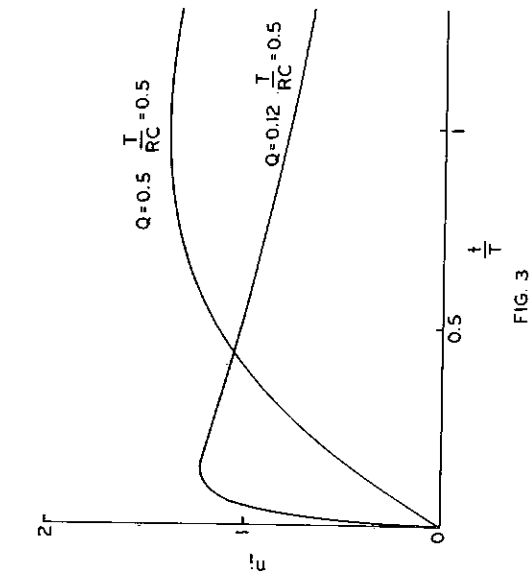

FIG. 3

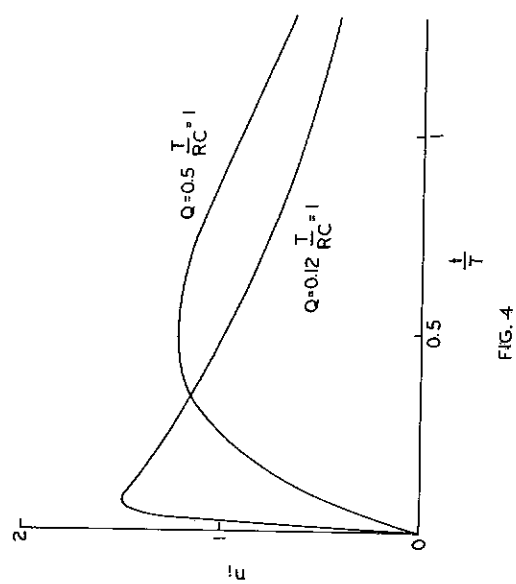

FIG. 4

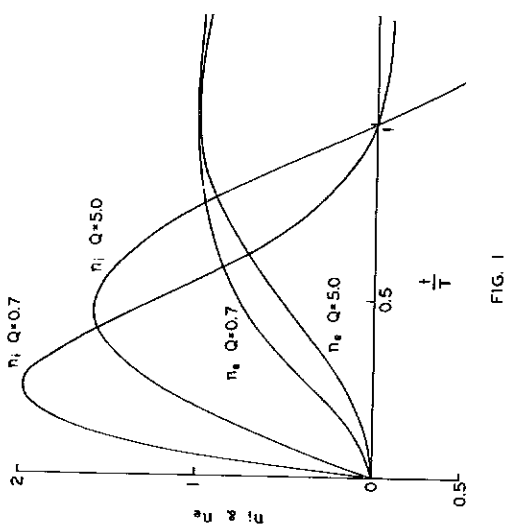

FIG. 1

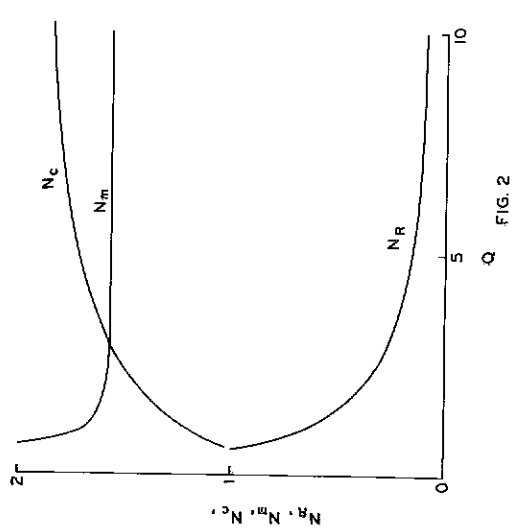

FIG. 2

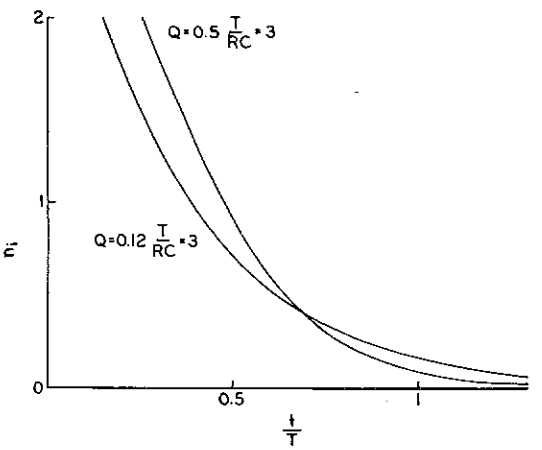

FIG. 5

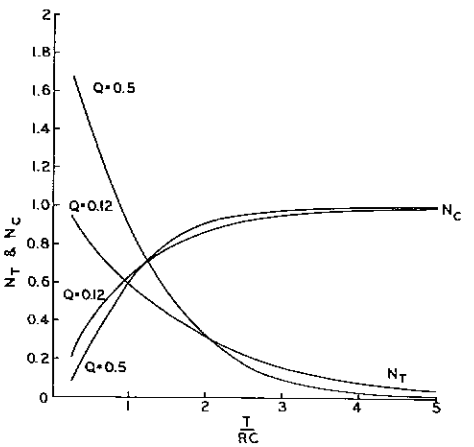

FIG.6

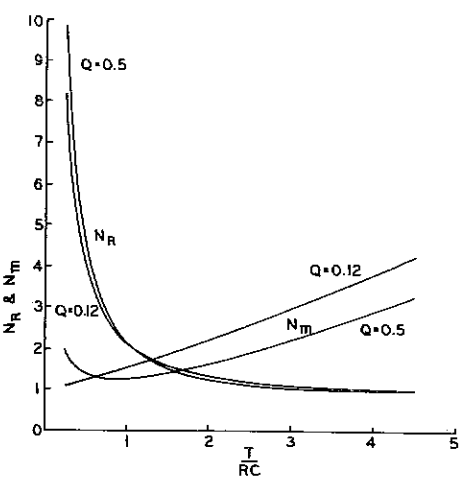

FIG. 7

and an N_C ratio of 1.06, so under conditions of complete discharge the condenser voltage would rise only 6% higher than normal. The maximum current for such a circuit would be 1.9 times the average current and the circuit would automatically cut off at zero current when the recharge is finished. Although the danger of over-volting the capacitors is now removed, there would still be the problem of high recharge current in the event of recharging from zero voltage, in which case the maximum current would tend to rise to 19 times the normal current. The recharge control equipment would have to have some provision for reducing such current in the event of a flashover or crowbar, and also at start-up times.

There seems to be no advantage in using the $Q < 1/2$ case, except on the grounds of simplicity, or perhaps to obtain a lower maximum recharge current at the expense of greater losses.

It is of interest to note that for the case of $Q < 1/2$ and $T/RC \leq 1$, N_R increases with increasing Q. This is because when the switch is opened with a finite current flowing, then the LI^2 energy in the inductance at that time is dissipated (presumably in the switching arc) and thus is lost to the circuit. When T/RC is less than one, the ratio of energy stored in the inductance to that dissipated in the resistance is such that increasing the Q also increases the total power loss.

Variable Resistance Recharging

Mr. J. F. Sheehan of Yale University has suggested a very interesting alternative to the LR current limiting network. This would replace the LR combination with a variable R, automatically controlled to keep the recharge current constant. The variable resistance would take the form of a hard tube.

The most useful case of this circuit would be when the recharge voltage E_o is equal to the maximum voltage E_1, and so the minimum variable resistance value is zero. This gives a dissipation value N_R of 1.0, so the power loss would be similar to the $Q = 0.75$ case outlined above. The maximum current ratio N_m is now the ideal value of 1.0, the N_C ratio is 1.0 and the current at the end of the charge is zero since there is no way for the capacitor voltage to rise above the recharge voltage.

Provided the current controlling action is automatic, the only effect of recharging a fully discharged bank would be to prolong the recharge period. The main disadvantage would be the complexity of such a circuit as compared with a passive LR combination.

Continuously Recharged Capacitor Systems

Some consideration has been given to the case which is often used; when recharge current is not zero at the start of the recharge period. This would occur if the switch was omitted in the $Q < 1/2$ case, or if the discharge repetition rate was greater than twice the ringing frequency in the $Q > 1/2$ case. An analysis of the recharge current in the latter case has been carried out.

The arrangement presents the difficulty that each recharge cycle depends upon the previous one, and there is no obvious indication as to how the current at the start of each recharge period will converge upon a steady value. Furthermore, this steady state will be upset by any irregularity in the pulsing rate. It is considered then that unless used with a $Q < 1/2$ and a large value of T/RC, in which case the initial recharge current will be very small, the continuous recharge system is likely to give less stable operation than one in which the recharge current is zero at the start of the recharge cycle. There would seem to be no real advantage of a continuous recharge circuit over one in which Q is a little greater than 1/2, and the recharge terminated by current reversal.

Conclusions

The optimum design of a circuit for recharging condenser banks of the type described above, would be one with a Q value about 0.75. If an active circuit is acceptable, then a constant current circuit would be preferable. It seems that a continuously recharged system would be less stable than one in which the recharge time is controlled.

WHEELER: If you look at the figure here, $I_m = 1.9$, and make a quick estimate of the peak power demand for a large installation, it turns out to be of the order of 60 MW for the instantaneous demand. This is reflected into the power line and the power companies will not be very happy about it. For this reason alone I think it may be necessary to go to a constant current-charging system.

STATUS REPORT ON THE COAXITRON DEVELOPMENT PROGRAM

G. W. Wheeler
Yale University

Several years ago, when the Yale Design Study Group proposed the use of 800 Mc/sec as the operating frequency for the waveguide section of the proton linac, it was recognized that suitable rf power sources were not available. Consideration was given immediately to this problem. It was generally agreed that negative grid triodes offer the best type of power source for proton linacs.

Work at RCA indicated that the "coaxitron" type of tube was promising. The coaxitron is a negative grid triode in which the resonant input and output circuits are contained within the vacuum envelope. The Yale and Los Alamos groups drew up and agreed on a set of performance specifications for an 800 Mc/sec coaxitron based on the estimated performance which RCA felt was reasonable. This has resulted in a fixed price contract between LASL and RCA for RCA to supply five prototype coaxitrons to meet certain performance specifications. The five tubes will be split between LASL and BNL for test and evaluation. The first tube is scheduled for delivery in November 1964 and then one tube per month.

The specifications for this tube are as follows. It is designated as the A15191.

Frequency (midband)	805 Mc/sec
Band width	15 Mc/sec
Gain	10 db (minimum)
Peak power output	1.25 MW
Pulse length	2.2 msec
Pulse rate	30 pps
Duty cycle	6.6%
Cathode	Thoriated tungsten filament
Output connector	Coax to waveguide transition
Input connector	1-5/8" Coax
Tuning adjustments	None
Operating mode	Zero bias, grounded grid
Plate output blocking capacitor	Internal
Plate voltage	$\sim$35 kV
Plate current	$\sim$100 A
Cathode area	$\sim$75 cm^2
Peak emission current	$\sim$300 A

The A15191 is scaled from the existing type A15038 which produces 5 MW peak power at 450 Mc/sec. At present, the A15191 design has progressed to the point where the cavity design has been verified by cold test measurements. The performance of the electronic circuitry has already been verified in other tubes. The grid-cathode structure is essentially identical with another coaxitron which exists. This is a 900 Mc/sec tube with the following demonstrated performance.

Frequency	~940 Mc/sec
Band width	~ 50 Mc/sec
Gain	11 db
Peak power output	1.4 MW
Pulse length	25 msec
Duty cycle	1%
Plate voltage	~35 kV
Plate current	~125 A
Cathode	Oxide Filament

MARTIN, J. H.: What is the average power output from the A15191?

WHEELER: Six per cent of 1-1/4 MW. This is hopefully conservative for the anode structure. The only experience we have is with the 400 Mc tube which does appear to be all right at that average power level.

VOELKER: You hope to get more gain than 10 db?

WHEELER: Yes. The more the better. They are already getting 11 db out of the 900 Mc/sec wide band tube and reducing the band width should improve the gain.

A POSSIBLE APPROACH TO THE INITIAL ADJUSTMENT OF A LONG LINAC

G. W. Wheeler and T. W. Ludlam
Yale University

In existing proton linacs, the maximum number of independent cavities is three. No serious problems have been encountered in adjusting the field level in each cavity and the relative phases of the cavities to the proper values. However, the initial adjustment of the multicavity linacs which are now being discussed[1] is a much more difficult problem. The reasons for this are clear. The effect of an improper adjustment at one point in the linac generally will not be observed until the beam has passed through several more cavities so that there is no direct way of determining the location of the improper adjustment. Furthermore, the adjustment of a particular cavity interacts with those for the following cavities. Initially, the setting of the quadrupole magnets is not very critical and it will be supposed that they can be set to the calculated values with sufficient accuracy to assure retention of the beam. Thus there are two major adjustments per cavity: the field level (E_o) in the cavity and its phase relative to the preceding cavity. Consequently, for the new linac injector proposed by the Brookhaven National Laboratory there are 122 adjustments.

There are two important stages in the adjustment. The first is an adjustment which is sufficiently good to assure the acceleration of the entire captured beam without the loss of particles at high energies. Numerical calculations indicate that if the field level is held to $\pm$ 1% and the intercavity phase to $\pm 2^{o}$, this situation will exist. The second stage of the adjustment involves reducing the beam energy spread and emittance to the smallest values which can be achieved. The success of these linacs particularly as injectors will be determined by the extent to which the adjustment errors can be reduced toward zero. It is generally agreed that the energy spread and emittance of a perfect linac would be entirely adequate for injection into a large synchrotron.

If all of the characteristics of the beam could be accurately measured at the end of each cavity, there would be no difficulty in adjustment. This unfortunately is impossible. The following quantities can be measured as indicated.

a) W and ΔW, the beam energy spread.

These quantities can be measured by magnetic analysis. Consequently the measurements can only be made at the injection point, at the

transition section and at the end of the accelerator. Beams of less than full energy may be drifted through the accelerator to the magnets without destroying the desired information. Accuracies of about 0.1% can be achieved. An alternative method involves time-of-flight techniques but requires considerable equipment and space.

b) I, the beam current.

Absolute measurement of the peak beam current is difficult but is not necessary for accelerator tune up. Relative measurements may be made with ease and considerable accuracy using beam current transformers. The transformer output is independent of energy and relative readings can be accurate to better than 1%. Thus if several transformers are calibrated relative to each other at one point, they may then be distributed along the accelerator and the differential outputs from them will be a sensitive measure of beam loss along the accelerator. However, the sensitivity of the transformers is only about 10 μA so that a peak beam current of at least 100 μA is needed for good measurements. Another sensitive method of detecting beam loss is to locate neutron or gamma detectors close to the structure to detect radiation due to lost beam. This system gives somewhat more detailed information as to the location of the beam loss.

c) The beam emittance.

The beam emittances can be fairly readily measured at low energies with considerable accuracy. At higher energies, the measurement can be done less readily. The measuring equipment is bulky and can be provided only at the injection point, at the transition and at the end of the accelerator. Some simpler systems which will give a rough measurement of x and y may be placed at more frequent intervals between cavities.

d) E_o, the average accelerating field in each cavity and φ_s, the synchronous phase.

An absolute measurement of E_o can be made to between 5 and 10% with carefully calibrated pickup loops in the cavities. A relative measurement of E_o between two cavities can probably be made to a few percent, and E_o may be held stable to 0.1%. There is no direct measurement of φ_s. If the energy gain in a cavity can be measured, then $E_o T \cos \varphi_s$ is known to the same accuracy. The transit time factor, T is fairly well known from cavity calculations. If E_o is decreased until $\varphi_s = 0$, it is possible in principle to measure the threshold value of E_o for which particles just gain the synchronous energy. This involves measuring a very small current and consequently has limited accuracy.

e) $\Delta\varphi$, the phase spread of the bunch.

The phase spread of the bunch can best be determined from a knowledge of ΔW. The center of the phase bunch may be measured with poor accuracy by observing the phase of a small resonant cavity between the accelerating cavities. This cavity will be excited by the beam at a phase corresponding to the "center of gravity" of the bunch.

f) $\Delta\varphi'$, the phase difference between adjacent cavities.

The phase difference between two cavities can be measured absolutely to a few degrees. The design value can be calculated accurately. The setting can be held to better than 1^{o}.

The following general procedures will be followed in order to tune up the accelerator with a minimum of activation of the structure. Initially, short beam pulses and reduced repetition rate will be used. The peak beam current will be limited to about 100 μA to remove the beam loading problems from the first tune-up attempt. The drift tube section should be completely tuned up before a serious attempt is made to tune the waveguide section. All measurements of the output beam from the drift tube accelerator will be done in the transition region between the two sections.

In what follows, it will be assumed that the beam from the drift tube section of the linac has been adjusted for best quality and that the transverse focusing of the beam in the waveguide section is well enough adjusted so that all particles which are longitudinally stable will be radially stable. The following procedure is suggested as a possible method of adjusting the waveguide section of the linac. Very extensive numerical calculations are needed to demonstrate that the procedure will actually lead to the desired result. Some preliminary calculations have been made using a program[2] which treats only the longitudinal motion of the axial particle.

If the field level (E_o) in each cavity and the phase difference between cavities ($\Delta\varphi'$) are set by absolute measurements to the design values, it is to be expected that particles will be lost at various points along the accelerator because of the errors. However, if the size of the bucket in each cavity is substantially increased, the entire beam can be retained in spite of sizeable errors in $\Delta\varphi'$. Since the initial tune up will be carried out at low beam current, the amplifier output, which will ultimately be transferred to the beam, is available to increase E_o above the design value. Calculations have shown that if E_o is increased by 15%, the entire beam can be retained for errors in $\Delta\varphi'$ of $\pm 5^{o}$ or more.

Since the design value of E_o should be well below the sparking limit, a 15% increase in E_o is possible. This will increase the bucket width from about 77^o to about 115^o. Throughout this procedure, the beam current is carefully monitored at several points along the accelerator.

The next step is to gradually decrease E_o in the first cavity until a noticeable decrease in beam current occurs. It will be necessary at the same time to decrease E_o slightly in the next few cavities in order to prevent the recapture of the particles which have become unstable in the first cavity. When the bucket in the first cavity has been shrunk so that some particles are outside of the stable region in the first cavity, the setting of $\Delta\varphi'$ for the first cavity is varied to minimize the loss. Here, $\Delta\varphi'$ is the phase difference between the last 200 Mc/sec cavity and the first waveguide cavity. This centers the injected bunch optimally in the first cavity. Now, E_o in the first cavity can be increased by a calculated amount to the design value. This will only be approximate but the exact value is not important. It should be noted that changing E_o causes the bucket to expand or shrink around $\varphi = 0$ and not around φ_s. Consequently, the value of $\Delta\varphi'$ which was just determined is no longer correct. A reasonably good calculated correction can be set in $\Delta\varphi'$ because now we are making changes in the relative (rather than absolute) values of E_o and $\Delta\varphi'$ and this can be done with considerable accuracy for changes of this magnitude.

At this point, all but the first cavity are turned off and the energy gain of that cavity is measured. If the average energy gain does not correspond to the calculated value, the cavity field will have to be tipped to make it do so.

The whole procedure is then repeated for subsequent cavities in a sequential fashion. When measuring the beam current decrease due to shrinking the bucket in cavities near the high energy end, magnetic analysis of the output beam will be required to distinguish between particles which have become unstable and those which have not since all will emerge from the end of the accelerator.

Repeating this entire performance a second time should further improve the adjustment. Once values of E_o and $\Delta\varphi'$ have been established for each cavity, it is the job of the level and phase servos to hold them there.

Preliminary numerical calculations indicate that the phase errors can be reduced by this procedure on the first attempt. However, the measurement of beam loss is not extremely sensitive and it will be necessary to examine the beam quality in order to achieve better

adjustment. Nevertheless the procedure seems promising at first look and further computations will be carried out.

Once the whole accelerator has been tuned up in the unloaded condition, the beam current can be increased until the effects of beam loading are observed. The automatic level and phase control systems must be adjusted to maintain the correct settings. At each stage the necessary adjustments can be made until the full beam current is (hopefully) reached.

LEISS: In making this analysis, you have assumed that subsequent buckets are in the correct place. Now, if you have a systematic deviation of the location of the subsequent buckets, have you assured yourself that in fact you are not building in systematic errors which you are trying to satisfy rather than putting the beam where you would like it? It seems possible that there is a trap here. In other words, are you presupposing that the problem is already solved?

WHEELER: No, we have not presupposed a solution. It is true that we have used only random errors distributed about the correct value and have not looked at the effect of gross systematic errors. However, by increasing E_o by an amount which is greater than any reasonable systematic error we can assure ourselves that E_o is well above the design value. Our assumption of $\pm 5^o$ phase error would account for a systematic phase error up to that value. A systematic phase error larger than this could be troublesome but I think that the system is flexible enough to handle it. Let me emphasize that there is a lot more work to do before we fully understand how to apply this method of tune-up.

BLEWETT: I should think that if you have a gross systematic error, no beam will come out and you will say, "Ah ha, I have a systematic error", and will look for it.

WHEELER: Yes. I think that there are a number of ways that you can detect gross systematic errors before you turn on the beam which implies that such errors can be eliminated.

FEATHERSTONE: There are at least two possible methods of controlling the relative phase of the cavities in a long string of cavities. One is to refer all the cavities to a reference line and the other is to refer each cavity to the preceding one. Is there a preferred way of doing this when you consider the actual tune-up process?

WHEELER: Yes, I think there is although I am not sure which it is. My own opinion is that it is better to measure the phase directly between two adjacent cavities. In either case you can have a systematic error in the phase detector.

TAYLOR: For about 18 months, we have been trying to get a rather similar measurement to work but so far we have not gotten consistent results. We have tried the following measurements. You have the bunch coming from the first tank and then you collapse the bucket in the second tank until you trap only a small current. You define this as a threshold and then you raise the level a little and shift the phase of the second tank to get back to the threshold current. The lowest tank level achieved gives you approximately the $\varphi_S = 0$ level and then the other levels can be converted to the corresponding φ_S. Making certain assumptions, the result should be two straight lines ($\varphi_S = \varphi$ and $\varphi_S = \varphi/2$) and the intercepts give you the phase width of the bunch. We have tried this several times. The very first time, we got two straight lines which intercepted the axis and gave us a phase width which agreed quite well with simple theory. We repeated this later and got two more lines with different slopes which gave us different intercepts. We still think that there is some way to go before you can use this technique as a measurement for setting phases but I agree with you that it could be useful.

CARNE: I think that the success of this technique depends on the beam performing many phase oscillations in one tank.

WHEELER: This could be correct. We find from our numerical calculations that we must shrink the buckets in a group of about four tanks at a time in order to get a clear indication of particle loss. This corresponds to about one phase oscillation wavelength near 200 MeV.

DICKSON: One has to be careful about the detector used here. A current transformer will accept all energies. Some sort of threshold detector might be better.

WHEELER: When a particle becomes unstable in phase at an energy of about 300 MeV or more, it will emerge from the end of the accelerator, even though its energy is incorrect. Magnetic analysis can be used to determine when particles have not been fully accelerated, or one can use a threshold detector as you suggest.

TAYLOR: I want to point out that this setup problem may be with us in 5, 6 or 7 years but that in the meantime the methods of measuring beam properties may have advanced to the point where one can get all of the

information required for a rational setting up. It does make one wonder about the distance between the tanks and if there are some tricks that can be used such as changing the stability limit at the end of the previous tank, as Lapostolle has suggested, to allow a little more space between tanks. I think that this would pay off.

PERRY: It seems to me that one might start at the high energy end to measure the E field level and determine from the energy whether or not you are above the accelerating gradient and then go progressively up the line toward the front end to determine what accelerating gradient you must have.

WHEELER: I don't think you can learn much about the proper phase setting by this approach.

PERRY: This is true, but it seems to me that knowing this gradient to begin with before you start worrying about phase you have an easier job in the phasing problem. You know how high you have to go to get 15% above accelerating gradients, for example.

FEATHERSTONE: I wonder if Blewett's technique of using the upper tail of the fish as a rather precise probe could be adapted to this technique?

WHEELER: I think that it can be done and could be of additional help.

REFERENCES

1. See for example:
"Design of a High Current 200 MeV Proton Linear Accelerator," NIRL/R/55, RHEL, 3/64, p. 19.

"A Proposal for Increasing the Intensity of the Alternating Gradient Synchrotron at the Brookhaven National Laboratory", BNL 7956, 5/64, p. 153.

"A Final Report on the Design of a Very High Intensity Proton Linear Accelerator as a Meson Factory at an Energy of 750 MeV", Yale University Y-12, 9/64, p. 111-113.

2. G. W. Wheeler and T. W. Ludlam, Minutes of the Conference on Proton Linear Accelerators, Yale University, October 1963, p. 29.

RF SUPERCONDUCTIVITY MEASUREMENTS

J. M. Dickson
Rutherford High Energy Laboratory

The feasibility of designing a proton linear accelerator with superconducting cavities has been studied by A. P. Banford at the Rutherford Laboratory. The work has been mostly on the measurement of the surface resistivity of metals at 4.2°K, since it was realized that it was vital to this project that a workable means of producing large areas of superconducting surfaces had to be devised, and that nearly all the other problems were easy by comparison with this one with the notable exception of the problem of beam loading. The ideas formulated in the first papers on this subject were based on results obtained with small samples of pure metals. The rf measurement work has had two aims (1) to measure the surface resistivity of superconducting electroplated metals and of superconducting alloys and (2) to attempt to build a small superconducting resonant cavity with low surface resistance.

The rf measurements consisted of the measurement of the Q of resonant devices at 4.2°K and comparison of the results with Q of a dimensionally similar resonant device of copper measured at room temperature. The ratio of the two Q's gives the "improvement factor", which is the factor by which the rf power loss of a resonator would be reduced relative to a similar copper resonator. The approach has been to try to use plating or other techniques which would be applicable to large areas and not to try to relate the results to the physical state of the surface. Most of the work has been with simple $\lambda/4$ resonant lines in the form of a hairpin, weakly coupled to a pulsed rf source and a detector. The Q was estimated from the decay rate of the detected pulse. The result for several surfaces are as follows:

1. Lead, extrapolated onto copper with a standard commercial fluoborate solution, has given improvement factors up to 15,000 (the theoretical limit at 400 Mc/s is 40,000). Solid "Specpure" lead wire gave slightly worse results.

2. Solid niobium wire, after electropolishing, yielded improvement factors of up to 13,000.

3. Niobium deposited from Nb Cl_5 vapor, or electroplated from a molten salt gave results similar to (2) after electropolishing.

4. Inhomogeneous superconductors, such as Pb-Bi eutectic and Nb_3 Sn gave very poor improvement factors ($\sim$50). This result can be explained by the filamentary nature of such materials, which is of course not a disadvantage when dc superconductivity is required.

5. Homogeneous alloys, such as Nb-Zr and Mo-Re gave improvement factors of about 2000. This can be explained simply by the fact that their resistivities fall rapidly below the critical temperature, but change very slowly above it, in contrast to the behavior of elementary metals.

Thus there seemed to be grounds for believing that large surfaces of lead or niobium could be prepared with suitably low surface resistivities. Some measurements on dielectrics at 4.2°K showed that PTFE (teflon) was the least lossy material tested and that it had a tan δ of about 2.5×10^{-6}.

The type of resonant cavity chosen was a half-wave coaxial line, short circuited at each end and split perpendicular to the axis at the central current node. All the cavities were made by electroforming in copper and subsequent electroplating with lead. It was intended that these cavities should be used at high power and that current carrying joints would be tested, but all tests were in fact made at low power. Ten sets of tests were made but the best improvement factor measured was 2000, while all the others were less than 1000. Variations in plating techniques, ambient magnetic field, thermal contact and liquid helium level were all tried to attempt to eliminate the cause of the poor results. An improvement factor of 2000 would mean that a 50 MeV proton linac would have an rf dissipation of 1 kW. A 4.2°K refrigerator for such a machine would cost about £ 400,000.

To account for the poor results one can postulate a residual resistivity to represent the unexpected extra losses, which can occur due to losses at joints, radiation through holes, etc. It can also include losses due to uncoated areas and parts of the surface held in the normal state magnetically or (unlikely) thermally. These areas would have an rf loss at 400 Mc/s about 4000 times larger than the ideal superconducting surface and if they totaled $1/200^{th}$ of the resonantor surface, the improvement factor would be reduced from the ideal 40,000 to the 2000 found experimentally. This degree of imperfection might also be expected to apply to the hairpin measurements, but it does not appear to do so. However, only the best results with hairpins have been quoted and some poor results ($\sim$4000) have been obtained with electroplated lead hairpins. Perhaps there is a statistical factor, which favors small surface areas.

These results can be compared with those obtained by other laboratories. At CERN Sussini using 260 Mc/s capacity loaded $\lambda/4$ coaxial resonators has never obtained improvement factors greater than 2000 to 3000 with lead and niobium. At Newcastle University Armitage using open ended 300 and 600 Mc/s $\lambda/2$ coaxial resonators has not exceeded an improvement factor of 40 yet with lead. At MIT Maxwell obtained an improvement factor of 50 with a 400 Mc/s coaxial resonator. At Stanford University Wilson obtained improvement factors of 2000 at 2856 Mc/s with a cavity which had a theoretical improvement factor of 3500. However, it must be noted that the normal (anomalous) surface resistivity scales as $f^{2/3}$ and the superconducting surface resistivity scales as f^2, so superconductivity of the whole surface is 14 times less important at this higher frequency. If $1/450^{th}$ of the surface was in the normal state, then the difference between 3500 and 2000 can be accounted for. Thus Wilson has been somewhat more successful in producing a homogeneous surface.

Other problems associated with a superconducting linear accelerator which have been studied include the effects of transient heat transfer and the relative merits of a conventional liquid nitrogen jacket and superinsulation. Thermal problems appear to be unimportant, even gross local overheating, whether steady or transient would not give trouble owing to the greatly enhanced diffusivity of metals at low temperatures. The extra cost of superinsulation would be offset by savings on liquid nitrogen after four years.

The rf tests have not been exhaustive and eventual success may yet be achieved by improved techniques and the expenditure of much time and effort. The results have, however, been sufficiently discouraging to inhibit further work on this problem at the Rutherford Laboratory, for the present.

SCHOPPER: I would like to comment on the beam loading problem. Gluckstern mentioned in the talk he gave here that according to his calculations, you get a limit of about 4 mA or several milliamperes, let us say.

DICKSON: Do you mean milliamperes or amperes?

SCHOPPER: Milliamperes instead of your 10 μA.

CARNE: Gluckstern gave 2 A as the limiting current for the new BNL injector for an estimated 1 M Ω/m for the deflecting mode, and, I think,

a frequency of 800 Mc/s. In view of the remarks of Walkinshaw, this current is probably of the order of 1 A. Now the limiting current varies inversely to shunt impedance of the deflecting mode, so that at a given frequency the limiting current will simply be reduced in ratio of the shunt impedances of the normal case and the superconducting case. Assuming that the deflecting mode exists at 400 Mc/s, where the improvement factor is 40,000, the limiting current will be down by the order of 40,000 from the limiting current of the normal situation, i.e. of the order of a few tens of microamps.

SCHOPPER: The main thing I want to point out is that you have an advantage in a superconducting linac in that you are working with CW which means that your peak current is equal to the average current. And so even 10 μA average current, I think, would not be too bad.

DICKSON: Well, one has the advantage as far as counting techniques are concerned. I think the advantage is probably a doubtful one in the case of CW beam loading. I don't think one is convinced that CW beam loading is any easier to cope with than pulse beam loading.

LEISS: I don't believe I can agree with this beam loading conclusion that you make. The beam loading is at a different frequency and it is not too hard to consider the possibility of a selective filter which keep the Q of that mode low and leaves the Q of the operating mode high. Admittedly with these leakage problems, it is nontrivial, but in principle it is probably no more difficult than many of the other problems involved. And so I just cannot see this limit.

CARNE: This selective loading may remove the deflecting mode, but in, for example, the disc-loaded guide, there are plenty of higher order modes which may cause deflection, and in CW operation there is time for them to build up. I doubt if one can load down all of them.

LEISS: I am sure that is true, but as you go higher and higher, you are almost guaranteed that the limiting currents go up. I agree there are many technical problems of a very formidable nature, but I don't believe that it is as discouraging as that.

DICKSON: Well, you see, the Rutherford Lab is in business for studying accelerators, not studying rf superconductivity as such. We feel that the present state of knowledge of the latter subject is sufficiently discouraging for us to abandon further work on a superconducting proton linac for the present. This is slightly changing the subject.

LEISS: But there are other people who are intensely interested in the ideas of superconducting machines.

DICKSON: Well, let them have a go.

ROWE: You were estimating what part of the surface area was a good surface in your cavities. Am I correct in thinking that what you did was make a copper cavity, say, and then cover it with lead, or were these cavities solid lead, for example?

DICKSON: The half-wave coaxial cavity we are talking about was one which was electroformed in copper over a plexiglass mold, in two halves, and then the mold was extracted and the inside of the copper cavity was electroplated. In all measurements a copper structure of the same physical dimensions was used for comparison and to find the improvement factor.

SCHOPPER: I want to mention another problem; that is the sparking. I think an advantage of a superconducting linac is that you can use high gradients. If you could go to higher gradients and somehow avoid sparking, then you could build a much shorter accelerator, which would be a saving.

DICKSON: O.K., but you put in two "ifs" which I do not think are really justified.

CARNE: You are suggesting that the sparking limit is a function of temperature. Now there may be something in this, but the sparking limit, we would like to say, is 17 MV per meter.

SCHOPPER: This was just my question. I was asking if anybody has any experience with sparking properties at low temperatures.

DICKSON: No, I haven't. There is one thing that can be said about sparking and it is just that you have still got the same stored energy in the cavity whether it is superconducting or not, because you have the same fields. So when you do get a spark, the same power will be dumped into the spark as in a normal machine, which is of the order of 50 Joules per 20 MeV cavity. 50 Joules might make a mark on the superconductor producing a normal area.

PERRY: The problem of sparking at low temperature, I think, is aggravated by the possibility of condensation of gasses on surfaces, which is an unknown quantity, I believe.

DICKSON: We have no data on this, but we recognize that is another problem.

DEUTERON ACCELERATION IN THE C. L. A. (CERN LINEAR ACCELERATOR)*

Th. Sluyters
Brookhaven National Laboratory

Acceleration of deuterons in the CLA using the 2π mode as employed for protons would require that the deuterons have the same velocity as the protons at every point along the linac structure. This would mean deuteron acceleration up to 100 MeV. This is far above any field level that is practically possible in the present machine. We can investigate the case where we use half the proton velocity in the 4π mode; so maintaining the same frequency of 202 Mc/s, the deuterons traverse one unit cell in two rf cycles. The alternating magnetic focusing properties are now identical for protons and deuterons, because the momenta of both particles are equal. Nonrelativistically speaking, this can be realized if the velocity of the deuteron is half the velocity of the proton; so the linac injection energy deuterons should be 270 keV instead of 540 keV for protons and linac final energy will be 25 MeV instead of 50 MeV for protons.

Approximately the energy gain for a synchronous particle per cell is:

$$W = e\bar{E}T\,L_n \cos \varphi_s$$

in which

e = electron charge

$\bar{E}$ = mean accelerating field

T = transit time factor

L_n = cell length

φ_s = synchronous phase angle.

Thus, for deuteron acceleration, the transit time factor T_D should be half the factor T_H for protons, if the other quantities are identical for both particles; if $T_D > 1/2\ T_H$, one has to diminish E and if $T_D < 1/2\ T_H$, one must look for means of increasing E.

---

*See: "A Theoretical and Experimental Comparison of Proton and Deuteron Acceleration in the CLA", CERN 64-22.

Courant (1962*) has calculated these ratios T_D/T_H for all gaps of the BLA, showing a reasonable drift tube geometry for deuteron acceleration.

Ratios of the energy gain per gap can be obtained by calculating the effective available voltage in the gaps for both particles, using theoretical values of the longitudinal electric field for the first cavity and experimental values for the second and third tanks:

$$R = \frac{\int_0^{\infty} E_x(x) \cos \frac{4\pi x}{\lambda} dx}{\int_0^{\infty} E_x(x) \cos \frac{2\pi x}{\lambda} dx} = \frac{\text{effective accelerating voltage for } D^+}{\text{effective accelerating voltage for } H^+}$$

These ratios were evaluated for the first and last gap of each tank (see Table I). The results show a less optimistic situation compared with Courant's results for the BLA and they suggest, for deuteron acceleration, appreciable tilting of the electric field in each cavity.

TABLE I

Cavity I		Cavity II		Cavity III	
Gap 1	Gap 42	Gap 1	Gap 41	Gap 1	Gap 27
0.2625	0.5137	0.6345	0.3598	0.7613	0.4942

A more extended investigation of axial motion has been made by calculating linac phase acceptances for both particles as a function of mean accelerating field and tilt using a mercury autocode program for proton acceleration written by A. Carne of the Rutherford National Laboratory. The approximations in this program are: symmetric gap fields, constant drift tube radius in each cell and acceleration independent of radial excursions.

The phase acceptances have been calculated as follows: at first the ideal tilt factors of the first cavity have been determined so that phase oscillations around a given phase angle are as small as possible

---

*E. D. Courant, "A Study of Possible Deuteron Acceleration", Conference on Linear Accelerators for High Energies, BNL, August, 1962.

($< 1^{o}$); then one searches for stable phase oscillations in the phase space. The tilt factors for the first cavity for synchronous deuteron acceleration compared to the tilt factors used for synchronous proton acceleration are shown in Fig. 1. Using these tilt factors, the linac acceptance for deuterons has been calculated for a stable phase angle of - 25 degrees, (see Fig. 2). On the basis of phase acceptance alone (so without radial loss), and a buncher peak voltage of 10 keV, deuterons are trapped for 80% between the initial phases 30^{o} and 314^{o}.

In practice, the flatteners in our cavities are fixed for synchronous proton acceleration and one can only impose from the outside a "linear" tilt gradient with tilt tuners positioned at the input and output end of each cavity. So it is more realistic to investigate deuteron acceptances with a linear change of electric field along the cavity.

Let us define acceptances in the energy phase plane as a product of the height of a bucket (stable energy range ΔE) and width of the bucket at mean injection energy (stable phase range $\Delta\varphi$), (see Fig. 3).

Figure 4 represents now proton and deuteron acceptances as a function of mean accelerating field for a set of negative tilts in the first cavity.*

The curves show that an increase in field level is necessary for deuteron acceleration in this drift tube structure and radio frequency and that tilt increase is more effective for deuterons than for protons. In practice, the increase in field level (which affects the whole cavity) is limited by radial losses, whereas the optimum tilt has not been reached.

The relation between acceptances, level and tilt for the second and third cavities are of less interest, because one can expect that the bunches can be captured in the respective buckets at appropriate level and/or tilt. Figures 5a and 5b show two typical deuteron buckets of the second cavity inside which an ellipse around an ideal deuteron bunch is drawn. Deuteron acceptances are here much less dependent on tilt compared with the first cavity.

Experimental deuteron acceleration has been investigated with a standard rf ion source assembly, producing deuteron beam currents up to 100 mA (10 μs pulse and 90% D^{+}). The beam performance for optimum machine conditions is given in Table II.

---

*Tilt is defined as $\frac{\Delta E}{E} \times 100\%$ in which ΔE is the rf electric field at output end minus the electric field at the input end of the cavity.

TABLE II

Preinjector	Source current	100 mA
	Beam current after column	60 mA
	Total emittance ($\frac{\text{area}}{\pi}$)	20 cm-mrad
	Linac input current	40 mA
	Injection energy	268 keV
Linac	Output current after first cavity (4.9 MeV)	7 mA
	Output current after second cavity (14.6 MeV)	7 mA
	Output current after third cavity (22.9 MeV)	7 mA
Inflector	Total beam emittance (90%)	< 3.0 cm-mrad
	Energy spread of 65% of the beam	< 100 keV

In the first cavity, approximately 17% of the beam was trapped and no beam losses occurred in the second and third ones. The final deuteron energy was 23 MeV with an energy spread of around 60 keV for 65% of the beam. The remaining part had a wide energy spread concentrated around an energy of 7.2 MeV.

There are two reasons for low trapping in the first cavity:

a) Axial phase losses. The range of the tilt tuners is limited to - 14%. Increase of rf level (affecting the whole cavity) should also increase the axial phase acceptance, however an optimum was reached, which finds its origin in stronger radial defocusing forces across the accelerating gaps for higher electrical field; this could not be compensated with the quadrupole focusing.

NOTE: For deuterons, always stronger focusing than for protons is necessary; this can be explained by comparing the radial force constant across the accelerating gaps; this constant is - 1/2 the axial force constant ω_φ^2, which is the square of the frequency of phase oscillations per unit length (Smith and Gluckstern, 1955*). The first cavity yields $\omega_\varphi(D^+)/\omega_\varphi(H^+) \approx 1.5$, so the defocusing forces for deuterons across the gaps are somewhat more than twice as large as for protons under equal machine conditions.

b) Radial losses. An important part of the beam is lost by improper matching at injection due to a smaller instantaneous transverse

*L. Smith and R. L. Gluckstern, Rev. Sci. Instr. 26, 220 (1955).

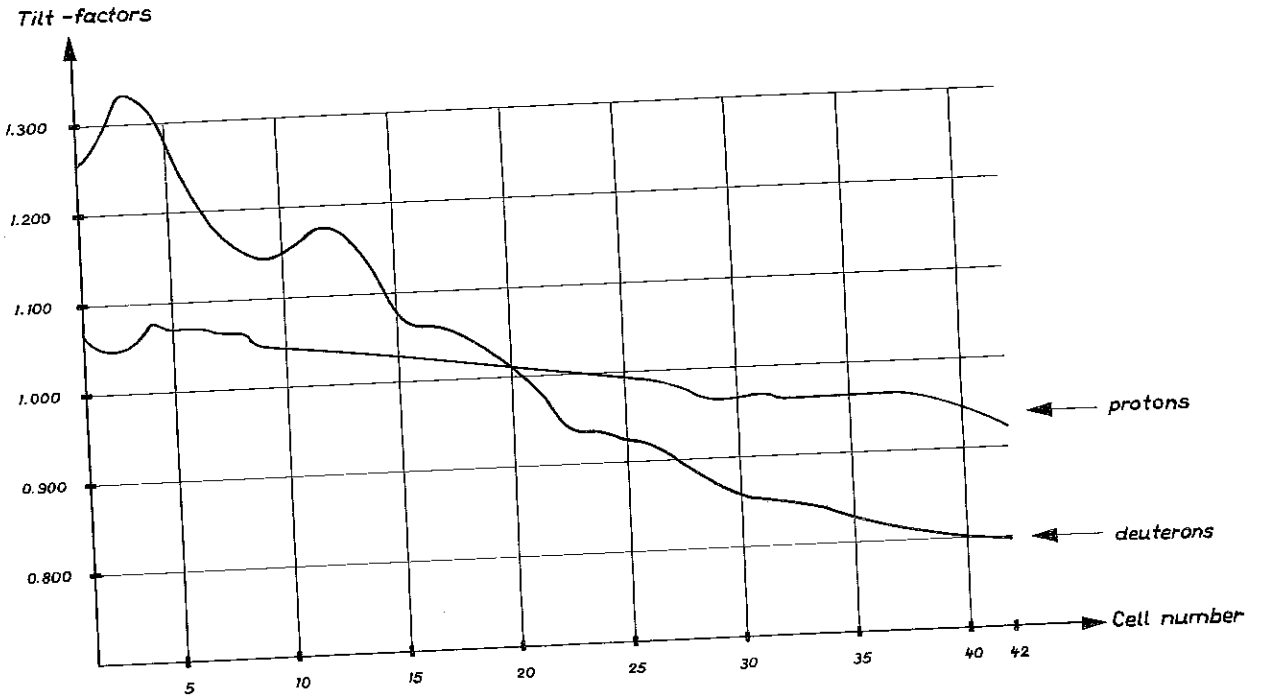

Fig. 1 Tilt factors for synchronous proton and deuteron acceleration in the first cavity.

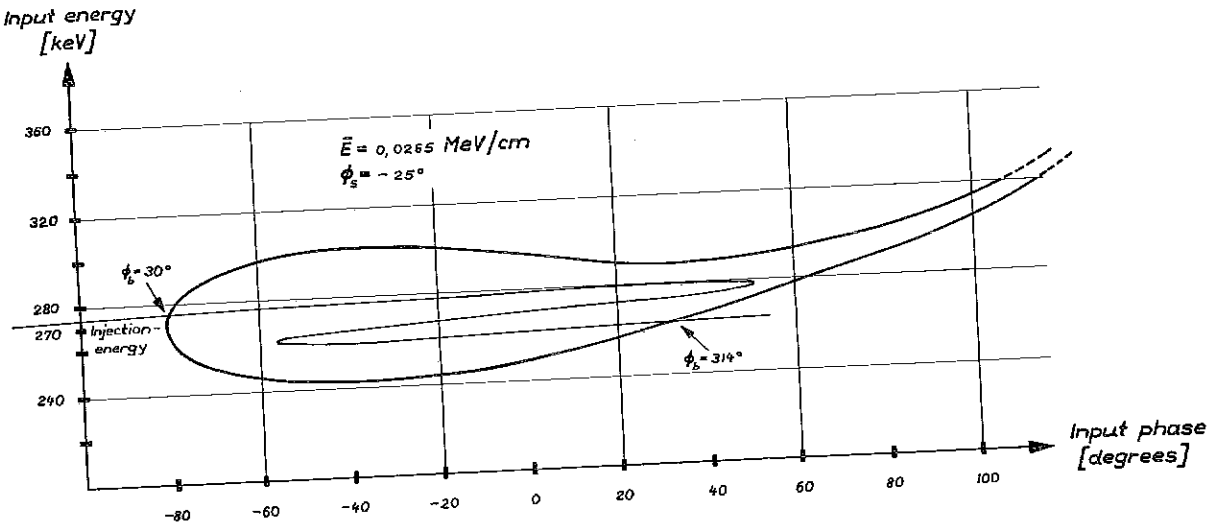

Fig. 2 Linac phase acceptance for deuterons with ideal tilt factors and a phase trapping curve for a buncher peak voltage of 10 keV. ϕ_b are particle phase angles at buncher position.

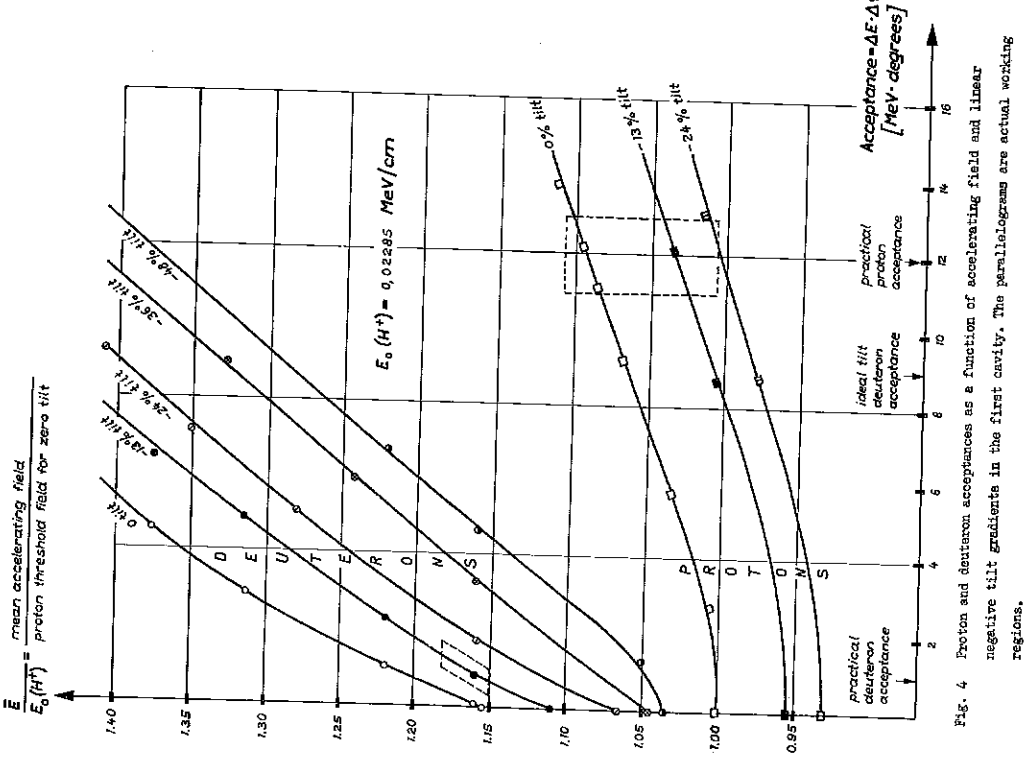

Fig. 4 Proton and deuteron acceptances as a function of accelerating field and linear negative tilt gradients in the first cavity. The parallelograms are actual working regions.

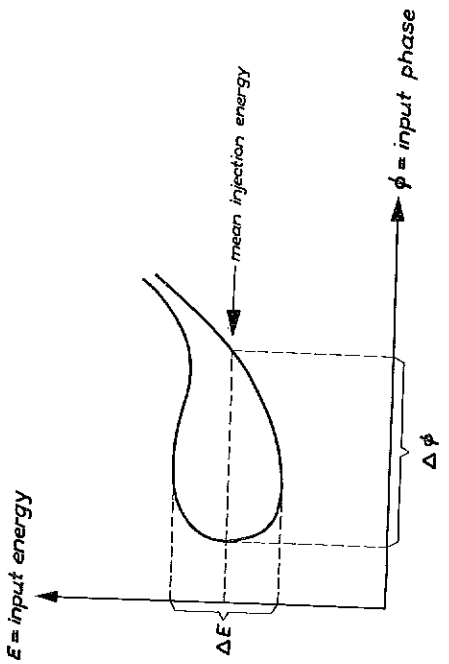

Fig. 3 Acceptance definition $\Delta E \cdot \Delta \phi$

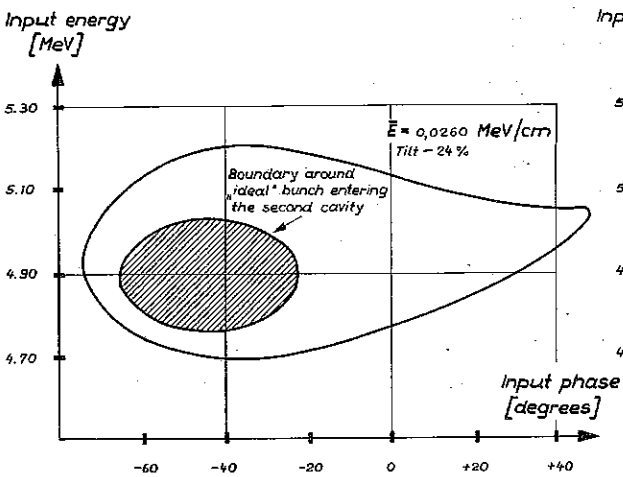

Fig. 5a Deuteron phase acceptance for the second cavity with positive tilt.

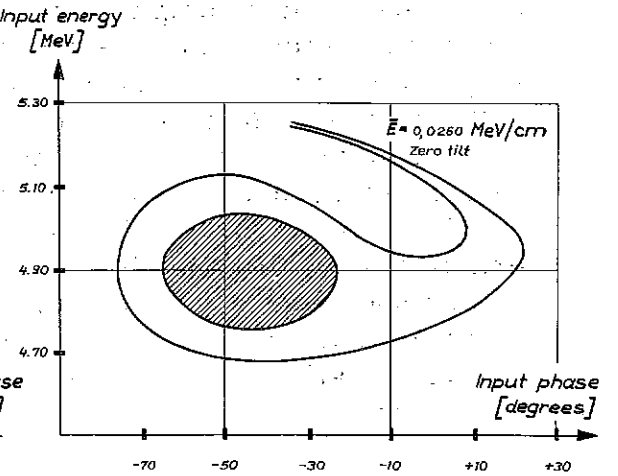

Fig. 5b Deuteron phase acceptance for the second cavity with flat field.

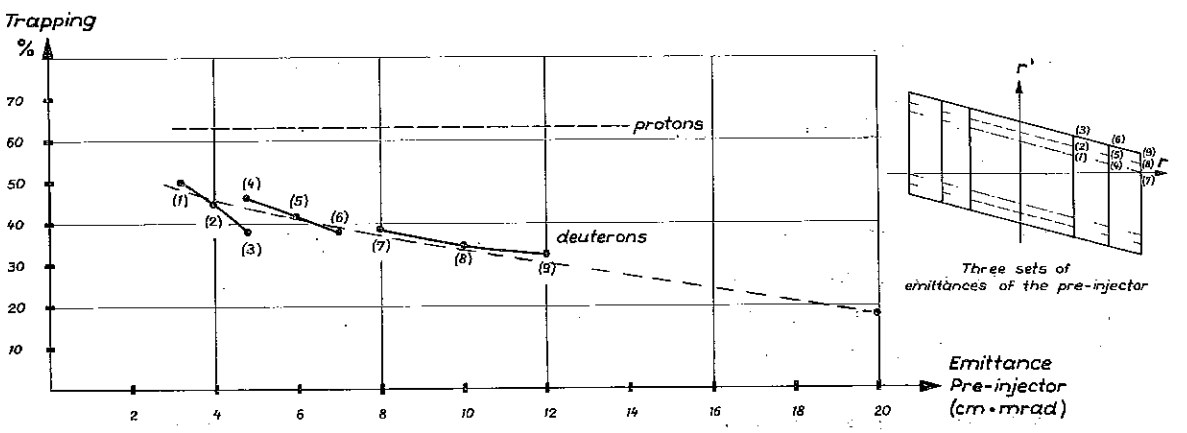

Fig. 6 Trapping for protons and deuterons as a function of injector emittances.

phase acceptance compared with protons. Therefore, smaller injector emittances should improve the trapping. Figure 6 shows an increase of trapping by a factor of three if the emittance diminishes to below 4.0 cm-mrad. At this injector emittance, the phase acceptance has been measured using optimum tilt and mean field conditions (see Fig. 7a). These results are compared with a theoretical phase acceptance. A buncher peak voltage of 7 keV suggests a theoretical trapping of 56%. In practice one measures 46%. The reasonable correspondence between theory and practice suggests that the present machine has an optimum trapping of around 50% for a preinjector emittance of around 4.0 cm-mrad; for this small emittance and low rf levels the radial focusing system is sufficient.

At the low energy side of the machine the radiation from deuteron interaction was 1 mrem/h or 7 n/cm^2/sec. This is a lower level than found from proton interaction with twice as much beam current. At the output end of the linac, a maximum dose rate of 20 mrem/h was measured.

SHAYLOR: I am very impressed with the fact that your ion source went well. We have a very elementary rf ion source in our Birmingham synchrotron and we started to accelerate deuterons about two years ago. Please don't ask me why. We had great trouble with the ion source; we had to get our witch doctor to say all sorts of interesting spells and to this day we don't really know why we cannot use commercial deuterium gas in it, but we have to use electrolyzed D_2O.

SLUYTERS: We have used commercial deuterium gas and normal operation of the source as if it were hydrogen gas except for the automatic flow control which was switched off.

SHAYLOR: I don't know why commercial gas would not work for us. Our injector is like your preinjector. We did not have trouble with the synchrotron, although it does not have beam control so we had to reprogram rf.

VAN STEENBERGEN: The emittance of the beam in the theoretical limit should be mass dependent. Was the emittance of the deuteron beam from the preinjector different from the corresponding emittance for an identical intensity of proton current?

SLUYTERS: Normalized to energy, the emittance was about twice as large as normal.

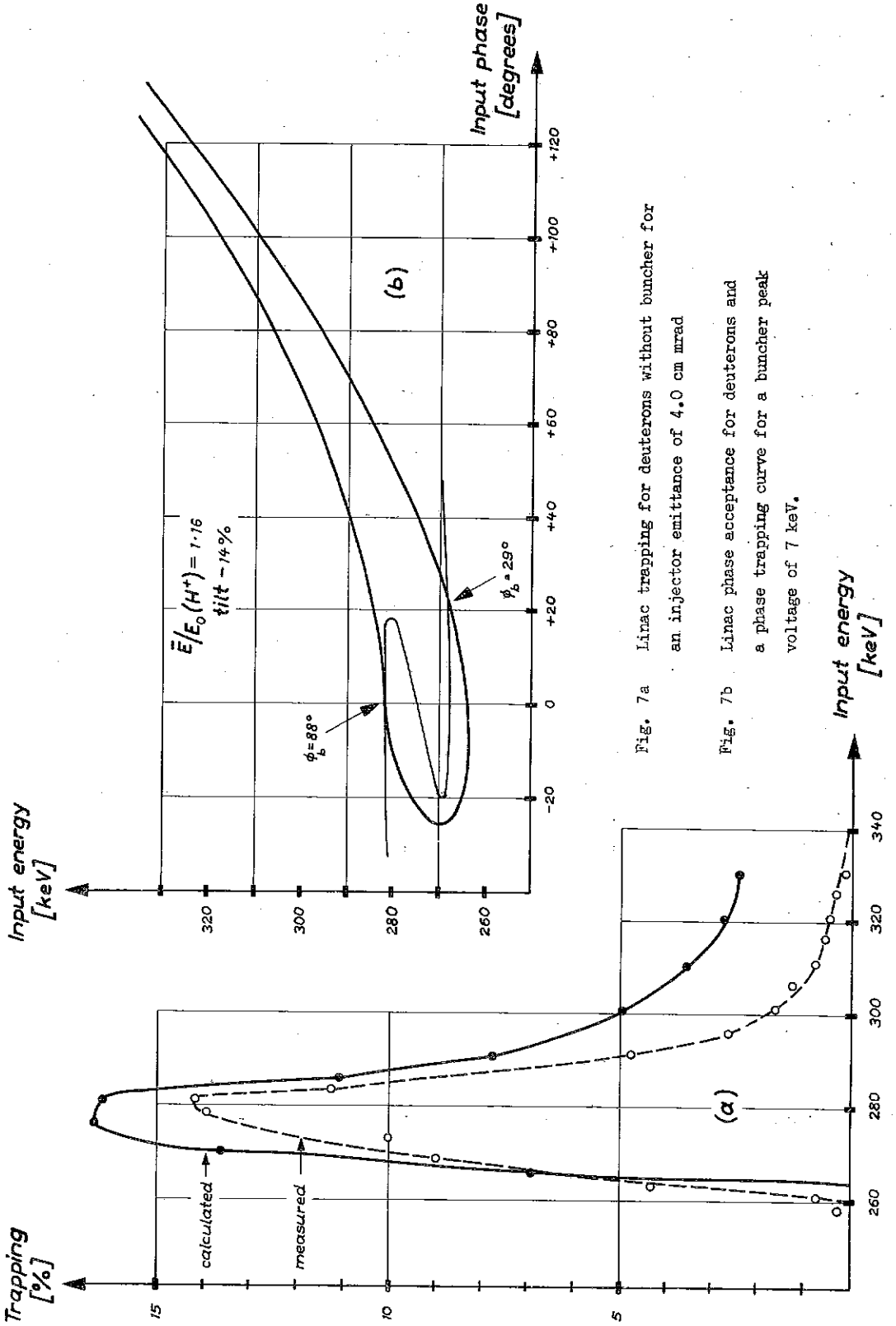

Fig. 7a Linac trapping for deuterons without buncher for an injector emittance of 4.0 cm mrad

Fig. 7b Linac phase acceptance for deuterons and a phase trapping curve for a buncher peak voltage of 7 keV.

VAN STEENBERGEN: The next question is regarding the longitudinal acceptance for deuterons. The calculated curve as shown here at a higher energy shows up the high energy acceptance tail in the fish diagram. The observed curve goes down to zero at the high energy end suggesting that you do not have a tail in the fish diagram.

SLUYTERS: There was a tail, but it was very low in intensity.

WADDELL: I was interested in your low background, when you were running the deuterons. I wonder, did you look for neutrons?

SLUYTER: Yes.

WADDELL: Then, does this not suggest that all of the loss was occurring essentially as one entered the machine, because certainly at energies of 4 or 5 MeV, the numbers of neutrons produced would have been very high.

BLEWETT: I think with protons the main capture loss is about 5 MeV, so with deuterons it should be about 1 MeV, should it not?

SLUYTERS: Yes. The main loss is during the first 10-15 drift tubes; this corresponds roughly with 1 MeV for deuteron acceleration. But, nevertheless, the background was much lower than we should expect.

FEATHERSTONE: I noticed in the first slide you showed us that the change of tilt required in going from accelerating protons to accelerating deuterons seemed to be in one sense in the first tank and in the opposite sense in the other two tanks. Do you use a constant g over ℓ ratio all the way through the machine as in the early Alvarez structures?

CARNE: In the first tank it is constant. Then the second two tanks have a varying g over ℓ .

FEATHERSTONE: So perhaps the fact that one had to change the tilt one way in the one tank and the other way in the other tanks is a reflection of the difference in design of the cavities.

SLUYTERS: In theory and in practice, the tilt has not an important influence on the capture as one can observe in Fig. 5.

THE ANL SECOND HARMONIC BUNCHER

W. Myers
Argonne National Laboratory

A multiple harmonic buncher system has been proposed for linacs by Dr. R. Perry[1] to improve the capture efficiency, or transmission, of the injected beam. With suitable choice of parameters, he has shown theoretically that it should be possible to secure an increase from 66% to 81% capture when using a second buncher operating at twice the linac frequency.

Such a buncher system has been designed and built, and this report will describe it briefly.

As is well known, a threefold improvement in capture over that provided normally by linac phase stability may be attained by bunching, i.e. applying a sinusoidal rf voltage across a gap where the rf phase is such that the synchronous particles undergo no energy change. Under these conditions, particles which differ in energy from the synchronous particles will be velocity modulated, and after traversal of a drift path, will arrive at the linac in a phase suitable for acceleration (see Fig. 1).

In order to increase the bunching efficiency still further one possibility is to replace the buncher sinusoid by a sawtooth wave of the form:

$$V = V_b \frac{\psi_b}{\pi} \qquad (-\pi \leq \psi_b \leq \pi) \qquad (1)$$

ψ_b = buncher phase

V_b = buncher gap voltage.

These two are plotted on the same scale in Fig. 2. It is seen that the sinusoid offers only a rough approximation to the optimum curve.

However, preliminary investigation of the nature of equipment required to generate a $\pm$ 20 kV sweep in 5 nsec, plus an ever faster retrace, indicated that an elaborate and expensive system would be needed if a sawtooth waveform were used.

Another possiblity would be to form a harmonic series approximation to the sawtooth, and this is the approach which we are developing. A total effective gap voltage V :

$$V = \sum_{1}^{K} \frac{(-1)^{n-1}}{n} \sin n\psi \qquad (2)$$

can be assembled across several individual buncher gaps, each one contributing a voltage term to the series. The net effect will be as if the total voltage were obtained in a single gap, since the individual gap separations will be small with respect to the drift distance. In Fig. 2b is shown the case where one buncher is running at the fundamental with another operating at the second harmonic. In Fig. 2d is the result when four gaps are driven at harmonically related frequencies. The gaps of such a system can be spaced closer together by locating the two higher frequency cavities inside the drift tubes of the others.

Theoretical phase space analyses to determine capture efficiencies have been made by plotting $\psi - \psi_s$ vs $W - W_s$ on an overlay of the ANL linac acceptance. The efficiency is found by dividing the absolute range of phase angle in radians enclosed in the linac acceptance by 2π (over total rf cycle). The equations relating the quantities plotted are for phase:

$$\psi - \psi_s = \psi_b - \frac{\psi_s T V_b}{2 V_o} \sum_{n=1}^{K} \frac{(-1)^{n-1}}{n} \sin n \psi_b \qquad (3)$$

and for energy:

$$W - W_s = e V_b T \sum_{n=1}^{K} \frac{(-1)^{n-1}}{n} \sin n \psi_b \qquad (4)$$

where

ψ	= particle phase	V_b	= buncher gap voltage
ψ_s	= linac synchronous phase	V_o	= potential of particle entering buncher
ψ_b	= particle phase at buncher	n	= order of harmonic
T	= buncher transit time factor		

Figure 3 shows the phase space diagram for a first plus second harmonic buncher system; the efficiency is about 81%. A similar plot for a four-harmonic buncher is shown in Fig. 4.

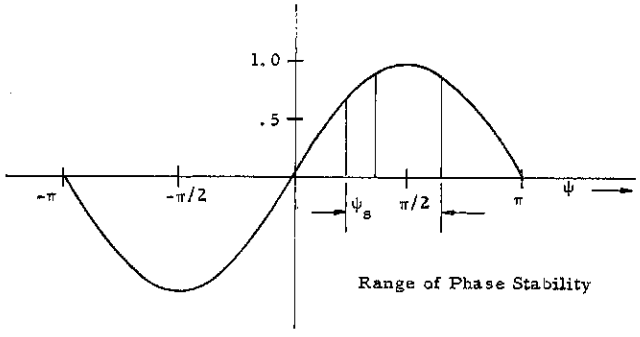

Linac RF Voltage Wave

Fig. 1

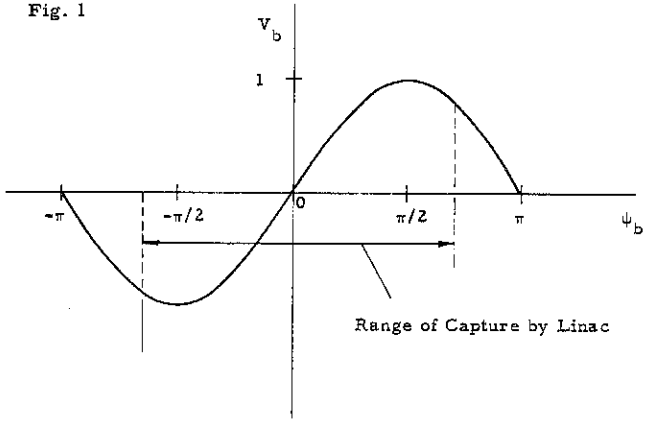

Sinusoidal Buncher Voltage

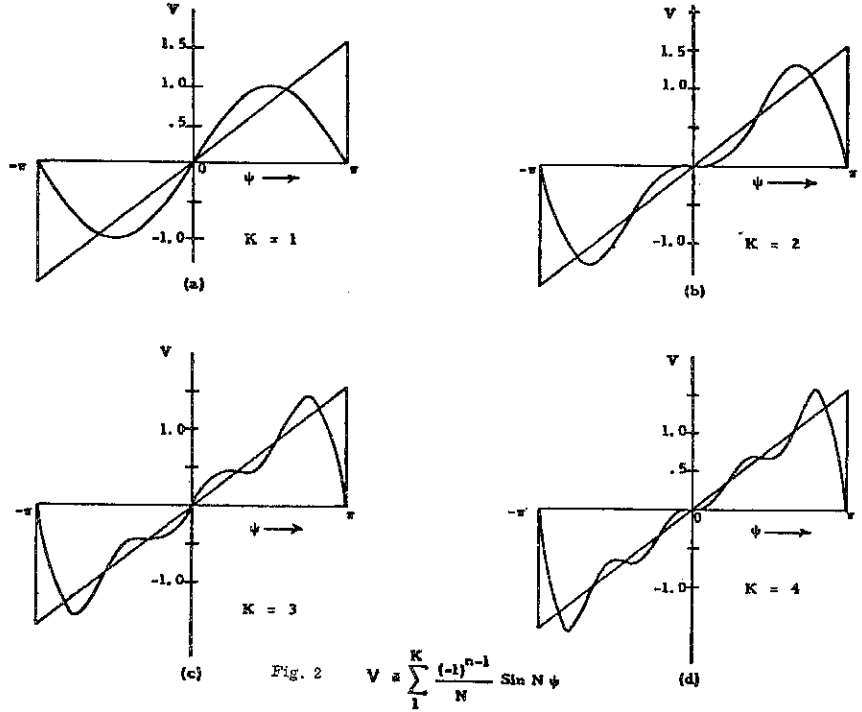

Fig. 2 $V = \sum_{1}^{K} \frac{(-1)^{n-1}}{N} \sin N\psi$

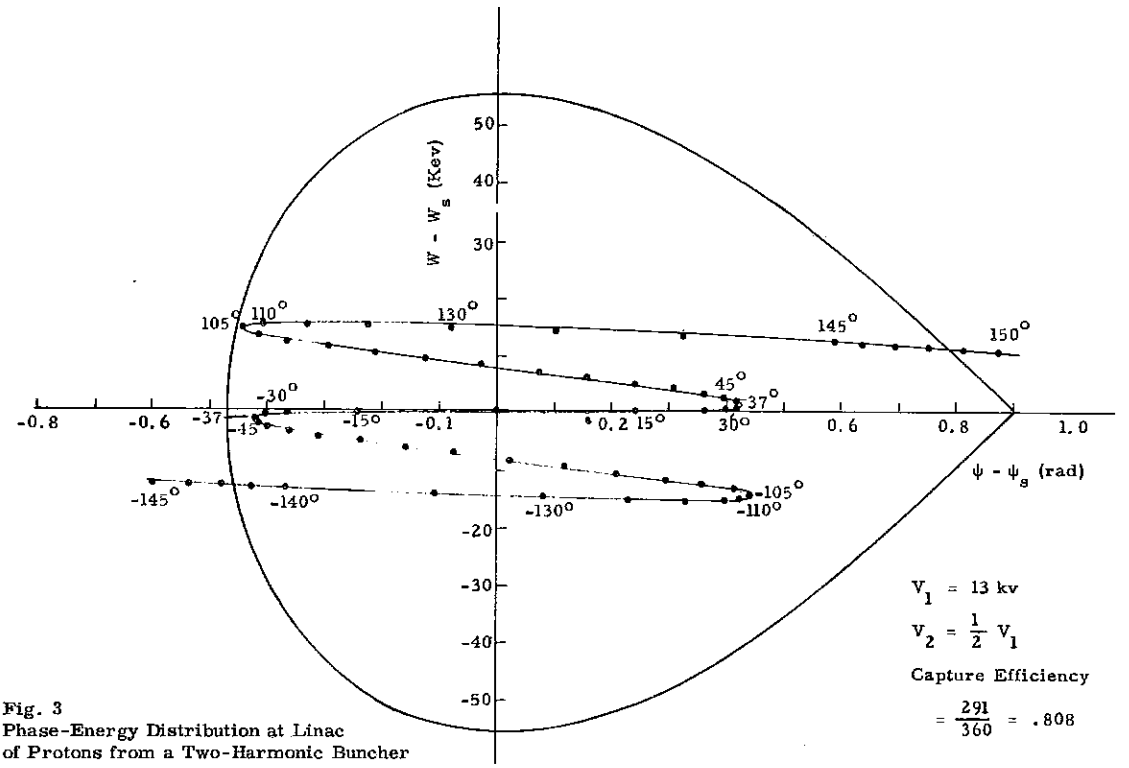

Fig. 3
Phase-Energy Distribution at Linac
of Protons from a Two-Harmonic Buncher

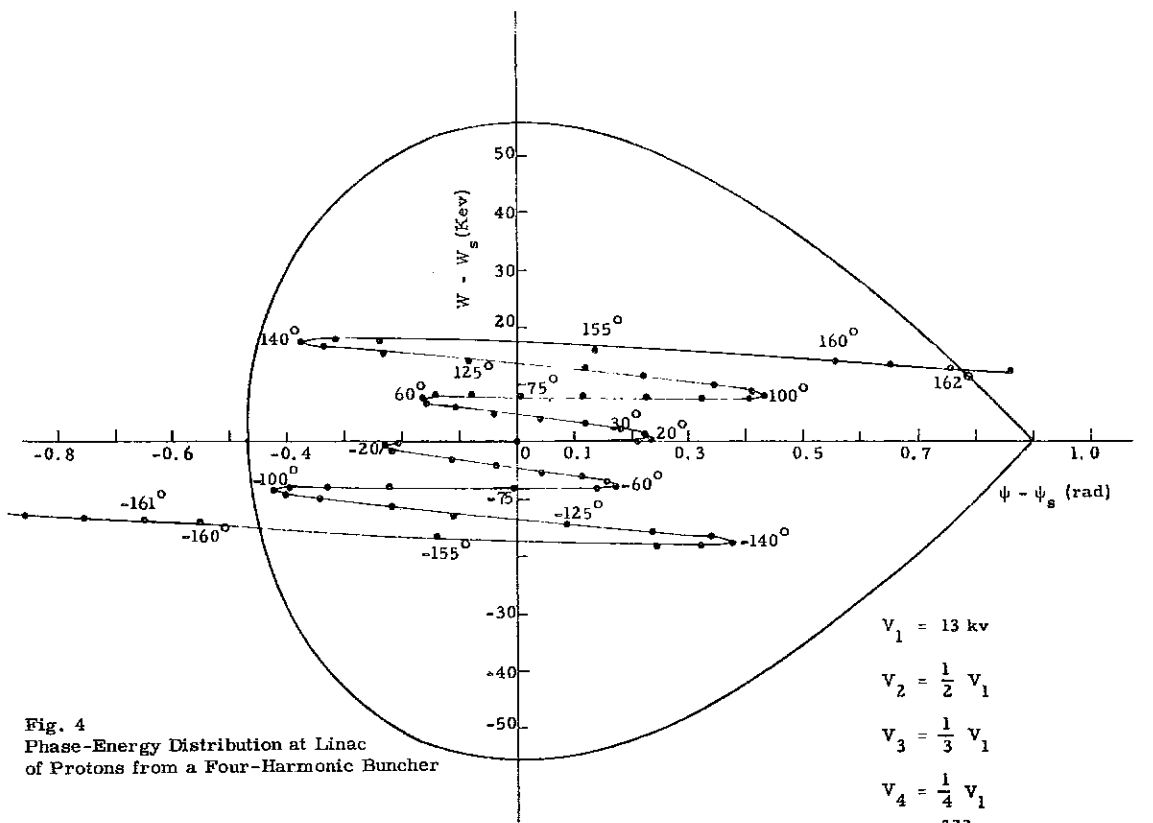

Fig. 4
Phase-Energy Distribution at Linac
of Protons from a Four-Harmonic Buncher

By noting that the first terms in Eq. (2) are the most important, it is not too surprising that a plot of capture versus number of bunchers (Fig. 5) taken from phase space data shows a pronounced roll-off after the second buncher is added. It was, therefore, decided to restrict the ANL system to the fundamental plus second harmonic. The complete second harmonic buncher system is shown in Fig. 6. The cavity was designed as a capacity-loaded radial line resonator; the dimensions and some details are shown in Fig. 7.

The cavity and the end plate were machined from OFHC copper. The end piece, which consists of a sandwich of two copper plates separated by a sheet of 1/16" teflon, provides for application of a 1 kV bias to prevent difficulties with multipactoring. Fine tuning of the cavity frequency is accomplished by rotating a 1" x 1/2" Cu "paddle." The level of rf excitation is observed by feeding a signal from the pickup loop to a diode detector and CRO. The gap is located approximately 2" from the first harmonic buncher gap.

The second harmonic buncher cavity is excited by a 400 Mc pulsed power doubler stage. The tube is an RCA type 7650 tetrode operated in the cathode drive configuration and delivers 500 watts output for 125 watts of drive. The input and output tank circuits are tuneable coaxial cavities. The plate power supply contains a large capacitor bank to obtain less than 0.5% droop during a 1 millisecond pulse, at a 10 pps repetition rate.

The source of 200 Mc drive power is a loop inserted near the low energy end of the linac. The phase shift control is placed in the drive line to avoid possible loading problems with the doubler, and to allow a slower tuning rate on the phase control.

In order to operate the doubler efficiently and obtain maximum power in the cavity, a double stub tuner is used to match the transmission line to the cavity. Transmission lines in most cases are RG8/U coaxial cable. The phase shifter is a standard General Radio unit, as are the stub tuner components.

Preliminary procedure for testing the SHB is to tune up the linac with the existing buncher for maximum transmission and observe the output current as the doubler is switched on and off.

It was anticipated that some preliminary results on the SHB would be available for presentation at this time. However, circumstances were such that no data was obtained in the limited time which was available for testing. Theoretically, 250 watts should suffice for cavity excitation;

however, no effect on the beam could be seen at levels of about 500 watts. The original estimate was based on the power taken by the first buncher, and may be low, since the Q of the present cavity is of the order of 1000. During the latest test, capture without the SHB was 55.5%.

No effect was observed on the beam as the doubler was switched on and off. The phase shift control has a range of $\sim 180^{\circ}$, so that the coupling loop may need to be rotated 180° to fall in the right phase range. Further trials will be made soon, and we expect to have it operational shortly.

OHNUMA: I don't know what kind of a beam your ZGS likes to receive from the linac, but unless you are very careful in designing this bunching system, the quality of the output beam could become lousy, because looking at the graph, the bunched beam is spread out very long, practically the entire area of the bucket. Since an increase in the phase spread automatically gives rise to an increase in the energy, unless you indeed require a very high intensity, sacrificing the beam quality, this may not be what you want. If you really want a very good quality of the beam, perhaps you should sacrifice the intensity a little bit, or capture efficiency of the buncher a little bit, and try to concentrate particles more around the center point.

MYERS: Yes, I can see what you mean. Our only thought here was just to try and see if it works basically as far as increasing the amount of beam that we can get. It may well be true that we experience an increase in phase space.

BLEWETT: Do you include grids in these buncher gaps?

MYERS: No, no grids.

BLEWETT: This is a question which we thought about a little at Brookhaven. We do have grids in the gaps of our first harmonic buncher for the reason that theoretically if you left the grids out you increased the emittance area by a factor of about two. Now I must admit that at one time the grids burned out, and the emittance area as far as we could see did not change.

HUBBARD: A comment on that too. We took the grids out of our buncher on the Highlac once also and the beam went down by quite a large factor, but I forget what it was.

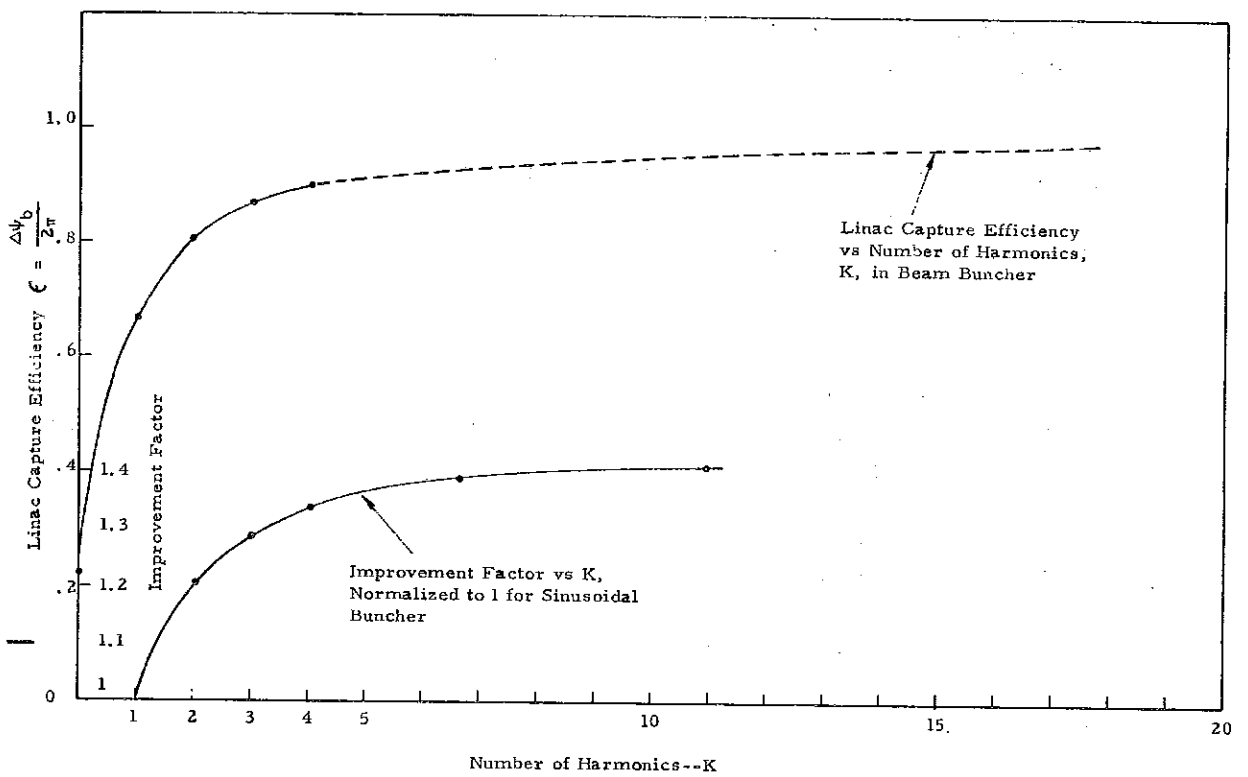
Linac Capture Efficiency $\epsilon = \frac{\Delta\psi_b}{2\pi}$
1.0
.8
.6
.4
.2
0
Improvement Factor
1.4
1.3
1.2
1.1
1
Linac Capture Efficiency vs Number of Harmonics, K, in Beam Buncher
Improvement Factor vs K, Normalized to 1 for Sinusoidal Buncher
1
2
3
4
5
10
15.
20
Number of Harmonics--K

FIG. 5

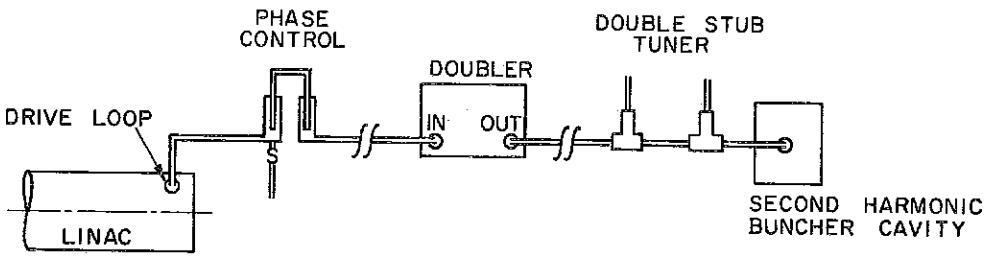
PHASE CONTROL
DOUBLE STUB TUNER
DOUBLER
DRIVE LOOP
IN
OUT
LINAC
SECOND HARMONIC BUNCHER CAVITY

FIG. 6

VAN STEENBERGEN: Do you have grids in the buncher of the 20 MeV linac injector for the Bevatron.

HUBBARD: Yes, there are grids.

PERRY: I would like to ask Ed, is it not possible to compensate for this divergence without grids by adjusting the matching quadrupoles?

HUBBARD: No, because it puts in a radial dependence of the change in energy of the beam you are putting in with the buncher.

BLEWETT: There is a Brookhaven internal report on this which should be in your files.

HUBBARD: Our buncher incidentally has a fairly large aperture, so we do not have to align it carefully in the transverse direction. This means that without grids we have a large radial dependence of the transit-time factor across it and this is why we think the grids are necessary.

VAN STEENBERGEN: I would like to make just one short comment to Rolland Perry with respect to the theoretical paper John mentioned. The focal length of the buncher gap lens, although modulated with the buncher frequency, is typically relatively long. If one has adjacent to the buncher a beam transport system with rather short focal lengths, then the buncher gap lens influence might be rather small. Further, it is possible to design the transport system such that a beam waist occurs at the location of the buncher gap. Therefore, I think whether one needs to worry about this time-dependent lens or not depends on the transport system around it.

REFERENCES

1. R. Perry, ANLAD-74, "Multiple-Harmonic Buncher for a Linear Accelerator", February 22, 1963.

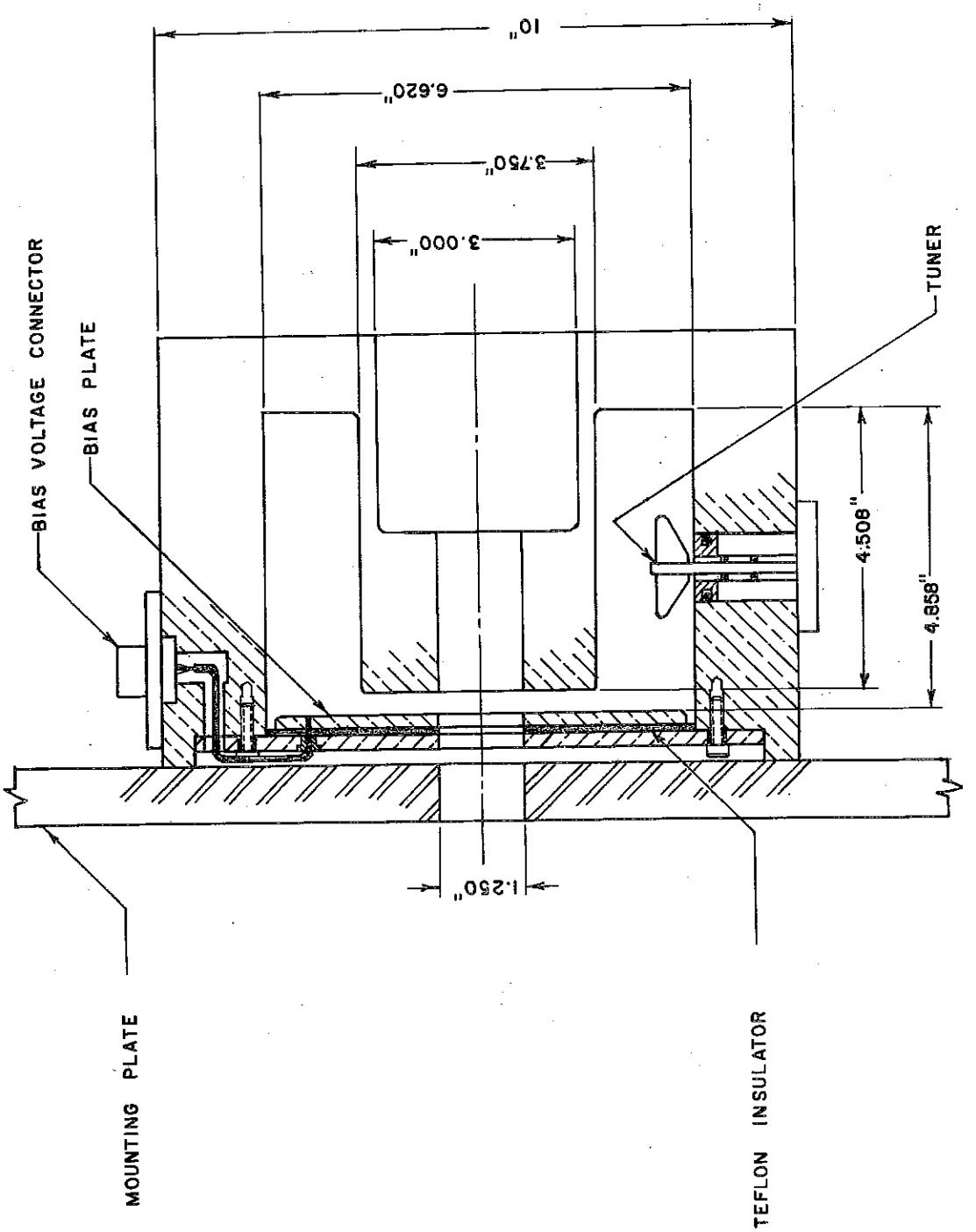

FIG. 7 SECOND HARMONIC BUNCHER CAVITY

A FAMILY OF IMPROVED LINAC BUNCHERS

R. Beringer and R. L. Gluckstern
Brookhaven National Laboratory and Yale University

Conventional bunchers use one or more gaps excited with fundamental frequency sinusoidal fields. They can be designed to inject about 2/3 of the dc beam into the admittance of a conventional drift-tube linac. However, the remainder of the particles (long tails) are not accelerated to the end of a long linac and will give rise to undesirable radiation and possible confusion in the beam-pickup instrumentation of a sophisticated multicavity linac.

Bunchers having several gaps with harmonically related sinusoidal fields[1, 3] are somewhat better but still have long tails. They are approximations to the saw-tooth buncher[1, 2, 3, 4] which has no tails and which can bunch all of the dc beam.

Unfortunately, no one seems to have a practical way of exciting a saw-tooth gap at frequencies as high as 200 Mc/s. Thus, other solutions are of interest.

The bunchers described here use an rf deflector to separate phase regions in space so that each phase region can be bunched independently with a sinusoidal field.

1. Isochronous Deflector

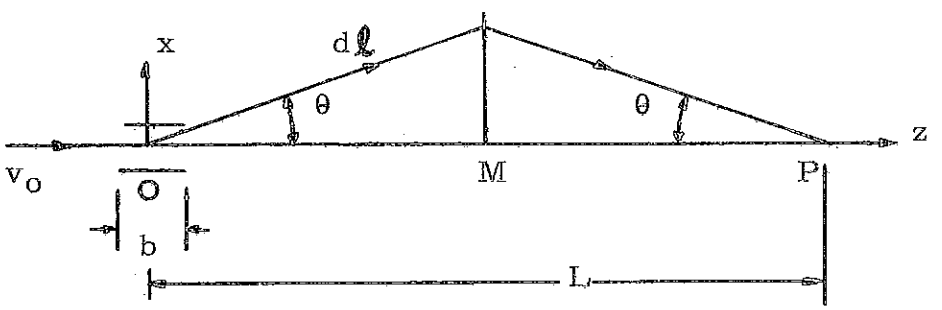

Consider an rf deflector at 0 with $E_x = E_o \sin \omega t$. The deflection angle is

$$\tan \theta = \frac{v_x}{v_o} = \frac{eE_o b}{mv_o^2} \sin \omega t ,$$

where dimension b includes a transit-time factor. M is a magnetic or electrostatic lens of unit magnification. If we approximate it as a thin lens, the elapsed time from 0 to P is

$$\frac{1}{v} \int_o^P d\ell = \frac{1}{\sqrt{v_o^2 + v_x^2}} \quad \frac{L}{\cos \theta} = \frac{L}{v_o} .$$

Thus the system is isochronous.

2. Isochronous Deflector - Redeflector

The angles θ at P can be eliminated by a second deflector since the system is isochronous. The particle arrives at P at time $t + L/v_o$ with transverse velocity $v_x = -(eE_o b/mv_o) \sin \omega t$. If we excite an identical deflector with field $E_x = E_o \sin (\omega t - \omega L/v_o)$, then all axial

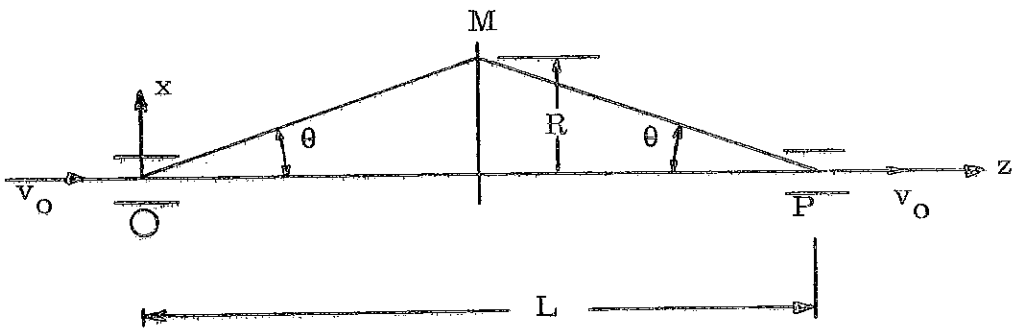

particles leave P with velocity v_o along z. This isochronous transport is also true for nonaxial particles incident at 0. Further, the field E_x need not be uniform over the aperture but only the same in the two deflectors provided that they are symmetrically placed with respect to M.

Phase errors $\Delta(\omega L/v_o) = -(\omega L/v_o)(\Delta v_o/v_o)$ arising from variations in v_o (dc preinjector voltage changes) give angular errors in the redeflected beam. These should be small compared to beam-emittance angles. The maximum angular error is

$$\frac{\Delta\theta_{max}}{\theta} = \frac{(\Delta v_x)_{max}}{v_o} = \frac{2\,\omega R}{v_o}\,\frac{\Delta v_o}{v_o} .$$

It is independent of L for a given maximum deflection R. In a typical case the errors are about one milliradian.

3. Deflector - Redeflector and a Bunching Gap

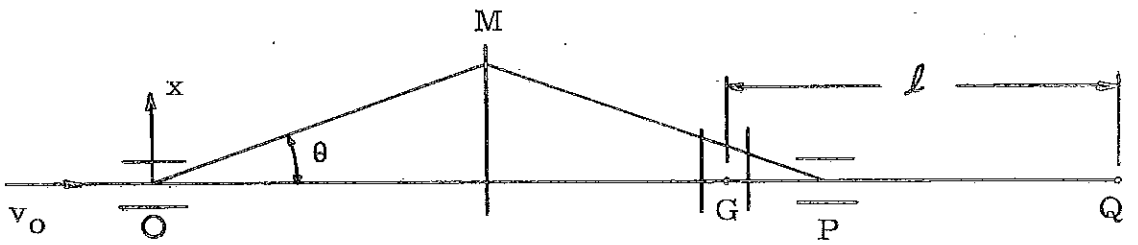

Near P, where the beam is still separated in space, we place a bunching gap with rf voltage

$$gE_z = -V_o \cos \omega t .$$

Particles leaving the gap have velocity

$$v = \sqrt{v_o^2 (1 + \tan^2 \theta) - \frac{2\,eV_o}{m} \cos \omega t} .$$

Since $v_o^2 \gg eV_o/m$, the angles θ are not changed to first order by the bunching voltage. (In the formula V_o includes another transit-time factor.) The elapsed time G to Q is

$$t' = \frac{\ell}{v_o\sqrt{1 - \frac{2\,eV_o}{mv_o^2}\cos\omega t}}$$

$$\cong \frac{\ell}{v_o} + B\cos\omega t$$

with $B = (\ell/v_o)(eV_o/mv_o^2)$. This is the ordinary buncher equation. The arrival time at Q is $t' + t + L/v_o$. This is expressed as an arrival phase at Q defined as

$$\phi = \omega t' + \omega t + \frac{\omega\ell}{v_o} + \text{const.}$$

As is well known, it is not possible to make ϕ the same for all particles. For our choice of zero phase the "long tails" come from the region $\pi < \omega t < 2\pi$. Note, however, that this region corresponds to negative θ, and hence a beam stop for all (or some) negative θ eliminates the long tails.

Suppose we make ϕ the same for $\omega t = 0, \pi/2, \pi$. Then $B = \pi/2\omega$ and $\phi = \pi/2 + \text{const.}$ for these three particles. Figure 1 shows the arrival phases of all particles from $0 < \omega t < 7\pi/2$. The abscissa is ωt and the ordinate $\phi = \omega t' + \omega t - \omega\ell/v_o - \pi/2$. If we stop all $\theta < 0$ particles, then all remaining particles (half of the dc beam) arrive at Q within 37° wide phase bands centered at $0, 2\pi, 4\pi, \cdots$. As usual, a compromise between ℓ, V_o, and the energy stability of the dc pre-injector is necessary in order to match the admittance of a given linac.

4. Deflector - Redeflector and Two Biased Bunching Gaps

Instead of stopping the beam particles with $\theta < 0$, let us provide separate bunching gaps for the positive θ and negative θ beams.

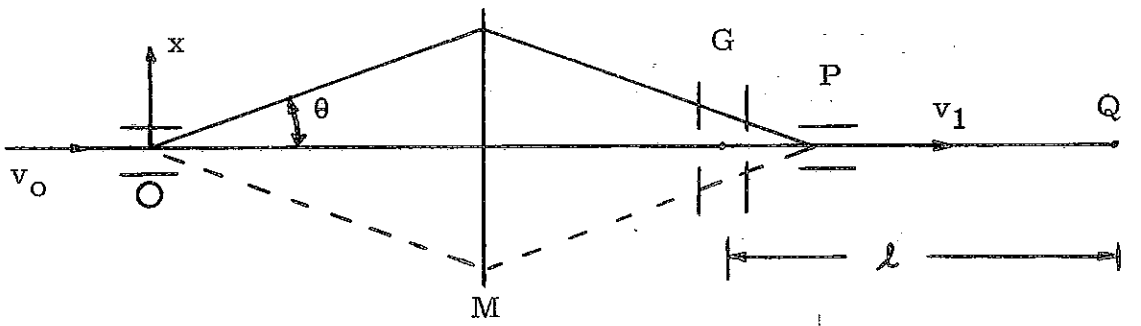

Let gap 1 have voltage $-V_o - V_o \cos \omega t$, for $\theta > 0$
and gap 2 have voltage $V_o + V_o \cos \omega t$, for $\theta < 0$.

The corresponding particle velocities in the drift space GQ are

$$v_1 = \sqrt{v_o^2 - \frac{2eV_o}{m}(1 + \cos \omega t)}, \quad \theta > 0$$

$$v_2 = \sqrt{v_o^2 + \frac{2eV_o}{m}(1 + \cos \omega t)}, \quad \theta < 0$$

and the elapsed times G to Q are

$$t_1' = \frac{\ell}{v_1} = \frac{\ell}{v_o\sqrt{1 - \frac{2eV_o}{mv_o^2}(1 + \cos \omega t)}}$$

$$t_1' \cong \frac{\ell}{v_o} + B(1 + \cos \omega t), \text{ for } \theta > 0, \text{ or } 2n\pi < \omega t < (2n + 1)\pi, \quad n = 0, 1, 2 \cdots$$

and

$$t_2' \cong \frac{\ell}{v_o} - B(1 + \cos \omega t), \text{ for } \theta < 0, \text{ or } (2n + 1)\pi < \omega t < (2n + 2)\pi, \quad n = 0, 1, 2 \cdots$$

With the choice $B = (\ell/v_o)(eV_o/mv_o^2) = \pi/2\omega$ the arrival phases are the same for $\omega t = 0, \pi/2, \pi, 3\pi/2, 2\pi$. Figure 2 shows the arrival phases for all particles as a function of the input phase to the buncher.

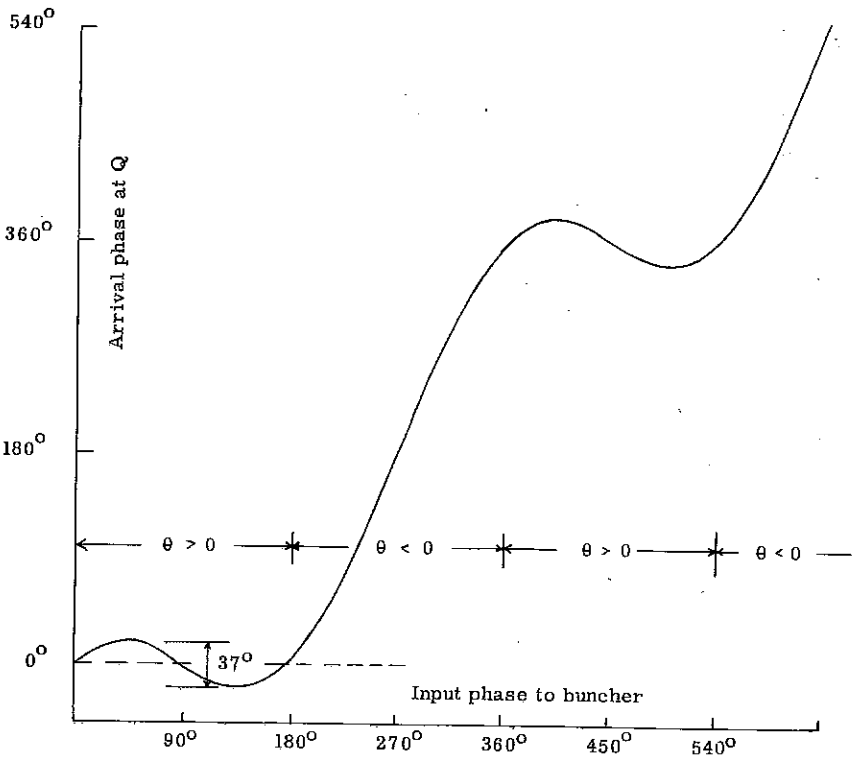

Fig. 1 - Phase of beam particles arriving at Q vs input phase to buncher for a single deflector and bunching gap.

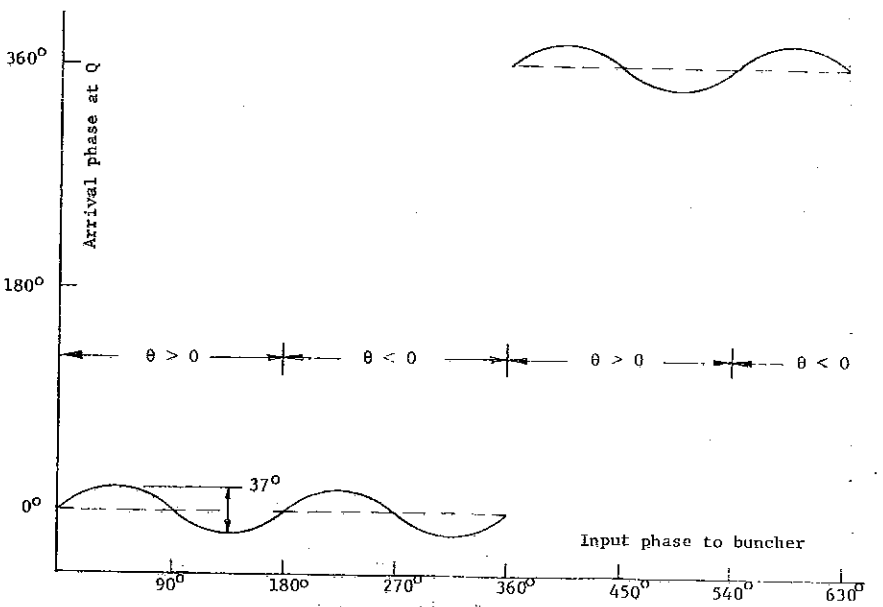

Fig. 2 - Phase of beam particles arriving at Q vs input phase for a two-gap fundamental frequency biased buncher.

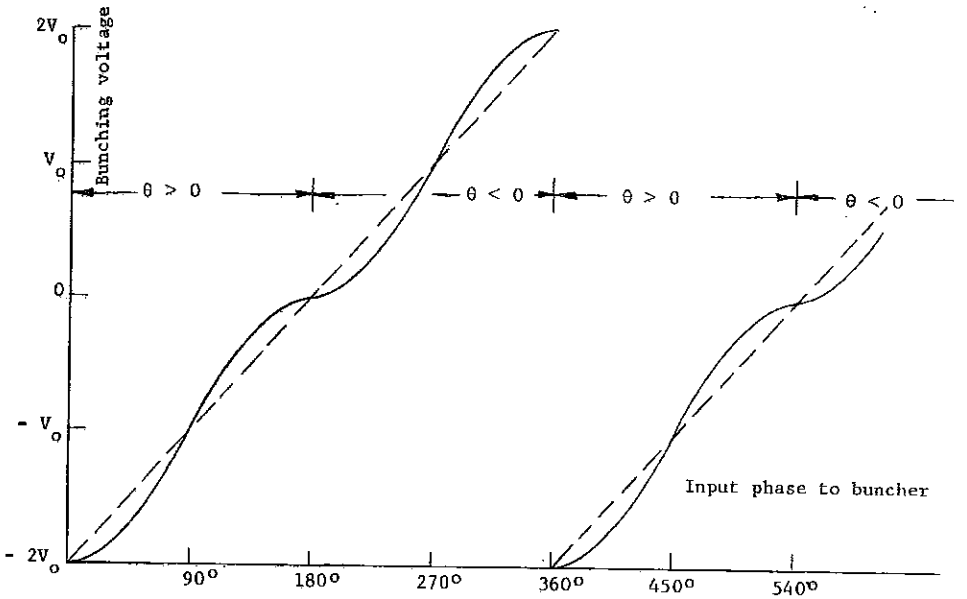

Fig. 3 - Bunching voltage waveshape for a two-gap fundamental frequency biased buncher.

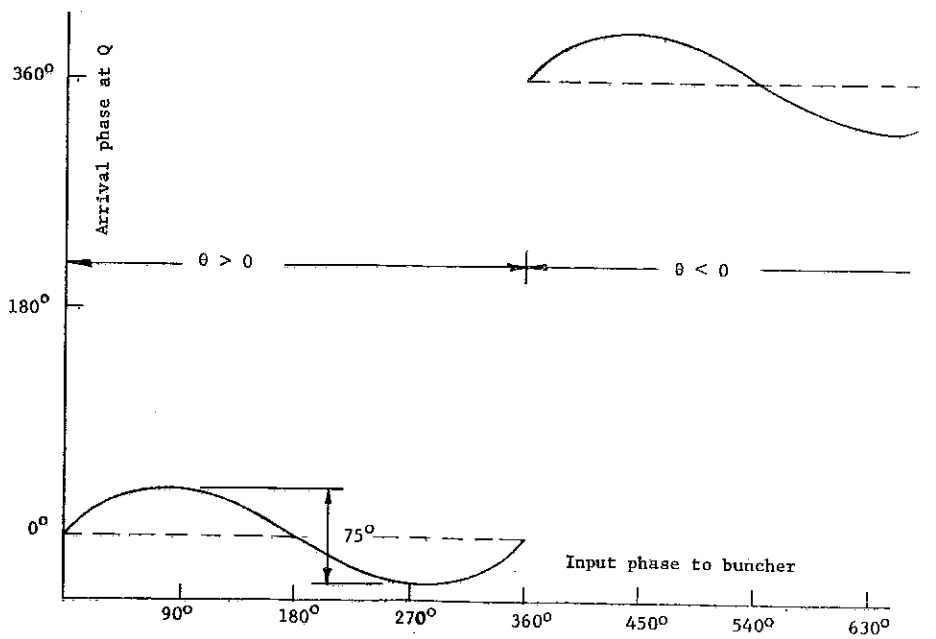

Fig. 4 - Phase of beam particles arriving at Q vs input phase for a two-gap second-subharmonic line-scan buncher.

The abscissa is ωt and the ordinate $\omega t' + \omega t - \frac{\ell\omega}{v_o} - \pi$. We see that all of the dc beam is bunched into 37° wide phase regions centered at 0, 2π, 4π, $\cdots$. The choice of V_o and ℓ is the same as for a conventional buncher.

The reason for the success of this buncher is easily seen if we plot the gap voltage vs input phase. This is shown in Fig. 3, and we see that we have provided nothing more than a good way of approximating a saw-tooth, but not, we note, by conventional Fourier analysis.

The buncher has one nontrivial complication. It requires a dc bias, either $\pm V_o$ for the two legs (or zero and $2 V_o$). These biases cannot be provided with electrostatic fields since the input beam is surrounded by an equipotential surface* (grounded beam pipe) and no arrangement of dc electrodes can accelerate or decelerate such a beam. However, an induction transformer can, in principle, provide a rectangular pulse of accelerating voltage. Since the linac is pulsed, this accelerating pulse should be of comparable duration (say 200 μsec). In a preliminary look, such a device appears feasible[5] for pulses of the order of 10 kV.

5. Subharmonic Deflector and Buncher

The need for dc bias can be eliminated if the alternate halves of input phase corresponding to $\pm\theta$ are bunched into separate linac buckets. This can be done with a subharmonic, $\omega/2$, deflector and buncher.

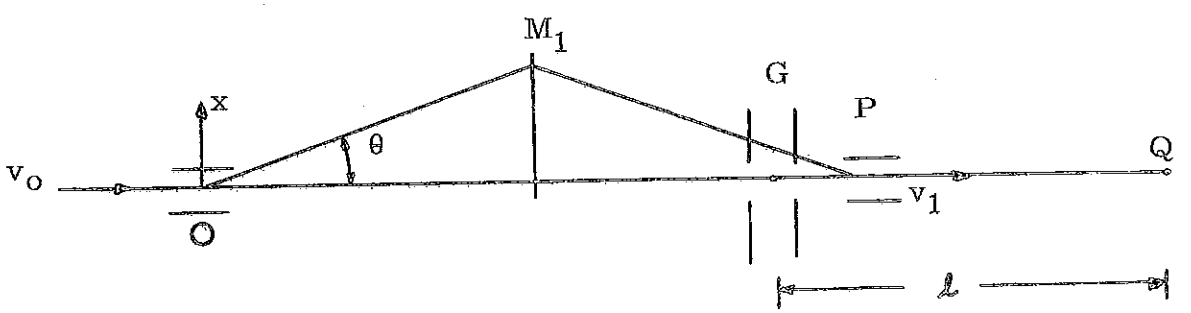

*This condition is imposed by the ion-source and accelerating column of the preinjector. However, one can conceive of devices in which the required dc bias can be provided in the incident beam. A klystron gun is such a device, and klystrons using these bunchers should have greatly improved efficiency.

Let gap 1 have voltage

$$-V_o \cos \frac{\omega}{2} t, \quad \theta > 0 \text{ or } 2n\pi < \frac{\omega}{2} t < (2n+1)\pi, \quad n = 0, 1, 2, \cdots$$

and gap 2 have voltage

$$V_o \cos \frac{\omega}{2} t, \quad \theta < 0 \text{ or } (2n+1)\pi < \frac{\omega}{2} t < (2n+2)\pi, \quad n = 0, 1, 2, \cdots.$$

At P we put a subharmonic redeflector. The elapsed times G to Q are

$$t_1' \cong \frac{\ell}{v_o} + B \cos \frac{\omega}{2} t, \quad \theta > 0$$

$$t_2' \cong \frac{\ell}{v_o} - B \cos \frac{\omega}{2} t, \quad \theta < 0$$

where $B = (\ell/v_o)(eV_o/mv_o^2)$. With the choice $B = \pi/\omega$ the arrival phases are the same for $\omega t = 0, \pi, 2\pi$. Figure 4 shows the arrival phases of all particles as a function of input phase to the buncher. The abscissa is ωt and the ordinate is $\phi = \omega t' + \omega t - \omega\ell/v_o - \pi$. Figure 5 shows the approximation to the saw-tooth for this case. Note that twice as large a bunching parameter B is required for this arrangement and that twice as large a phase spread (75^o) is produced as compared with the biased two-gap buncher.

6. Conical-Scan Deflector and Buncher

The essential feature of all of these bunchers is the separation of phase regions in space and the application of appropriately phased sinusoidal bunching voltages to the separated beams. This can be accomplished in a more general way by a two rather than a one-dimensional deflection. In particular, conical-scan deflectors appear promising.

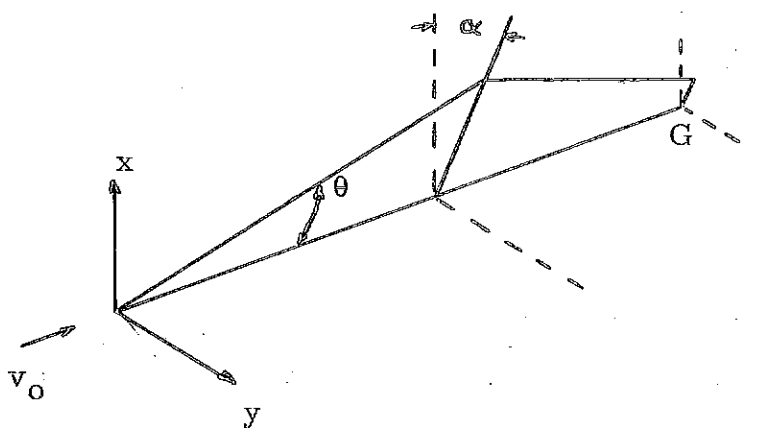

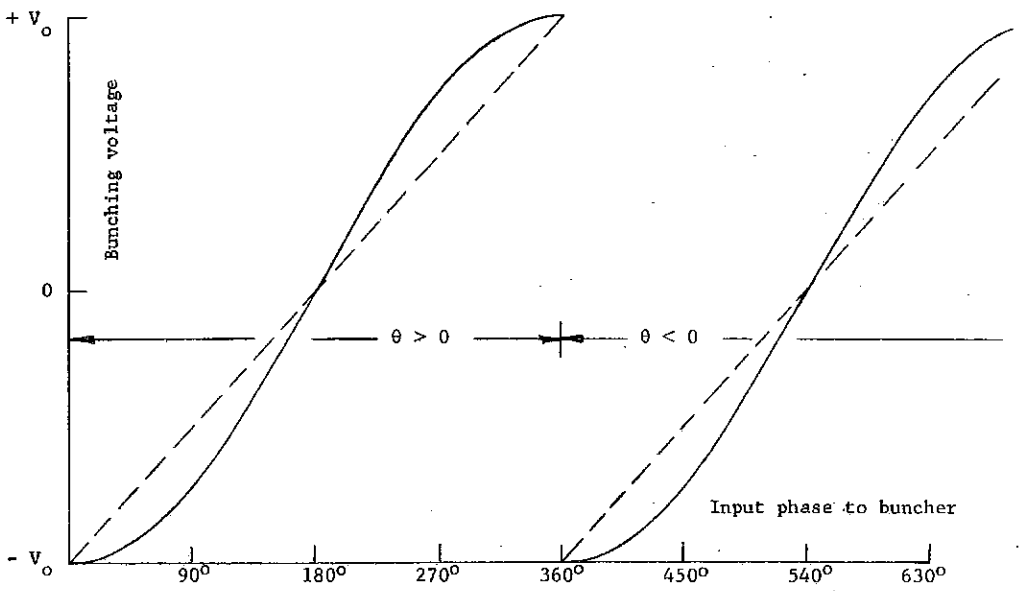

Fig. 5 - Bunching voltage waveshape for two-gap second-subharmonic line-scan buncher.

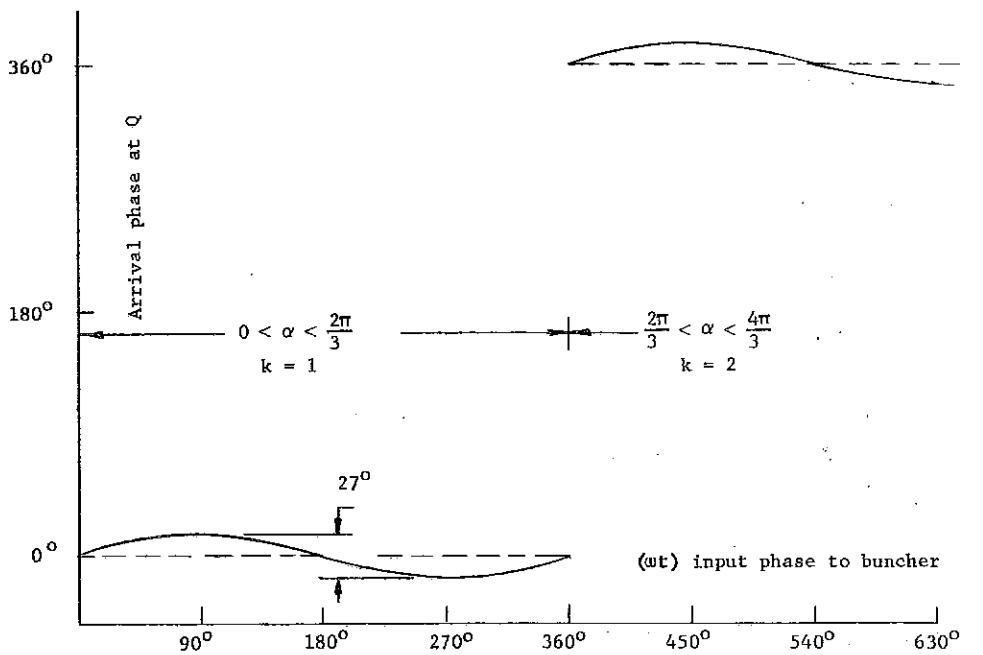

Fig. 6 - Arrival phase for a three-gap third-subharmonic conical-scan buncher.

Consider a deflector at 0 consisting of two perpendicular electric fields in quadrature extending a distance b along z.

$$E_x = E_o \cos \frac{\omega}{p} t$$

$$E_y = E_o \sin \frac{\omega}{p} t , \quad p = 2, 3, \cdots .$$

The deflection angle θ is constant,

$$\tan \theta = \frac{v_r}{v_o} = \frac{eE_o b}{mv_o^2} ,$$

where b includes a transit-time factor. The azimuth angle of the beam is $\alpha = \frac{\omega t}{p}$, where t is measured when the particle is at 0. The beam is scanned on a cone at uniform angular velocity. A plane parallel to xy at G is divided into p sectors in α, each sector containing a bunching gap with voltage

$$gE_z = - V_o \cos \left(\frac{\omega t}{p} - \frac{2 \pi k}{p} + \delta \right) .$$

The gaps are numbered with increasing α by k = 1, 2, $\cdots$ p. Note that after p cycles of the linac frequency ω the scan repeats exactly. The elapsed time G to Q is

$$t' \cong \frac{\ell}{v_o} + \frac{\ell}{v_o} \frac{eV_o}{mv_o^2} \cos \left(\frac{\omega t}{p} - \frac{2 \pi k}{p} + \delta \right) ,$$

and the arrival phase at Q is

$$\phi = \omega t + \omega t' + \text{const.} = \omega t + \omega B \cos \left(\frac{\omega t}{p} - \frac{2 \pi k}{p} + \delta \right) + C ,$$

with $B = (\ell / v_o)(eV_o / mv_o^2)$.

As in the previous case, the phase shift from gap to gap is so arranged that each 2π region of ωt is bunched into a separate linac bucket. The appropriate constants are

$$\delta = \frac{\pi}{p} + \frac{\pi}{2}, \quad C = - \pi , \quad \omega B = \pi / \sin (\pi / p) .$$

With this choice the arrival phase at Q is

$$\phi = \omega t - \pi + \frac{\pi}{\sin \frac{\pi}{p}} \cos \left[\frac{\omega t}{p} + \frac{(1 - 2k)\pi}{p} + \frac{\pi}{2} \right].$$

A large p yields a very close approximation to the saw-tooth since the sinusoidal voltage in the gap is being used only in the linear region where it changes sign. Figures 6, 7, 8, 9 show the arrival phase and bunching voltage vs ωt for p = 3 and p = 4. The p = 2 case is the same as for one-dimensional deflection.

7. Bunching Voltage and Drift Length

The conventional choice of bunching voltage and drift length should be re-examined for the very narrow bunches proposed here. For large bunching voltage and short drift length the phase shifts produced by dc voltage fluctuations of the preinjector are small but the velocity spread in the bunched beam is large. An optimum design is a compromise between these.

Assume that an optimum design is one which gives the best beam quality in longitudinal phase space at the input of the first linac tank. For a tank with uniform accelerating field and a bunch which occupies only a small part of the stable longitudinal phase region, the locus of a particle as it undergoes phase oscillations is the ellipse[6]

$$\left(\frac{w - w_s}{w_s} \right)^2 - \frac{2\, eE_o\, T}{m_o c^2 \beta_s} (\phi - \phi_s)^2 \sin \phi_s = \text{const.},$$

where $(w - w_s)$ is the energy deviation for the phase deviation $(\phi - \phi_s)$. The other symbols have the usual meanings. An optimum design fills a given ellipse along both axes and thereby achieves the smallest possible ellipse.

Consider a typical first tank for a proton linac.[7] At its input

$$\omega = 2\pi \ 200 \text{ Mc/s}, \quad \lambda = 1.5 \text{ m}, \quad \phi_s = -30^\circ, \quad E_o = 1.7 \text{ MV/m},$$

$$\beta_s = 0.04, \quad T = 0.9 .$$

For the four-gap buncher the maximum phase error is 7.5°. Suppose we choose an ellipse with semi-axis $\phi - \phi_s = 10.4^\circ = 0.18$ rad whose other semi-axis is $w - w_s = 19.0$ keV. This determines the bunching voltage, $V_o = \sqrt{2}\ 19.0 = 27$ kV, and the drift length from $\omega B = \sqrt{2}\ \pi = \ell \omega e V_o / m v_o^3$, $\ell = 2.36$ m. We now assume a dc

voltage stability for the preinjector which gives a phase error $10.4^{\circ} - 7.5^{\circ} = 2.9^{\circ}$ in the drift length 2.36 m. The relation is $\Delta\phi = (\omega \ell / v_o)(\Delta v_o / v_o) = 2.9^{\circ}$ giving $\Delta v_o / v_o = 0.204 \times 10^{-3}$ or $\Delta(1/2\, m v_o^2)/(1/2\, m v_o^2) = 0.41 \times 10^{-3}$ which is about the limit of stability of existing Cockcroft-Walton machines. As usual, the energy deviation $\Delta(1/2\, m v_o^2) = 0.31$ keV is a negligible addition to $w - w_s = 19$ keV. The design is an optimum filling of an ellipse of semi-axis 10.4° for the dc stability cited.

8. Second-Order Terms in the Bunch Width

Even an ideal saw-tooth buncher does not produce a bunch of zero phase width.[4] For very narrow widths it is necessary to examine this effect.

For the conical-scan buncher the arrival phase at Q, including second-order terms and for the choice of parameters which gives first-order zeros at $\omega t = 0, \pi, 2\pi$ is

$$\phi = \omega t - \pi + \frac{\pi}{\sin \frac{\pi}{p}} \cos\left(\frac{\omega t}{p} - \frac{2\pi k}{p} + \frac{\pi}{p} + \frac{\pi}{2}\right) + \frac{3 v_o}{2 \omega \ell}\left[\frac{\pi}{\sin \frac{\pi}{p}} \cos\left(\frac{\omega t}{p} - \frac{2\pi k}{p} + \frac{\pi}{p} + \frac{\pi}{2}\right)\right]^2 .$$

The maximum errors in ϕ due to the first-order term occur near* $\omega t = \frac{\pi}{2}, \frac{3\pi}{2}$ and are

$$\Delta\phi_1 \cong \pm \pi\left(\frac{\sin(\pi/2p)}{\sin(\pi/p)} - \frac{1}{2}\right) .$$

Errors due to the second-order terms occur at $\omega t = 0, 2\pi$ and are

$$\Delta\phi_2 = \frac{3}{2}\frac{v_o}{\omega \ell}\pi^2 = \frac{3\pi\beta\lambda}{4\ell} .$$

For the four-gap case discussed above $\Delta\phi_1 = \pm 7.5^{\circ}$ and $\Delta\phi_2 = 3.4^{\circ}$. The distorted phase bunch for this case is shown in Fig. 10. There is no net increase in the 15° phase width but there is some distortion

*The maximum arrival phase errors occur at those ωt which are the solutions of $\cos(\omega t/p)\cot(\pi/p) + \sin(\omega t/p) = p/\pi$. For large p, $\omega t \cong 0.42\pi$, 1.58π. The errors themselves are almost the same as at $\pi/2$, $3\pi/2$ for all values of p.

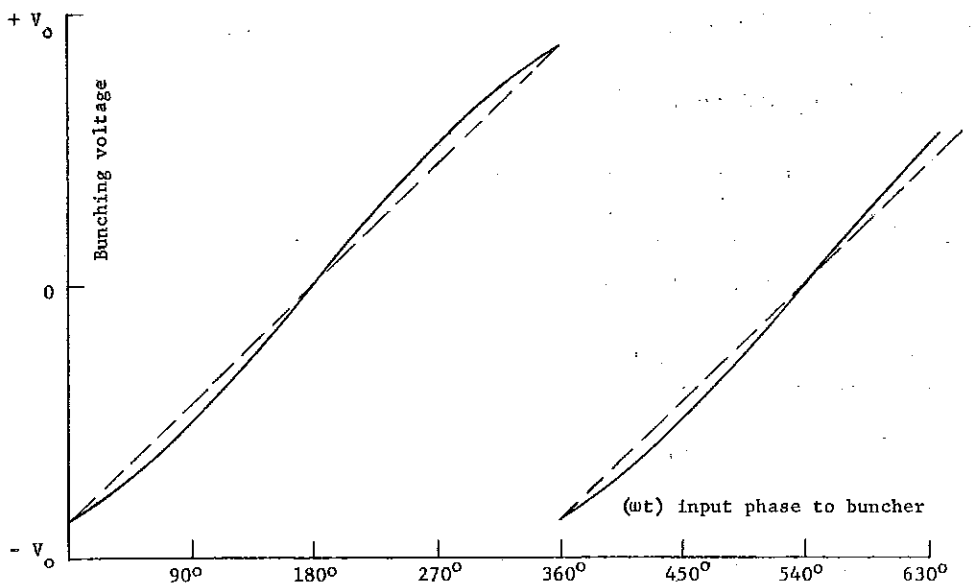

Fig. 7 - Bunching voltage waveshape for a three-gap third-subharmonic conical-scan buncher.

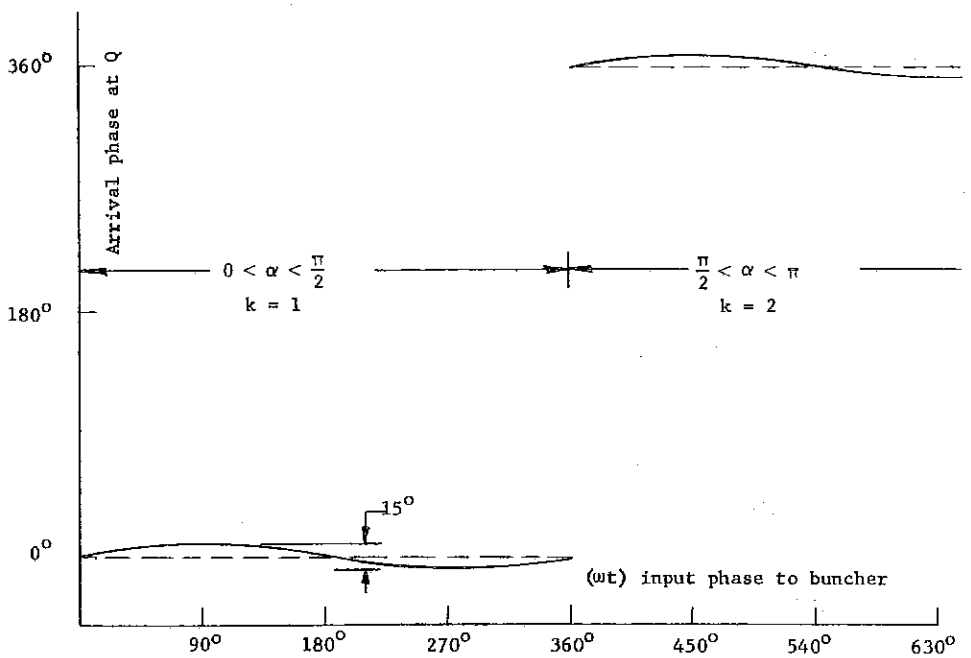

Fig. 8 - Arrival phase for a four-gap fourth-subharmonic conical-scan buncher.

around $\omega t = \pi$ which could be removed by a slightly different choice of the bunching phase and amplitude. In sum, the second-order terms are not negligible but do not seem to cause any trouble.

9. Parallel-Plate Deflector

It is clear that the deflection angles should be somewhat larger than the beam emittance angles at the deflector. Since the latter are, say, 0.5^{o} for a 1 cm radius proton beam at 750 keV, the desired deflection angles are in the range 10^{o} - 20^{o}.

Consider a one-dimensional deflector consisting of a pair of parallel plates driven by rf voltages balanced to ground.

$$V_2 = -\frac{1}{2} E_o h \cos \frac{\omega t}{p}$$

$$V_4 = \frac{1}{2} E_o h \cos \frac{\omega t}{p} .$$

Ignore, for the present, the longitudinal fields in the end gaps, and consider only the deflection. Measure t_o when the particle reaches 0. The force equation is

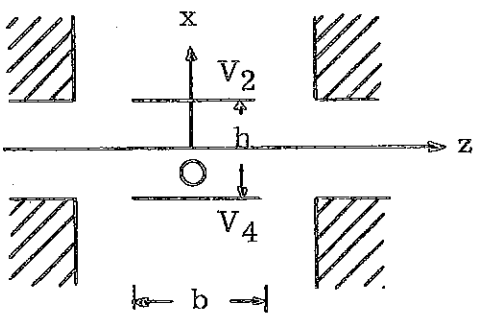

$$m \frac{d^2x}{dt^2} = eE_o \cos \frac{\omega t}{p} .$$

The transverse velocity as the particle leaves the plates at $z = b/2$, $t = t_o + b/2 v_o$ is

$$v_x = \frac{dx}{dt} = \frac{2 eE_o p}{m \omega} \sin \frac{\omega b}{2 p v_o} \cos \frac{\omega t_o}{p} .$$

Maximum deflection for a given E_o occurs for $\frac{\omega b}{p v_o} = \frac{2 \pi b}{p \beta_o \lambda} = \pi$.

For this choice

$$v_x = \frac{dx}{dt} = \frac{2}{\pi} \frac{eE_o b}{m v_o} \cos \frac{\omega t_o}{p}$$

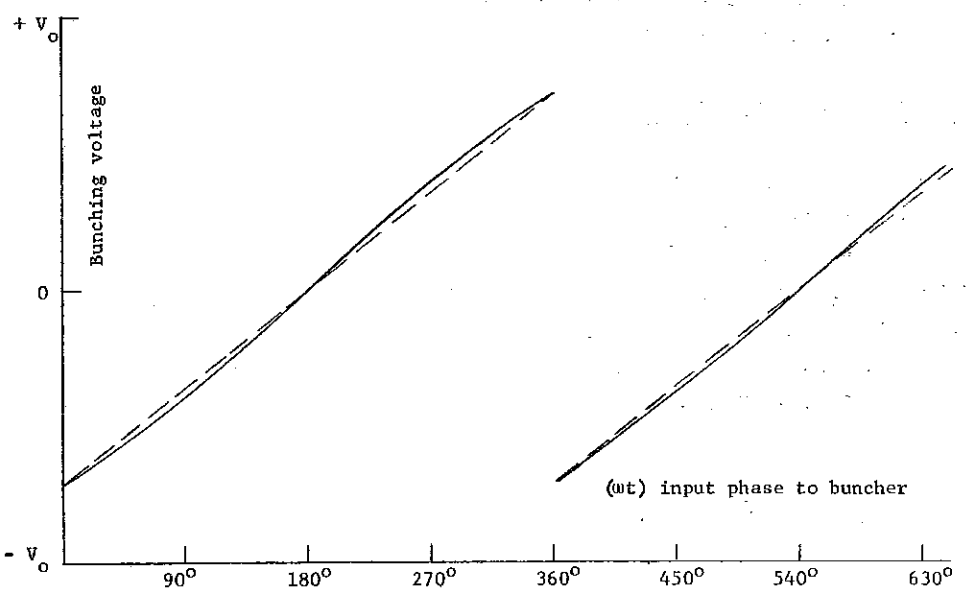

Fig. 9 - Bunching voltage waveshape for a four-gap fourth-subharmonic conical-scan buncher.

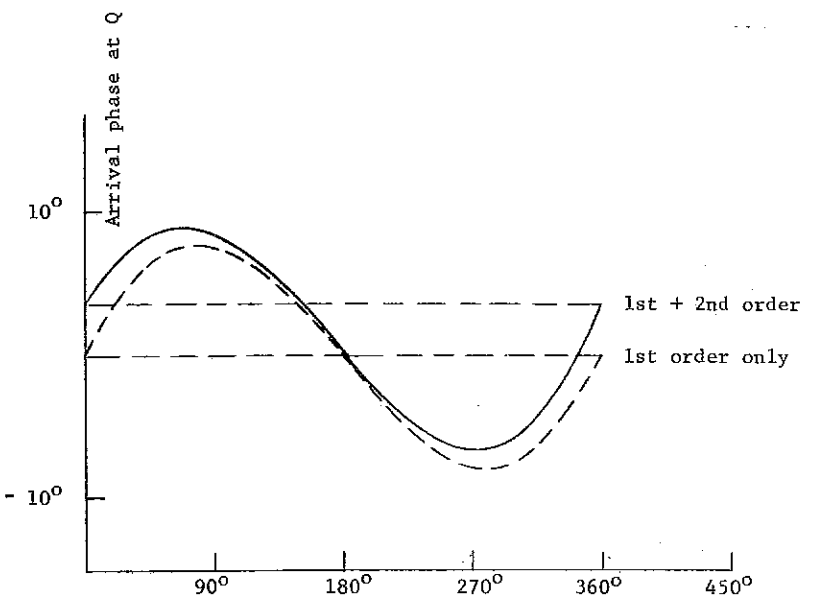

Fig. 10 - Effect of second order terms in a four-gap fourth-subharmonic conical-scan buncher.

For 10° maximum deflection with p = 4, λ = 1.5 m, β_o = 0.04, E_o = 3.4 MV/m and for 20°, E_o = 7.1 MV/m. These are high but probably attainable field strengths, but they would not be attainable for a fundamental frequency deflector (p = 1).

10. Crossed-Field Deflector

A conical scan deflector requires two mutually perpendicular sets of plates (or their equivalent). Consider two such plate sets, with each pair of plates balanced to ground. In general, the mere application of voltages in quadrature will not produce a uniform E field rotating at frequency ω/p, and the uniformity in space and time depends on the electrode shape. A typical case is four equal segments of a circular cylinder with voltages

$$V_1 = -V_3 = -E_o\, a \sin\frac{\omega t}{p}$$

$$V_2 = -V_4 = -E_o\, a \cos\frac{\omega t}{p} .$$

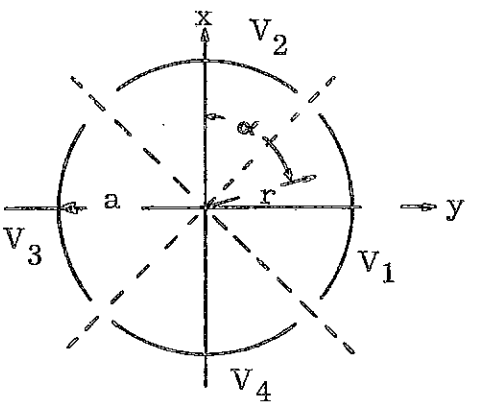

The electrostatic potential at r = a, t = 0 has the boundary value

$$V(\alpha) = \sum_{n=1,3,5\cdots} a_n \cos n\alpha$$

where

$$a_n = \frac{1}{\pi}\int_{-\pi}^{\pi} V(\alpha)\cos n\alpha\, d\alpha = -E_o\, a\,\frac{\sin(n\pi/4)}{(n\pi/4)} .$$

Thus, at r = a and t = t the boundary potential is

$$V(\alpha, t) = -E_o\, a \sum_{n=1,3,5\cdots} \frac{\sin(\frac{n\pi}{4})}{(\frac{n\pi}{4})}\left[\cos n\alpha \cos\frac{\omega t}{p} + \cos n(\alpha - \tfrac{\pi}{2})\sin\frac{\omega t}{p}\right] .$$

The potential in the region of the axis can be expanded in terms of dipole, sextupole, etc. terms varying as $(r/a)^1$, $(r/a)^3$, etc. respectively. (Note that even n terms, e.g. quadrupole, are absent.) Thus the deflecting

fields near the axis are

$$E_r = -\frac{\partial V}{\partial r} = E_o \frac{2\sqrt{2}}{\pi}\left[\cos\left(\alpha - \frac{\omega t}{p}\right) + \left(\frac{r}{a}\right)^2 \cos\left(3\alpha + \frac{\omega t}{p}\right)\right.$$

$$\left. - \left(\frac{r}{a}\right)^4 \cos\left(5\alpha - \frac{\omega t}{p}\right) - \left(\frac{r}{a}\right)^6 \cos\left(7\alpha + \frac{\omega t}{p}\right) + \cdots\right],$$

$$E_\alpha = -\frac{1}{r}\frac{\partial V}{\partial \alpha} = E_o \frac{2\sqrt{2}}{\pi}\left[-\sin\left(\alpha - \frac{\omega t}{p}\right) - \left(\frac{r}{a}\right)^2 \sin\left(3\alpha + \frac{\omega t}{p}\right)\right.$$

$$\left. + \left(\frac{r}{a}\right)^4 \sin\left(5\alpha - \frac{\omega t}{p}\right) - \left(\frac{r}{a}\right)^6 \sin\left(7\alpha + \frac{\omega t}{p}\right) + \cdots\right],$$

a series of vectors rotating at increasing rates, with alternate directions of rotation and alternate signs by pairs. The deflection is not truly conical but a scalloped cone depending on the initial radius of the beam particle. Since appreciable gaps in α must be provided to insulate adjacent electrodes, the higher multipoles will be somewhat larger than indicated. On the other hand, since the transit time is an appreciable fraction of a period, the rapid rotation of the higher multipoles will tend to average to zero and, more important, they are small near the axis.

The dynamics of deflection is more conveniently treated in (xy) where the fields are:

$$E_x = E_o \frac{2\sqrt{2}}{\pi}\left\{\cos\frac{\omega t}{p} + \frac{1}{a^2}\left[(x^2 - y^2)\cos\frac{\omega t}{p} - 2xy\sin\frac{\omega t}{p}\right]\right.$$

$$\left. + \frac{1}{a^4}\left[(-x^4 - y^4 + 6x^2y^2)\cos\frac{\omega t}{p} + (4xy^3 - 4x^3y)\sin\frac{\omega t}{p}\right] + \cdots\right\}$$

$$E_y = E_o \frac{2\sqrt{2}}{\pi}\left\{\sin\frac{\omega t}{p} + \frac{1}{a^2}\left[(y^2 - x^2)\frac{\sin\omega t}{p} - 2xy\cos\frac{\omega t}{p}\right]\right.$$

$$\left. + \frac{1}{a^4}\left[(-x^4 - y^4 + 6x^2y^2)\sin\frac{\omega t}{p} + (4x^3y - 4xy^3)\cos\frac{\omega t}{p}\right] + \cdots\right\}$$

The equations of motion

$$m\frac{d^2x}{dt^2} = e E_x$$

$$m\frac{d^2y}{dt^2} = e E_y$$

are coupled and too complicated for exact solution. An approximate solution is obtained by integrating twice for the pure dipole field, substituting these x, y into the sextupole term, and integrating this equation once to obtain the deflection angles. For the transit time $(\omega b/pv_o) = \pi$, the approximate (pure dipole) solutions are

$$m\frac{dx}{dt} = e E_o \frac{2\sqrt{2}}{\pi}\frac{p}{\omega}\left[\sin\frac{\omega t}{p} + \cos\frac{\omega t_o}{p}\right]$$

$$m\frac{dy}{dt} = e E_o \frac{2\sqrt{2}}{\pi}\frac{p}{\omega}\left[-\cos\frac{\omega t}{p} + \sin\frac{\omega t_o}{p}\right]$$

$$m x = e E_o \frac{2\sqrt{2}}{\pi}\frac{p^2}{\omega^2}\left[-\cos\frac{\omega t}{p} + \left(\frac{\omega t}{p} - \frac{\omega t_o}{p} + \frac{\pi}{2}\right)\cos\frac{\omega t_o}{p} + \sin\frac{\omega t_o}{p}\right]$$

$$m y = e E_o \frac{2\sqrt{2}}{\pi}\frac{p^2}{\omega^2}\left[-\sin\frac{\omega t}{p} + \left(\frac{\omega t}{p} - \frac{\omega t_o}{p} + \frac{\pi}{2}\right)\sin\frac{\omega t_o}{p} - \cos\frac{\omega t_o}{p}\right]$$

$$\tan\theta = \frac{e E_o 4\sqrt{2}\, p}{m v_o \pi \omega} = \frac{e E_o b 4\sqrt{2}}{m v_o^2 \pi^2}$$

where t_o is the time at which the particle reaches 0. The effect of the sextupole field is three scallops on the cone of trajectories. The amplitude of the scallops is approximately $\Delta\theta$ where

$$\frac{\Delta\theta}{\tan\theta} = \frac{\pi}{2a^2}\left(\frac{e E_o 2\sqrt{2}\, p^2}{m \pi \omega^2}\right)^2$$

$$= \frac{1}{8\pi}\frac{b^2}{a^2}\tan^2\theta .$$

For $\theta = 10^o$ and a maximum error $\Delta\theta/\tan\theta = 0.1$ the deflector radius must be greater than $b/9$, and if it is $b/3$, the error is 10 times less. The effect is not serious. In any case, a symmetrically placed re-deflector cancels the aberration.

11. Parallel Plates in Tandem

There is another solution to the conical scan deflector which uses smaller apertures for a given aberration and hence lower voltages for a given deflection. This consists of two independent sets of parallel plates mutually perpendicular and in tandem. Such a deflector cannot give a cone but it can produce a circular trace at the buncher. The analysis is not given here, being essentially the same as Section 9 above.

12. Twisted Parallel-Plate Deflector

Another conical-scan deflector which can be thought of as the limiting case of parallel-plate pairs in tandem is a pair of parallel plates, twisted with a uniform pitch, so that the field rotated uniformly with z. If the plate separation is small as compared with the pitch, the field is approximately uniform

$$E_x = E_o \cos kz \sin\left(\frac{\omega t}{p} + \phi\right)$$

$$E_y = E_o \sin kz \sin\left(\frac{\omega t}{p} + \phi\right) .$$

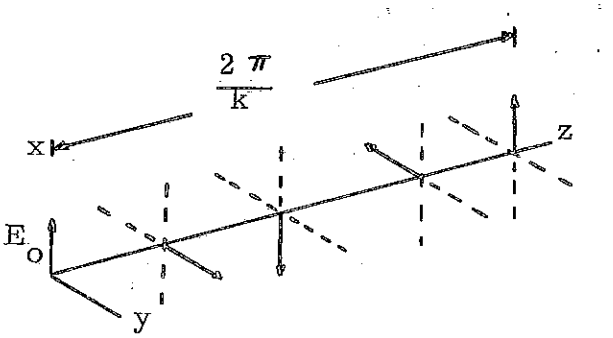

An axial particle of velocity v_o enters the deflector at $t = 0$, $z = 0$ and emerges at $t = T$, $z = b$. The radial velocities at emergence are

$$\dot{x} = \frac{eE_o}{2m}\left\{\left[\frac{1 - \cos\left(\frac{\omega T}{p} + kv_o T\right)}{\frac{\omega}{p} + kv_o} + \frac{1 - \cos\left(\frac{\omega T}{p} - kv_o T\right)}{\frac{\omega}{p} - kv_o}\right]\cos\phi\right.$$

$$\left. + \left[\frac{\sin\left(\frac{\omega T}{p} + kv_o T\right)}{\frac{\omega}{p} + kv_o} + \frac{\sin\left(\frac{\omega T}{p} - kv_o T\right)}{\frac{\omega}{p} - kv_o}\right]\sin\phi\right\}$$

$$\dot{y} = \frac{eE_o}{2m}\left\{\left[\frac{1 - \cos\left(\frac{\omega T}{p} + kv_o T\right)}{\frac{\omega}{p} + kv_o} - \frac{1 - \cos\left(\frac{\omega T}{p} - kv_o T\right)}{\frac{\omega}{p} - kv_o}\right]\sin\phi\right.$$

$$\left. - \left[\frac{\sin\left(\frac{\omega T}{p} + kv_o T\right)}{\frac{\omega}{p} + kv_o} - \frac{\sin\left(\frac{\omega T}{p} - kv_o T\right)}{\frac{\omega}{p} - kv_o}\right]\cos\phi\right\}.$$

For a conical scan $\dot{x}/\dot{y} = \pm \tan(\phi - \phi_o)$ which gives three types of solutions

a) $kv_o = \omega/p$ with $\omega T/p = \pi n$, $n = 1, 2, \cdots$

$$\dot{x} = \frac{eE_o}{2m} \pi n \frac{p}{\omega} \sin \phi$$

$$\dot{y} = \frac{eE_o}{2m} \pi n \frac{p}{\omega} \cos \phi \quad .$$

In this arrangement the velocities continue to grow with the length: the x and y impulses are in step with the particle everywhere, a sort of synchronous deflecting mode.

b) $\omega T/p - kv_o T = 2\pi n$, $n = 1, 2, \cdots$

$$\dot{x} = \frac{eE_o}{2m} \frac{1}{\frac{\omega}{p} + kv_o} \cos (\phi - \phi_o)$$

$$\dot{y} = \frac{eE_o}{2m} \frac{1}{\frac{\omega}{p} + kv_o} \sin (\phi - \phi_o)$$

$$\tan \phi_o = \frac{\sin (\frac{\omega T}{p} + kv_o T)}{1 - \cos (\frac{\omega T}{p} + kv_o T)} \quad .$$

c) $\omega T/p + kv_o T = 2\pi n$, $n = 1, 2, \cdots$

$$\dot{x} = \frac{eE_o}{2m} \frac{1}{\frac{\omega}{p} - kv_o} \cos (\phi - \phi_o)$$

$$\dot{y} = -\frac{eE_o}{2m} \frac{1}{\frac{\omega}{p} - kv_o} \sin (\phi - \phi_o)$$

$$\tan \phi_o = \frac{\sin (\frac{\omega T}{p} - kv_o T)}{1 - \cos (\frac{\omega T}{p} - kv_o T)} \quad .$$

For (b) and (c) the deflection does not grow with n. Solutions (a) give the largest deflections for a given E_o and b, and the deflection of

solutions (c) is the weakest. We also note that the twist is greatest for solutions (a), and the aberrations, which are related to the twist, are largest for (a). However, the synchronous mode (a) seems to be the most attractive for an actual design.

There are two kinds of aberrations produced by a twisted field. One is the lack of conical symmetry of the deflections (x_1, y_1) at emergence even though the velocities are without aberration; this is inherent in the twisted plates in lowest approximation. The second kind is a velocity aberration induced by the nonuniformity of the field across the aperture because of the twist. That is, a twisted uniform field cannot, in fact, be produced because it is not a solution of Laplace's equation. We consider the deflection aberration first.

For solutions (a) with $kv_o = \omega/p$ and $\omega T/p = \pi n$, the deflections at emergence for a uniform, twisted field, are

$$x_1 = \frac{eE_o}{2m} \frac{p^2}{2\omega^2} n\pi \, (\cos\phi + n\pi \sin\phi)$$

$$y_1 = \frac{eE_o}{2m} \frac{p^2}{2\omega^2} n\pi \, (\sin\phi + n\pi \cos\phi) .$$

The variation of $r_1 = (x_1^2 + y_1^2)^{1/2}$ with ϕ is an aberration. The magnitude of the aberration is

$$\frac{|\Delta r_1|_{max}}{(r_1)_{av.}} = \frac{n\pi}{1 + n^2\pi^2}$$

which is largest for $n = 1$ and varies approximately as $1/n$. Figure 11 shows the deflections for the worst ($n = 1$) case. We note, in particular, that a particle which enters when the field is a maximum ($\phi = \frac{\pi}{2}$) does not undergo a pure x deflection although its radial velocity at emergence is along x. For large n, this distortion disappears and r_1 becomes a circle.

While the effect is large in a relative sense for small n, it is not necessarily serious since the deflections (x_1, y_1) are usually small as compared with the deflections produced by drift with velocities (v_x, v_y) which are, in the uniform field approximation, without aberrations.

Now we consider the velocity aberrations. As we mentioned, a twisted uniform field is not a solution of Laplace's equation, but it can be the dominant term in a true solution. Write the potential as

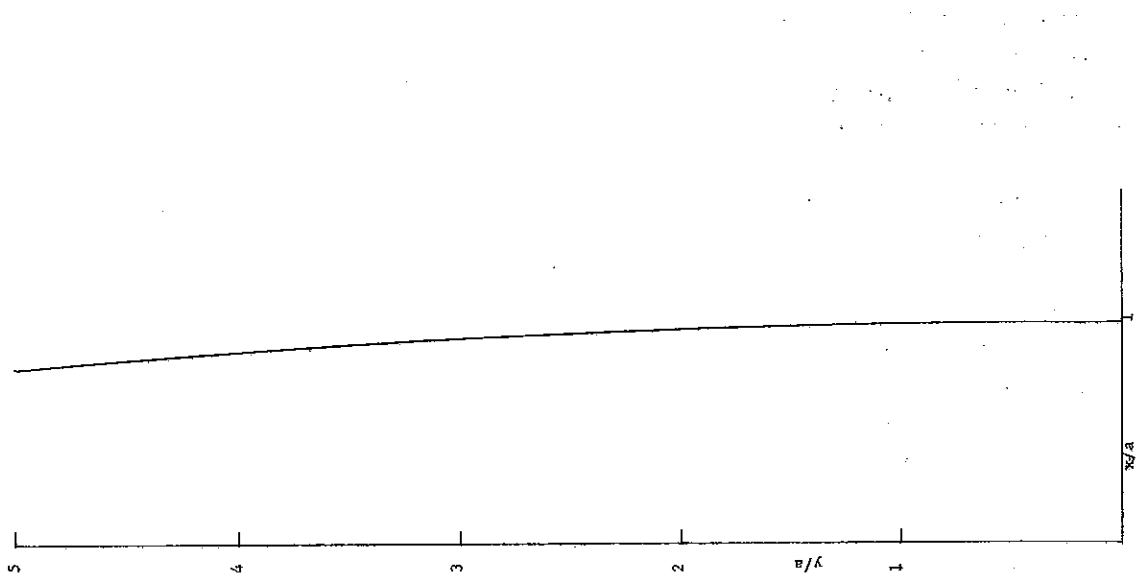

Fig. 12 - Plate shape for a pure $I_1(kr)$ field with $ka = \frac{1}{4}$

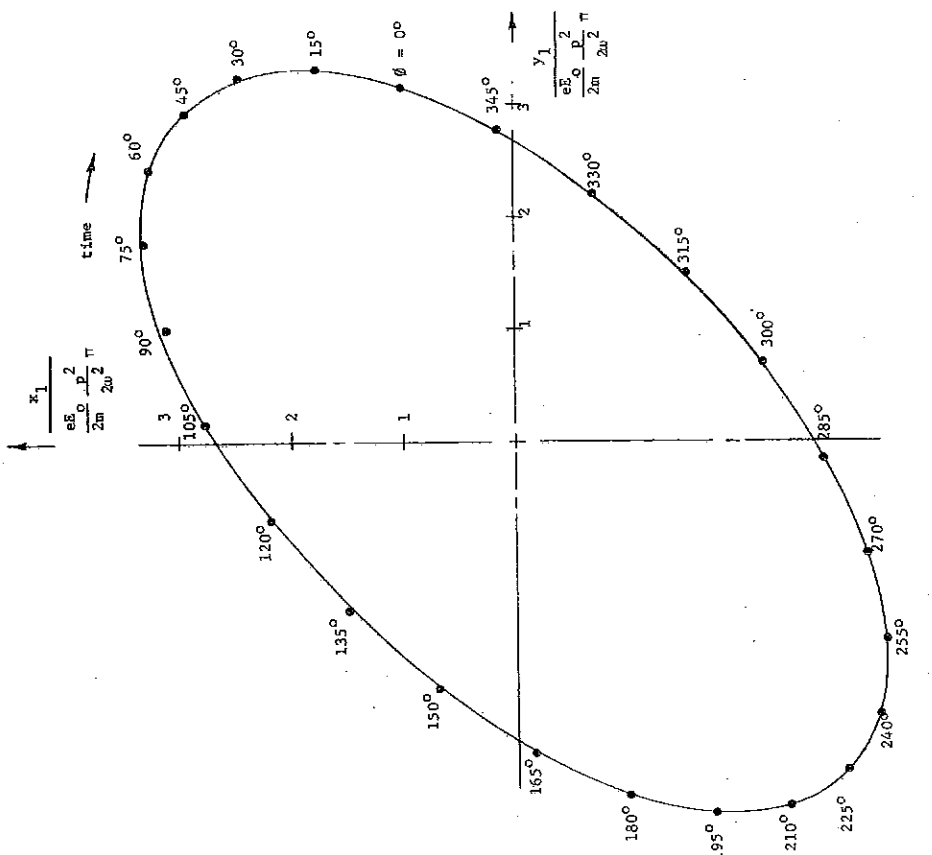

Fig. 11 - Deflections on emergence from twisted plate deflector for n = 1. Points labeled with entrance phase.

$$V = - E_o f(r) \cos(\theta - kz) \sin\left(\frac{\omega t}{p} + \phi\right)$$

where $f(r) \to r$ as $r \to 0$. With this V, Laplace's equation in cylindrical coordinates is

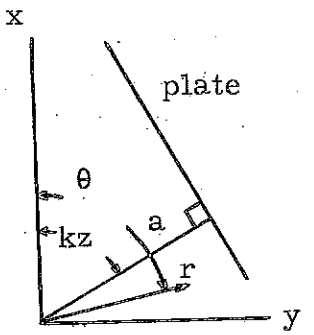

$$\frac{d^2 f}{dr^2} + \frac{1}{r}\frac{df}{dr} - \left(k^2 + \frac{1}{r^2}\right) f = 0 ,$$

the modified Bessel equation with solutions

$$f = S_1 I_1 (kr) .$$

Setting the plate potential at $- V_o$ for $\theta = kz$, $r = a$

$$V = - \frac{V_o}{I_1 (ka)} I_1 (kr) \cos(\theta - kz) \sin\left(\frac{\omega t}{p} + \phi\right) .$$

If $ka << 0$, $I_1 (ka) \cong ka/2$ and

$$V \cong - V_o \frac{r}{a} \left\{1 + \frac{1}{8} k^2 r^2 + \frac{1}{192} k^4 r^4 + \cdots\right\} \cos(\theta - kz) \sin\left(\frac{\omega t}{p} + \phi\right) .$$

The plates must be shaped to give this solution, and the polar equation of the plates is obtained by setting $V = - V_o$. Figure 12 shows the plate shape for $2\pi/k = 24$ cm, $a = 3/\pi$ cm, i.e., $ka = 1/4$.

Assume that the plates are shaped to give a pure $I_1 (kr)$ solution. We wish to know the aberration produced by the terms in r^3, r^5, etc. Keeping only the term in r^3

$$E_x = E_o \left\{ \cos kz + \frac{1}{8} k^2 (3 x^2 + y^2) \cos kz \right\} \sin\left(\frac{\omega t}{p} + \phi\right)$$

$$E_y = E_o \left\{ \sin kz + \frac{1}{8} k^2 (3 y^2 + x^2) \sin kz \right\} \sin\left(\frac{\omega t}{p} + \phi\right) .$$

The equations of motion can be solved, as before, by iteration. When this is done for a twist such that $kv_o = \omega/p$, we find that the emergence velocities are of the form

$$\dot{x} = \frac{eE_o}{m} \frac{p}{\omega} \left\{ \frac{1}{2} n\pi + \frac{1}{8} k^2 \left(\frac{eE_o}{2m} \right)^2 \frac{p^4}{\omega^4} F(\phi) \right\}$$

where $|F(\phi)| < 10$ for all ϕ. For a 10^o deflection with $p = 4$, $n = 1$, the second term is about two thousandths of the first term. The conical aberrations due to the velocity are thus negligible.

Even so, the pure $I_1(kr)$ solution is not the best for small aberrations. Consider the general potential of a uniformly twisted field

$$V = - E_o f(r) \cos n(\theta - kz) \sin \left(\frac{\omega t}{p} + \phi \right)$$

which obeys

$$\frac{d^2 f}{dr^2} + \frac{1}{r} \frac{df}{dr} - \left(n^2 k^2 + \frac{n^2}{r^2} \right) f = 0$$

with solutions

$$f = S_n I_n (n kr), \quad n = 1, 3, 5 \cdots .$$

The general solution is, therefore,

$$V = - \sum_{n=1, 3 \cdots} S_n I_n (n kr) \cos n(\theta - kz) \sin \left(\frac{\omega t}{p} + \phi \right)$$

with

$$\frac{V_o}{E_o} = S_1 I_1 (ka) + S_3 I_3 (3 ka) + \cdots .$$

We can choose the constants S_n in various ways. We can eliminate the terms $r^n \cos(\theta - kz)$ for $n = 3, 5, \cdots$ by setting $S_3 = S_1/27$, $S_5 = S_1/125$, $\cdots$. The aberrations are then confined to terms of the type $r^n \cos^m (\theta - kz)$ with $n = 3, 5, \cdots$, $m = 3, 5, \cdots n$, with smaller coefficients than with the pure $I_1(kr)$ solution as well as smaller contributions by the integrals. An optimum choice requires detailed computations which we have not carried out.

13. Twisted Ribbon Deflector

As we shall see in Section 18, the twisted-plate deflector suffers from an asymmetric fringing field which causes unwanted bunching. This suggests a hybrid device which combines the best features of the twisted-plate and the segmented-cylinder deflectors. It would consist of p conducting ribbons wound helically on a cylinder and driven with the

usual push-pull voltages. The dominant deflecting field would be approximately uniform over the aperture and by rotating in both time and space it could give synchronous deflection.

Write for this dominant term

$$E_x = E_o \cos \left(\frac{\omega t}{p} + kz + \phi\right)$$

$$E_y = E_o \sin \left(\frac{\omega t}{p} + kz + \phi\right) .$$

As written, the expression gives clockwise rotation with t. If $k > 0$, the helix is clockwise also. The synchronous solution occurs for $kv_o = - w/p$. Then, since $z = v_o t$

$$\dot{x} = \frac{eE_o t}{m} \cos \phi$$

$$\dot{y} = \frac{eE_o t}{m} \sin \phi$$

$$x = \frac{eE_o t^2}{2\,m} \cos \phi$$

$$y = \frac{eE_o t^2}{2\,m} \sin \phi .$$

The device has unit transit time factor, can be cut to any length, and has E, r, and $\dot{r}$ in phase everywhere. The counter directions of rotation of E in t and z means that the particle sees a uniform E as it proceeds along z. The scan is purely conical.

The device also has other solutions, some of which may be very useful. It is possible to cancel $\dot{r}$ while preserving r and thus to scan conically without radial velocities. This removes the necessity for a lens. An obvious way to do this is to place two identical deflectors in tandem with the second one out of phase by π with the first. The second removes the $\dot{r}$ but allows r to grow to twice its value at the exit of the first deflector. At the transition between the two there is a natural bunching gap.

Another way to achieve zero $\dot{r}$ is to operate nonsynchronously. Let $kv_o = - f\,\omega/p$ where $0 < f < 1$. If we set $(1 - f)\,\omega T/p = 2\,\pi\,n$, where n is an integer and T is the emergence time, we find on emergence that

$$\dot{x}_1 = \dot{y}_1 = 0$$

$$x_1 = -\frac{eE_o}{m}\frac{T^2}{2\pi n}\sin\phi$$

$$y_1 = \frac{eE_o}{m}\frac{T^2}{2\pi n}\cos\phi \ .$$

The deflection is greatest for $n = 1$. The vector r_1 rotates in the same sense as E at emergence and is perpendicular to it, leading by $\pi/2$. If now we place in tandem an identical device, the second out of phase by π, (i.e. reversed voltages), the particles crossing the gap between them are bunched by the fringing fields between facing electrodes. The bunching is correct (early particles are decelerated) and, with some electrode shaping near the gap, this simple system may incorporate all of the desirable features of a conical scan subharmonic buncher. We have not yet studied any of the more complex features of such a system.

14. Rf Drive for Deflectors

The excitation of either the one-dimensional, four-plate conical scan or twisted-plate deflectors should be push-pull, balanced to ground. Since the voltages are high, the circuits should be resonant. In the region of 50 Mc/s where the $p = 4$ deflector operates, coaxial lines are convenient elements. A possible design can be derived from a half-wave line open at both eneds, with a plate attached to each end and the line folded to bring the plates together. The device is push-pull with respect to the outer conductor. For the four-plate deflector, two such circuits could be arranged to feed two pairs of push-pull plates in time quadrature. Because of the crossed polarization, the interaction will be small even though the E fields occupy the same space.

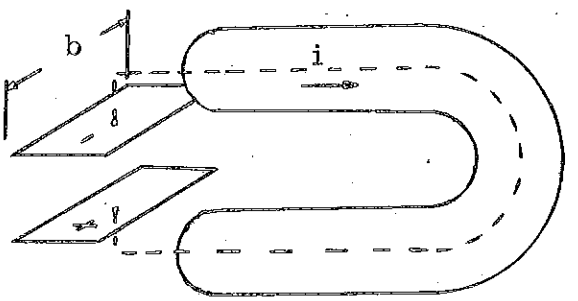

15. Lenses

For one-dimensional deflection the lens should be a true lens in the sense that it have the same focal length for all deflection angles. There are a variety of well-known electric and magnetic lenses which have this property for small angles and some which are quite good up to the maximum angles of interest here. In general, they will not be exactly isochonous if they focus exactly, and conversely. These aberrations should be examined in any serious design, but we have not done so.

We have considered in more detail lenses for the conical scan arrangement. Here, since the cone angle is almost constant, the lens may have large aberrations for angles other than the cone angle; the important property to preserve is isochronism as a function of the azimuth angle. Since lenses which are figures of revolution are automatically isochronous in this sense, we have considered two such types which show some promise: coaxial electrostatic systems and magnetic solenoids.

Consider a lens of two coaxial circular cylinders with potentials $\pm V$ of the correct magnitude to give a symmetrical path. The first integral of the equation of motion is

$$\dot{r}^2 - \dot{r}_o^2 = - \frac{4\,eV}{m \ell n \frac{R_2}{R_1}} \ell n \frac{r}{r_o},$$

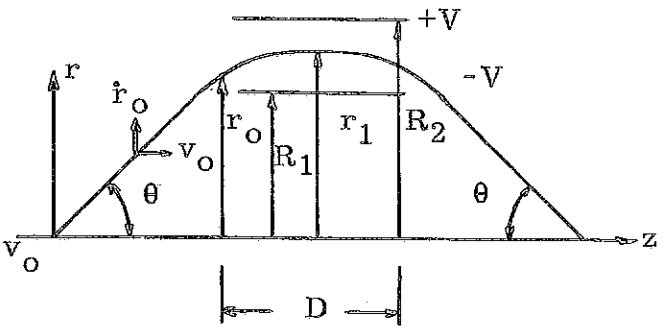

which determines the potential from

$$\frac{2\,eV}{\frac{1}{2} m v_o^2} = \tan^2 \theta \, \frac{\ell n \frac{R_2}{R_1}}{\ell n \frac{r_1}{r_o}} .$$

The second integral can be written

$$\frac{D}{v_o} \sqrt{\frac{eV}{\ell n \frac{R_2}{R_1}}} = 2 r_1 \int_o^{w_o} e^{-w^2} dw = r_1 \sqrt{\pi}\ \mathrm{Erf}\,(w_o)$$

which determines the length D, where $w^2 = \ell n \frac{r_1}{r}$.

There are many other coaxial systems, all with rather similar properties. For the angles θ of interest here, the well-known concentric-sphere-segment lens is not attractive since it is too short and hence requires very large potentials. There is a large family of shapes intermediate between spheres and cylinders which consist of various arcs rotated around z. None of those examined have any important advantages over the cylinder lens.

All of these coaxial electrostatic systems have one serious technical difficulty - the support of the center electrode which lies completely inside the beam sheath. It could conceivably be cantilevered from a ground plane (perhaps part of the buncher) whose annular beam slot was not complete but rather segmented. This appears very unattractive, particularly if the electrode is at a large negative potential, which requires an insulated cable crossing the beam sheath.

Solenoids avoid this difficulty since the coil can be completely external. Consider a uniform axial field B. A particle deflected through angle θ describes a helix on a cylinder of radius R where

$$B = \frac{mv_o \, c \tan \theta}{eR}$$

and

$$L = \frac{2 \pi R}{\tan \theta} \quad .$$

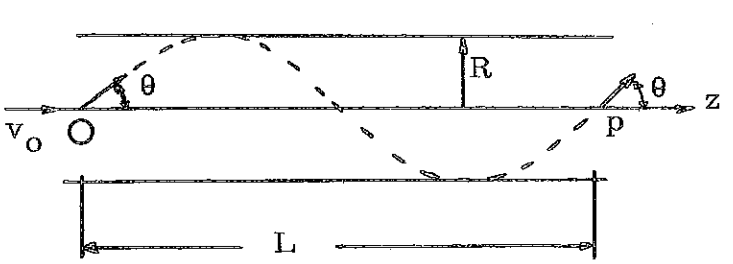

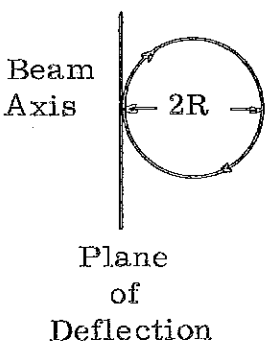

As the beam is scanned conically at frequency ω/p, the cylinder rotates in the same sense and at the same frequency, and the original beam cone is reconstructed at point P. The inside diameter of the solenoid coil must be at least 4 R. The plane of the bunching gaps can be anywhere between P and the 0 to P midpoint, and any radius of the bunching annulus from zero to 2 R can be arranged, depending on this position. For $\theta = 10^{o}$ and $\frac{v}{c}\Omega = 0.04$ a possible design choice is R = 10 cm, B = 2200 gauss, L = 360 cm. For an air solenoid the required current density in the winding would be about 2400 A/cm^2, which is feasible. Iron cladding could improve the efficiency, and there is no necessity for uniformity of B with either r or z so long as the field is axially symmetric.

As a lens, an ideal solenoid reconstructes the input transverse phase space. Thus it acts like a thin lens of unit magnification and focal length L/4.

Lenses which are not figures of revolution, such as electric or magnetic strong focusing triplets, may be sufficiently isochronous. They have one important property; for feasible fields they can have short focal lengths and so permit close spacing between the buncher and redeflector while preserving a large beam radius at the buncher. However, it is just this condition (large θ) which enhances the lack of isochronism. In a serious design these conflicting properties should be studied but we have not done so. As we shall see in the next section, the buncher - redeflector spacing is one of the most difficult problems in the whole scheme, and a successful design must minimize this spacing by a careful choice of the lens system and the transverse beam optics.

16. Redeflection Errors

One of the serious difficulties in the whole scheme is the angle errors introduced at the redeflector arising from the fact that the beam is partially bunched when it is redeflected. The errors are small for long drift lengths and short buncher - redeflector spacings but there are technical limits on both of these and near these limits the errors are not negligible.

Consider a conical scan beam converging to P from the bunching gap G. If the bunching is made correct at Q, the arrival phase at P is

$$\phi = t + \frac{z_o}{\ell} \frac{\pi}{\sin \frac{\pi}{p}} \cos\left(\frac{\omega t}{p} - \frac{2\pi k}{p} + \frac{\pi}{p} + \frac{\pi}{2} \right) + C \ .$$

At P the transverse velocities are

$$v_x = -v_o \tan\theta \sin\frac{\omega t}{p}$$

$$v_y = -v_o \tan\theta \cos\frac{\omega t}{p} \quad .$$

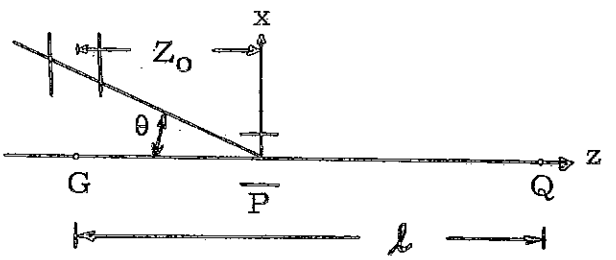

With the redeflector we add the velocities

$$v'_x = v_o \tan\theta' \sin\frac{\phi}{p}$$

$$v'_y = v_o \tan\theta' \cos\frac{\phi}{p} \quad .$$

If $z_o = 0$, $\tan\theta = \tan\theta'$, and $C = 0$, the beam is redeflected without errors. We find that no adjustment of phase (i.e., C) or amplitude (i.e., $\tan\theta'$) reduces the errors, so we remove this generality by setting $C = 0$, $\tan\theta = \tan\theta'$ and write for the angle errors,

$$\Delta\theta_x = \frac{v'_x + v_x}{v_o} = \tan\theta \left(\sin\frac{\phi}{p} - \sin\frac{\omega t}{p}\right)$$

$$\Delta\theta_y = \frac{v'_y + v_y}{v_o} = \tan\theta \left(\cos\frac{\phi}{p} - \cos\frac{\omega t}{p}\right) .$$

Figure 13 shows the angle errors for $p = 4$, $z_o/\ell = 0.1$ as a function of $\frac{\omega t}{p}$ for one complete scan. The points are labeled with $\omega t/p$ values to show the variation in time. The discontinuities in the errors make it essentially impossible to compensate them by changes in the voltage waveform. For the case of Fig. 13 the maximum angle error is $0.078 \tan\theta$ or 0.8^o for $\theta = 10^o$.

For angle errors up to a few degrees, the errors are linear in z_o/ℓ. Thus for $p = 4$, $z_o/\ell = 0.2$ the maximum error is $0.156 \tan\theta$.

These redeflection-angle errors add randomly to the beam emittance angles and hence the transverse phase space of the beam is degraded. This can be serious, depending on the design of the linac and the tolerances on its output beam quality.

Although complex voltage waveforms at the redeflector are not effective in reducing the errors, a second conical scan redeflector near the first linac gap is of some help. At the bunching point Q all of the particles on a single arc of Fig. 13 are essentially simultaneous. The addition of a small deflection voltage equal to the radius of the arc and

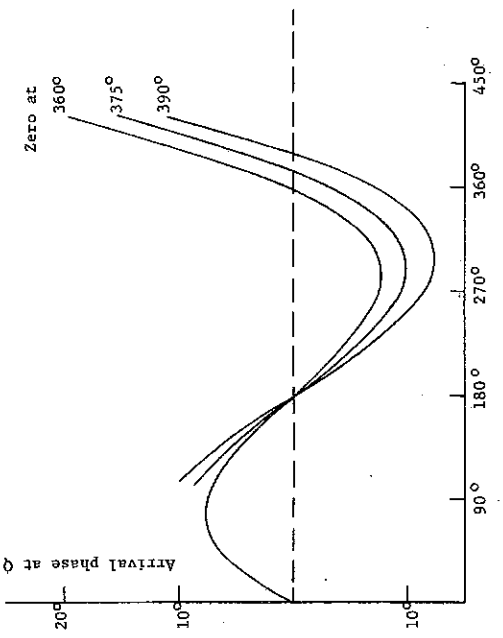

Fig. 14 - Arrival phase for a p = 4 buncher for several choices of the phase at the outer zeros.

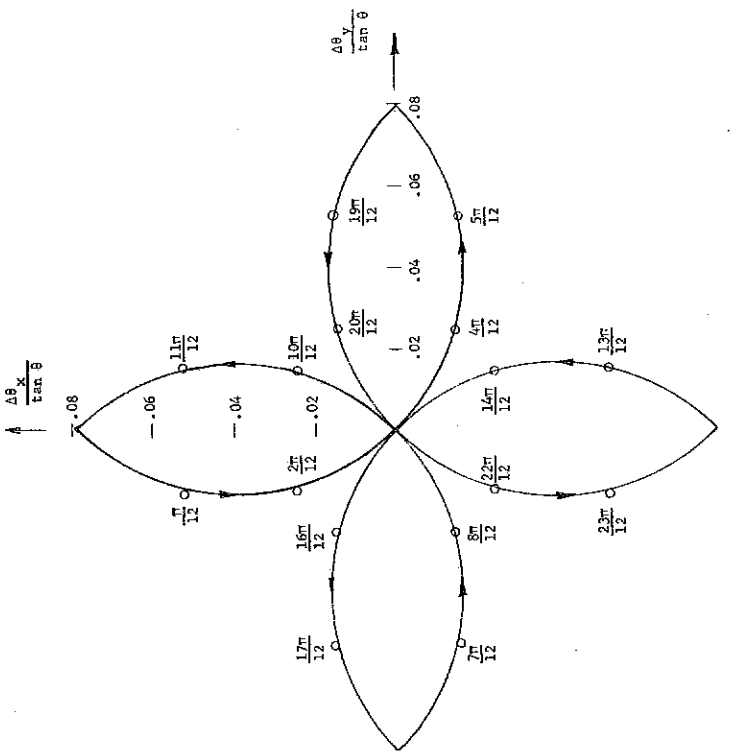

Fig. 13 - Redeflection-angle errors for a fourth-subharmonic conical-scan redeflector located at one-tenth of the drift length for bunching.

of frequency $\omega t/p$ converts Fig. 13 into a circle of radius $0.078 \tan \theta/\sqrt{2}$ and thus reduces the errors by a factor $\sqrt{2}$.

17. The Buncher

For conical deflection the buncher is a set of p annular segments of mean radius R_B, each differing in phase from its neighbor by $2\pi/p$, where ω/p is the scanning and bunching frequency. The ratio of the arc length of a segment to the beam diameter should be large enough so that the beam does not spend too much time overlapping adjacent segments. It is not necessary to reduce this time to an extremely small value since the phase regions just outside the ideal boundaries are no worse than those just inside. For example, for p = 4 (see Fig. 8), the maximum arrival phase error (7.5°) which occurs at $\omega t = 285^\circ$ is not exceeded until ωt reaches 390°. If it is so arranged that at $\omega t = 360^\circ$ the beam center crosses to the next segment and at 390° the trailing edge crosses, then the diameter of the beam is equal to $\frac{\pi}{12} R_B$. If the beam diameter is 1 cm, then R_B must be at least 3.82 cm.

If it is desired to use larger beam diameters (or smaller buncher radii), the arrival phase error can be optimized by choosing a bunching voltage which gives a zero in arrival phase at an ωt somewhat greater than 360° with some sacrifice in the maximum arrival phase error. This is shown in Fig. 14. If, for the p = 4 case, we place the arrival phase zeros at -15°, 180°, 375°, the maximum arrival phase errors is $\pm 10^\circ$, which is not exceeded until ωt reaches 408°. Thus the usable phase overlap is increased from $390^\circ - 360^\circ = 30^\circ$ to $408^\circ - 360^\circ = 48^\circ$ with a corresponding increase in the allowable beam diameter.

For subharmonic bunchers the low frequency and the electrode complexity make drift tube bunchers attractive. For even p the electrodes at opposite ends of a bunching circle diameter are push-pull balanced to ground. Thus the buncher circuits can be the same half-wavelength folded coax that were suggested for the deflector. The two bunching gaps are separated by half a period of ω/p which is a length $\beta_0 \lambda\, p/2$. For p = 4, the maximum electrode-to-electrode voltage is $\sqrt{2}$ times the voltage to ground and gap g_2 must exceed g_1. For p = 6, these voltages are equal, and for larger p the electrode-to-electrode voltage continues to diminish. The region of the beam sheath deleted by the gaps g_2 can be used on the ground plane for radial straps to support its central disk. Because of the circuit balance, no current flows on these straps. The central annuli of the buncher electrodes require similar straps from the outside annuli; these radial grids will be needed anyhow for good beam dynamics. Such grids will carry current.

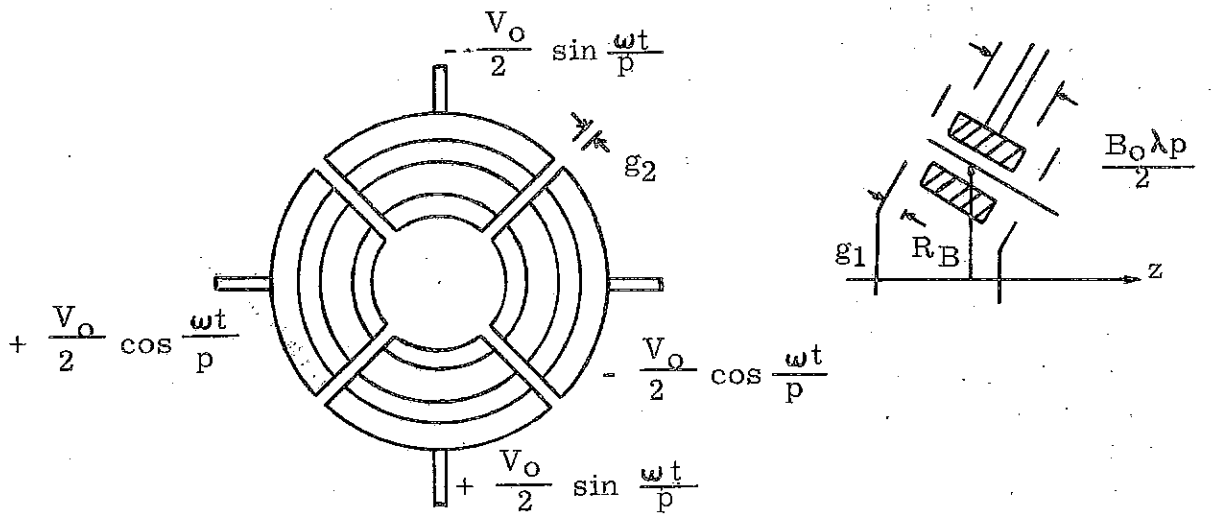

18. Bunching Due to End Effects in the Deflectors

When one attempts to formulate an actual design, it is found that the deflection fields are larger than typical bunching fields. This suggests that the ever present E_z at the ends of a deflector can give a large, and probably undesirable, bunching effect. If we neglect the beam diameter, these effects will occur only at the exit of the deflector and entrance of the redeflector for deflectors which are balanced to ground and hence have $E_z = 0$ on the z axis.

The segmented-cylinder deflector appears to be relatively free of such bunching effects. In the rotating dipole approximation the deflections at emergence (with $\omega b/pv_o = \pi$) are

$$x_1 = \frac{eE_o}{m}\frac{2\sqrt{2}}{\pi}\frac{p^2}{\omega^2}\,2\left(\sin\frac{\omega t_o}{p} + \frac{\pi}{2}\cos\frac{\omega t_o}{p}\right)$$

$$y_1 = \frac{eE_o}{m}\frac{2\sqrt{2}}{\pi}\frac{p^2}{\omega^2}\,2\left(-\cos\frac{\omega t_o}{p} + \frac{\pi}{2}\sin\frac{\omega t_o}{p}\right)$$

which is a constant radial deflection rotating around z with frequency ω/p and a constant phase delay relative to the deflecting field which it

encounters as it emerges. Hence each particle encounters the same fringing field relative to its path and the end effect is equivalent to a dc acceleration and of no importance. The higher multipoles do not behave in this cooperative manner. However, their size can be suppressed by a large aperture-to-deflection ratio and in addition they will fall off more rapidly with z than does the dipole field. We have not actually calculated their residual bunching effects.

The twisted plate deflector has a relatively large and undesirable bunching effect in lowest approximation. The fringing field does not rotate but merely oscillates in time and each ray on the emergent cone receives a different z impulse. Particles which emerge with maximum $\pm$ x deflection traverse the fringing field when it is a time maximum and are decelerated along z, whereas particles with maximum $\pm$ y deflection lie in the plane of zero E_z and also cross near the time zero. The deflector acts like a buncher of frequency $2\omega/p$.

If the z impulses were not too large, they could be compensated in a four-gap buncher by operating the two $\pm$ pairs at different voltages. However, the effect is large. It can be calculated if the fringing field shape is known. For parallel plates spaced by 2 a with potentials $\pm V_o$ the potential is given by a Schwartz-Christoffel transformation of a segmented plane, and can be written

$$\pi \frac{x}{a} = 1 + \ell n \left[\frac{\pi (V/V_o - z/a)}{\sin \pi (V/V_o + 1)} \right] + \left[\frac{\pi (V/V_o - z/a)}{\sin \pi (V/V_o + 1)} \right] \cos \pi (V/V_o + 1)$$

where the origin of x, y is in the median plane in-line with the edge of the plates. Figure 15 shows some of the equipotentials and a typical exit trajectory. Since the latter crosses some of the equipotentials, there is a z impulse. For the example shown a numerical integration gives

$$mv_o \Delta v_z \cong - 0.3\ eV_o$$

which is clearly intolerable since V_o is always larger than the peak voltage of the proposed bunchers. It is possible, but unlikely, that plate shaping or auxiliary electrodes in the fringing gap could lower substantially this z impulse. The same conclusions hold for simple one-dimensional deflection by parallel plates.

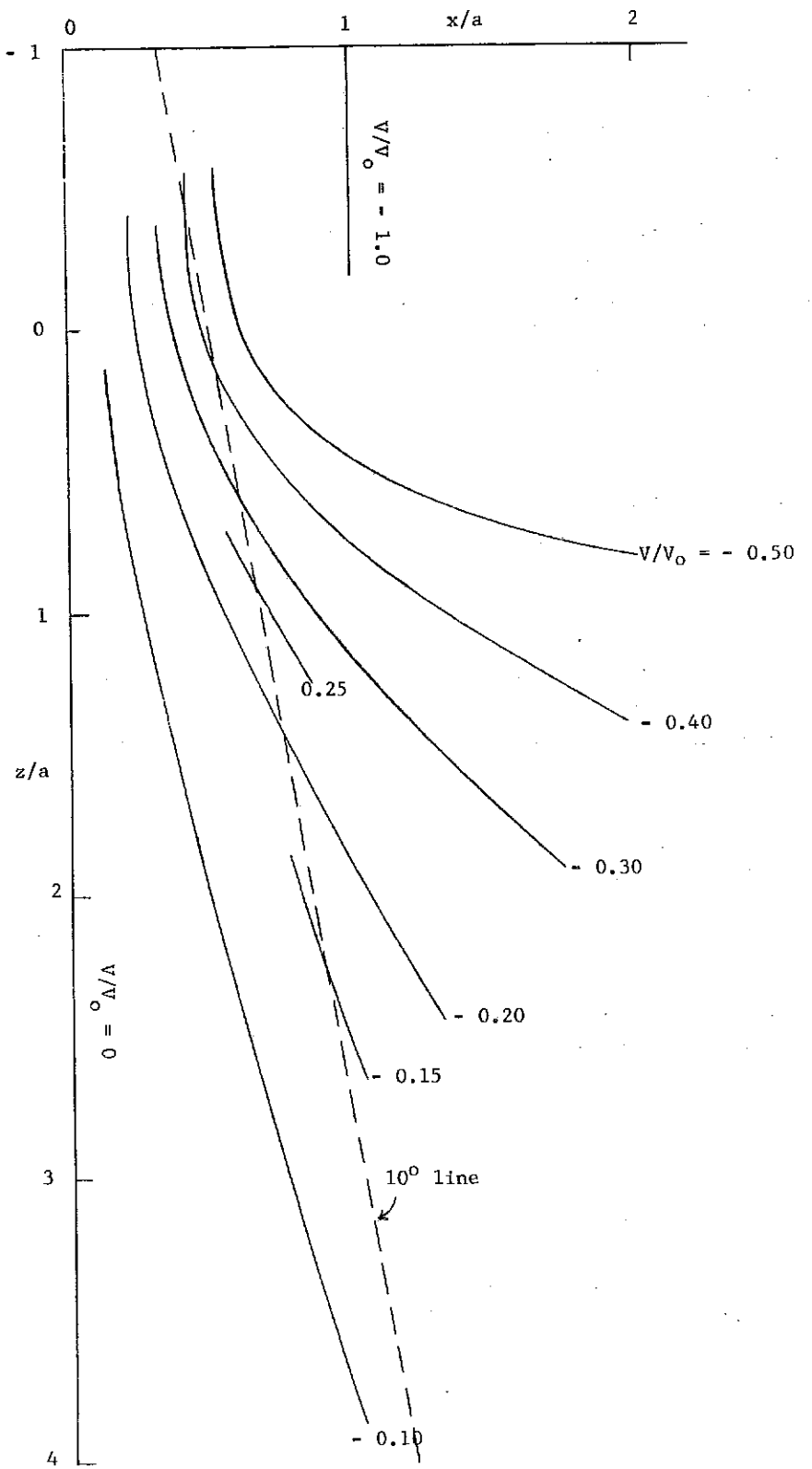
0
1
x/a
2
- 1
0
1
2
3
4
z/a
V/V$_o$ = - 1.0
0 = $^o\Delta/\Delta$
V/V$_o$ = - 0.50
- 0.40
- 0.30
- 0.20
- 0.15
- 0.10
0.25
10^o line

Fig. 15

19. Remarks

We have made some attempts to put together the various devices discussed into a system. These attempts have not been very successful because of the conflicting requirements and inadequacies of the components. Chief among these are (a) unwanted bunching by the deflection fields, (b) very high fields in the deflectors, and (c) redeflection errors. It is too early to be sure that these cannot be resolved and it is to be hoped that they can, for the general principle seems both sound and attractive. At this time the simple system of two nonsynchronous twisted ribbon deflectors seems to warrant careful study.

WHEELER: The engineering problems on this tailless buncher are formidable, but a good deal of thought has been given to them and it seems that reasonable solutions are at least possible.

MARTIN, J. H.: I do not want to deviate our discussion too far from linacs, but occasionally linacs are used to feed other machines, such as synchrotrons, and in ours, for example, we would like to be able to chop a beam or do something like this at something like 4 Mc. Now I have also heard of plasma oscillations occurring in ion sources in the few megacycles region and heard of people talking about bona fide chopping devices and so forth. Now I am wondering if anyone has ever tried to take advantage of plasma oscillations in an ion source in such a way that you actually chop the beam at the ion source at frequencies like 5 Mc?

WHEELER: Not that I have heard of.

VAN STEENBERGEN: I think at the AGS we have been most pronouncedly plagued in the past with those particular oscillations and we had a number of observations on them. It is not a single frequency, it is a whole pattern of frequencies and it is not predictable in the sense that one could use a particular frequency.

MARTIN: Well, if this kind of oscillation occurs as in certain kinds of electronic circuitry, you can encourage it to oscillate, usually at one single frequency, so I am proposing here essentially to drive an ion source at a frequency of your choosing and a phase of your choosing.

WHEELER: When are you going to try it?

MARTIN: Maybe we will get to it.

LAPOSTOLLE: Well, I will only comment to say that this (the tailless buncher) may be a difficult scheme to realize, but it is very similar to an rf separator, and rf separators are being built. I don't think it will be so much of a difficulty to built such a device.

WHEELER: I think its virtues are worth a good deal of effort.

REFERENCES

1. J. E. Leiss, Conference on Proton Linear Accelerators, Yale University October 21-25, 1963, p. 267.

2. S. Ohnuma, ibid., p. 273.

3. R. Perry, ibid., p. 279.

4. R. Beringer, Yale Design Study Technical Note RB-1, October 26, 1963.

5. M. Plotkin, private communication.

6. L. Smith, Handbuck der Physik, Vol. XLIV, p. 371.

7. Yale Study on High Intensity Proton Accelerators, Final Report, April 1964.

NIMROD INJECTOR

N. D. West
Rutherford High Energy Laboratory

(Presented by H. Wroe)

General Status

The Nimrod Injector is at present operating with a 600 keV proton beam current of 38 mA which, with the buncher, gives 18 mA at 15 MeV. The maximum 15 MeV beam current achieved has been 24 mA.

Emittance plots of the 600 keV and 15 MeV beams are shown in Fig. 1. An estimated 90% of the 600 keV beam current can be contained within an ellipse of area 7 π cm-mrad, and 90% of the 15 MeV beam within an ellipse of area 3.3 π cm-mrad.

The 600 keV beam is currently badly misaligned from the axis of the dc accelerating column, and this fact, together with the effect of aberrations, would explain the asymmetries of the 600 keV emittance. The accelerating column assembly, however, can be steered to align the beam on to the linac axis.

The mode of operation at present is to set up the injector to a standard beam condition. This means that all controls are set to predetermined levels. The 15 MeV beam current produced under these standard conditions is usually within 10% of the nominal, from week to week. The alignment of the beam as it leaves the linac is checked occasionally by means of a pair of four-jaw defining apertures. The results of the measurement are used to calculate the adjustments to a set of four steering magnets required to align the beam to the axis. The misalignments found are usually small, and the beam is only realigned infrequently.

Multipactor Experience

The occurrence of multipactoring in the Nimrod injector linac and the method of inhibiting it by coating the drift-tube faces with carbon black were reported at the Brookhaven Linear Accelerator Conference in 1962. Since then, it has been found possible to leave the faces of the first ten drift tubes uncoated, and to coat the remaining drift-tube faces only over four small areas, corresponding roughly to the positions of the quadrupole pole tips. This has considerably reduced the sparking problem. The effectiveness of the carbon black is demonstrated by the

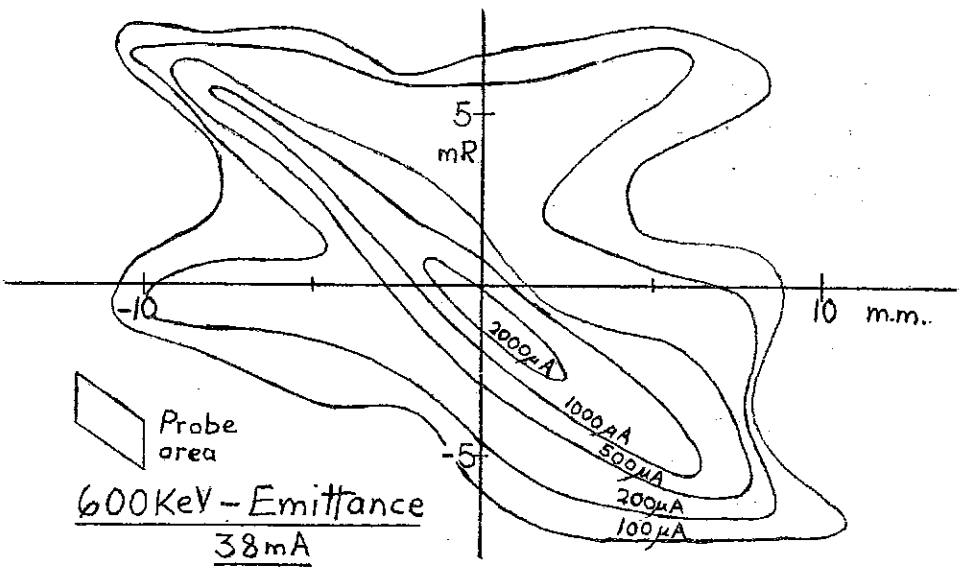

600 KeV – Emittance
38 mA

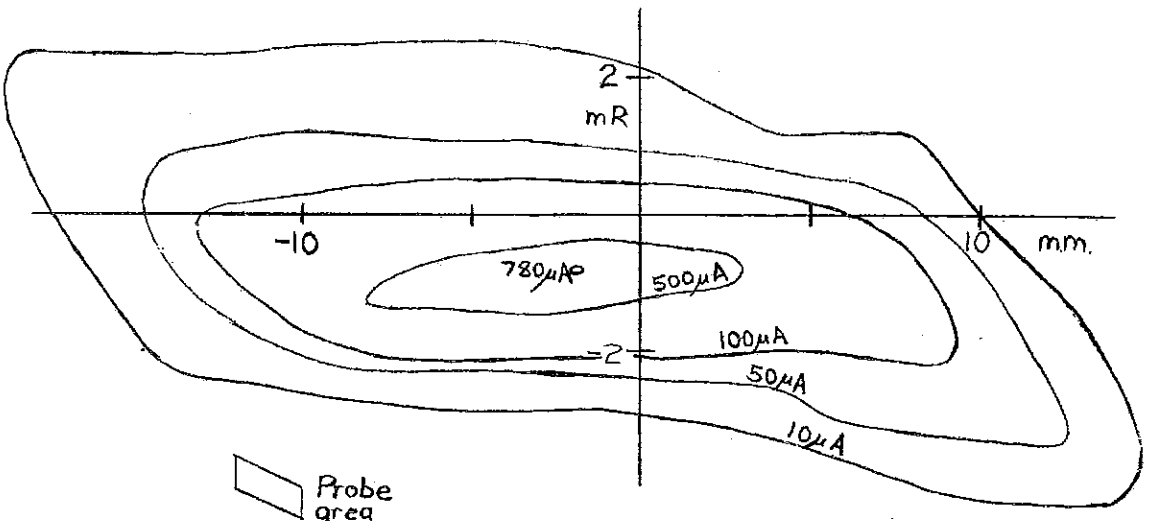

15 MeV – Emittance
18 mA

Fig. 1 Nimrod Injector

fact that the linac will still multipactor if the quadrupoles are switched off.

Similar multipactor trouble has been experienced with the buncher and debuncher cavities. It may be significant that the copper used in their construction was not oxygen free. Both of these single gap cavities were designed to allow a whole cavity end wall to be biased by a dc voltage of up to about 6 kV, but in neither case did the bias prevent multipactoring.

With the buncher cavity, a carbon black coating on the whole of each drift tube and end wall was found to be effective for a time, but eventually multipactoring occurred between the drift-tube faces. A gap splitter, capable of being biased, was then fitted. This consisted of a thin plate suspended at the center of the gap, parallel to the end walls, and of diameter equal to that of the drift tubes. For good measure, the gap splitter, as well as the other cavity surfaces, was carbon blacked. The cavity now operates without multipactoring even with no bias applied to the gap splitter.

In the case of the debuncher, carbon blacking the drift tubes and end walls failed to prevent multipactoring to the end walls. A gap splitter was then fitted, of diameter nearly equal to that of the cavity, and biasing it appeared to eliminate the multipactoring. Subsequently, it was discovered that the cavity was in fact operating at a high multipactor level and eventually operation became unstable. Inspection of the cavity showed that the multipactoring had occurred between the cavity end wall and the cylindrical wall, very close in the corner of the cavity, where there are low fields even at high gap voltages. Finally, all surfaces of the cavity were carbon blacked, including the cylindrical wall and the gap splitter, and since then multipactor-free operation has been possible.

The carbon black used is dispersed in alcohol and painted on the surfaces by brush. The presence of large carbon blacked surfaces does not appear to have any significant effect on the cavity Q factor or on the vacuum pressure.

BLEWETT: I have the greatest difficulty in understanding these remarkable experiences with multipactoring.

WHEELER: Some years ago at Yale, we built a single cavity proton linac operating at 50 Mc/sec. The resonator was a quarter wavelength coaxial

cavity, shorted at one end and capacitatively loaded at the other end where the acceleration took place. Therefore this resonator had radial electric fields except in the accelerating gap. The post loaded TM_{010} resonator that Wroe has mentioned also must have radial electric fields near the end walls. Now, in this coaxial resonator, the electric field between the post and the outer wall varies continuously from zero to the maximum gap field so that there will always be some point at which the voltage is correct for multipactoring. We tried every known scheme to suppress the multipactoring except carbon black. The method which finally worked was a high rate rise of the rf drive, which was accomplished by an oversized rf system.

BLEWETT: The only difference between this and other machines seems to be in the frequency. I can't believe that the 50 Mc drop in frequency could be responsible for all of these extraordinary effects.

DICKSON: On the last slide that you showed, there was scalloping on top of the drive pulse. Have you looked at the frequency of this scalloping in the same way as has been done on other linacs?

WROE: No. You will have to ask Nigil West about that.

WHEELER: That looks a little bit like an oscillation in the drive system.

INFORMAL DISCUSSION OF SPARKING PHENOMENA

SWENSON: We are fortunate to have a representative in this room of practically every proton linear accelerator in the world (Brookhaven, Argonne, CERN, Rutherford, Minnesota, New and Old Bevatron Injector, and the original Alvarez Linac). I have a short list of general questions which I would like to pose to a representative of each of these linacs. These questions were chosen to reveal the type of information which you as a group have and to stimulate a discussion on sparking phenomena. The questions that I have go something like this. Is sparking a problem in your linac? If so, where are the sparks? Why are they there rather than at other places?

HUBBARD: If we start talking about "why", we'll be here for a week.

SWENSON: I would also like to ask you if you have evidence that the sparking is beam dependent, dependent on the vacuum pressure, or dependent on surface contamination. Another question might be for what gradient would you build your next linac? And of course aside from answers to these questions, I would like to have any comments that you feel are pertinent.

Perhaps I should try to define the purpose of this session. The economics of linac design favors pushing the cavity excitation up to some level which is considered safe from the standpoint of sparking. There is very little reliable information on what the safe limit is. And there is no popular description of the nature of the sparking process which is observed in proton linacs. That is, there is no model of the process which explains why the sparks are where they are. Another important point is, how reliable must this linac be? That is, can we stand some sparking and can we allow some time for conditioning after the tank has been opened to air? I know there are some in this room who feel that the future linacs should be very conservative in their electric gradients and if this is the case, perhaps it is not necessary to understand the sparking phenomena.

VAN STEENBERGEN: That last comment I did not get. Why should future linacs be conservative in electric gradients?

HUBBARD: I will write three numbers on the board if you like. In 1948 the Lawrence Radiation Laboratory built a 200 Mc per second linac with a gradient of 0.9 MV/ft. In 1952 we built another with a gradient of 0.6 MV/ft, and in 1961 another linac with a gradient of 0.5 MV/ft.

LAMB: In 19-- something, it will probably be 0.4. It makes a great deal of difference what the application is. For an injector for a machine that costs x times the cost of any linac you are going to put on it, you can certainly afford to run it at half that gradient if you don't get spark one.

FEATHERSTONE: Do you worry about spark one?

LAMB: After it is baked in, you do, I think. You just don't want any sparks.

WHEELER: I think we tend to agree with that.

VAN STEENBERGEN: But isn't that demanding a bit too much. I mean, in all high voltage experiences, one normally expects some conditioning of a particular device under consideration, resulting in usually significant improved performance with regards to maximum electric fields, etc.

LIVDAHL: In January, we were open to air for one week. We did lots of things. Granted, we did not remove drift tubes, but after a week we pumped down late one afternoon. We came in the next morning, and in 30 minutes we had operating gradient. I do not think we had seen more than probably 200 sparks in that time and within an hour we were 10% over gradient, which is where we like to operate.

BLEWETT: Was the tank open to room air, dry nitrogen, or what?

LIVDAHL: It accidently got let up on kleenex and alcohol.

FEATHERSTONE: I think it is fair to say that often when a tank of the Minnesota linac has been down to air and has been pumped overnight, we can establish beam in half a day. It is another story, though, when we have gotten the drift tubes well coated with oil.

VAN STEENBERGEN: From that point of view, I feel again that the gradients could be made higher. It should be a rare occasion that one has to open the tank to air. In that case, conditioning periods of even a day or so would be acceptable.

HUBBARD: But if you are at a point where it requires a lot of conditioning, you are at a point where it will spark occasionally, even after you have done it.

SWENSON: Let me try the first question. Is sparking a problem in your linac?

BLEWETT: (On the BNL linac.) We have some color photographs of the first few drift tubes in our linac. Horrible as the drift tubes look, they still feel smooth to the touch.

VAN STEENBERGEN: Our experience is that in normal operation sparking is not a problem. These photographs look horrible, but we feel that this happens during the first half week after you have had the tank open.

BLEWETT: We feel it is important that the new injector operate at a 30-pulse per second repetition rate to speed up conditioning.

LIVDAHL: Our conditioning is done at 10 pulses per second which is higher than the current possiblities at Brookhaven and at Berkeley.

VAN STEENBERGEN: Let me make it clear that we do not see any deterioration of the sparking situation with time. We have never opened the linac to clean or treat the drift tube surfaces because of sparking.

LIVDAHL: (On the ANL linac.) I do not consider sparking a problem in the Argonne linac. I have seen no spark marks on any drift tube beyond the 20th gap.

BLEWETT: I think we can go even farther and say that we have seen no sparks beyond the 5th gap.

TAYLOR: (On the CERN linac.) I would say that sparking in our linac is a fault condition, that is, we open up the linac and find, for example, a faulty contact between the drift tube stem and the liner. When the linac is working properly, we just do not lose pulses because of sparking. We might have trouble for a day after being up to air for a week or so. The sparking damage that we see is concentrated on the first ten drift tubes.

DICKSON: (On the Harwell linac.) Sparking is not a problem now in the Harwell linac. A couple of years ago it used to be a problem in Tank one. We do not have direct evidence, but we think it was due to water vapor in the tank. I think I told some of you that we found some of the copper in the drift tubes to be porous to water. Since we have cured the porosity problem, we have a very short run-in time at 50 cps, at 1% duty cycle, and the linac seems to operate properly just for years with no problem. We see a few sparks on the first ten drift tubes but they do not bother us.

FEATHERSTONE: (On the Minnesota linac.) Sparking has never really been a problem on the Minnesota linac. The first cavity is a low gradient cavity, like the old Bevatron injector, and it just never sparks. We do

see evidence of sparks on the drift tubes of the second and third tanks. There is no apparent concentration of the sparks in any particular place along the length of the linac. They seem to appear at random.

SWENSON: I might say at this point in regard to the Minnesota linac that I calculated the fields in the vicinity of the drift tubes at three different places, that is, at both ends and at the middle, of their second and third tanks. There are some fairly small radii of curvature on the corners of the drift tubes at the high energy end of Tanks 2 and 3, and I got some electric fields on the metallic surfaces of 28 and 26 MV/m, respectively. I can present a table which compares some actual calculated quantities for the Minnesota linac with similar quantities in some of our latest linac designs.

	Units	Minnesota Linac	MURA Design Run 30547	MURA Design Run 30525
Energy	(MeV)	39	39	195
E_{ave} over cell	(MV/m)	3.0	2.8	2.3
E_{ave} over gap	(MV/m)	12.0	9.8	5.1
E_{max} on axis	(MV/m)	11.7	8.1	6.8
E_{max} on metallic surface	(MV/m)	28.3	15.1	13.4

By all the criteria listed in the left-hand column, the MURA designs are conservative in comparison to the Minnesota linac. However, it might be an error to assume that the critical criteria is listed in the table. Additional information is available on these calculations in a MURA Technical Note TN-467.

FEATHERSTONE: Incidentally, the location of the sparks that we do see does not coincide with the location of the peak fields on the drift tube surface. We tend to get a concentration near the bore radius.

REMARK: That is probably where the field is the highest.

CARNE: May I throw some wood on the fire at this point? It was mentioned in the PLA Progress Report for 1963* that we have done a redesign of our Tank 1, and we were quite concerned about breakdown. We have

*PLA Progress Report 1963, pp. 8-10, NIRL/R/60, January 1964.

done a whole series of electrolytic tank measurements to determine the electric field gradients across the drift tube surface. If you plot the field distribution along the drift tubes surface, you get a peak in the distribution where the outer radius of curvature meets the flat of the drift tube; you get a uniform distribution across the drift tube flat and another peak in the distribution near the radius of curvature of the bore hole. If we now plot surface fields against drift tube number (we have 41 + 2 half drift tubes in our machine) as in the sketch below, we find for the inner radius a surface electric field which goes from about 13 million volts per meter down to about 10. The field for the outer radius is initially less than for the inner radius, crossing over at about 6 or 7 MeV. So for the first 6 MeV it is the field near the inner radius of curvature that is critical. This may throw some light on the fact that the sparking seems to be concentrated in the first few MeV and that the sparks seem to be concentrated on the flat drift tube faces, or near the radius of curvature on the bore.

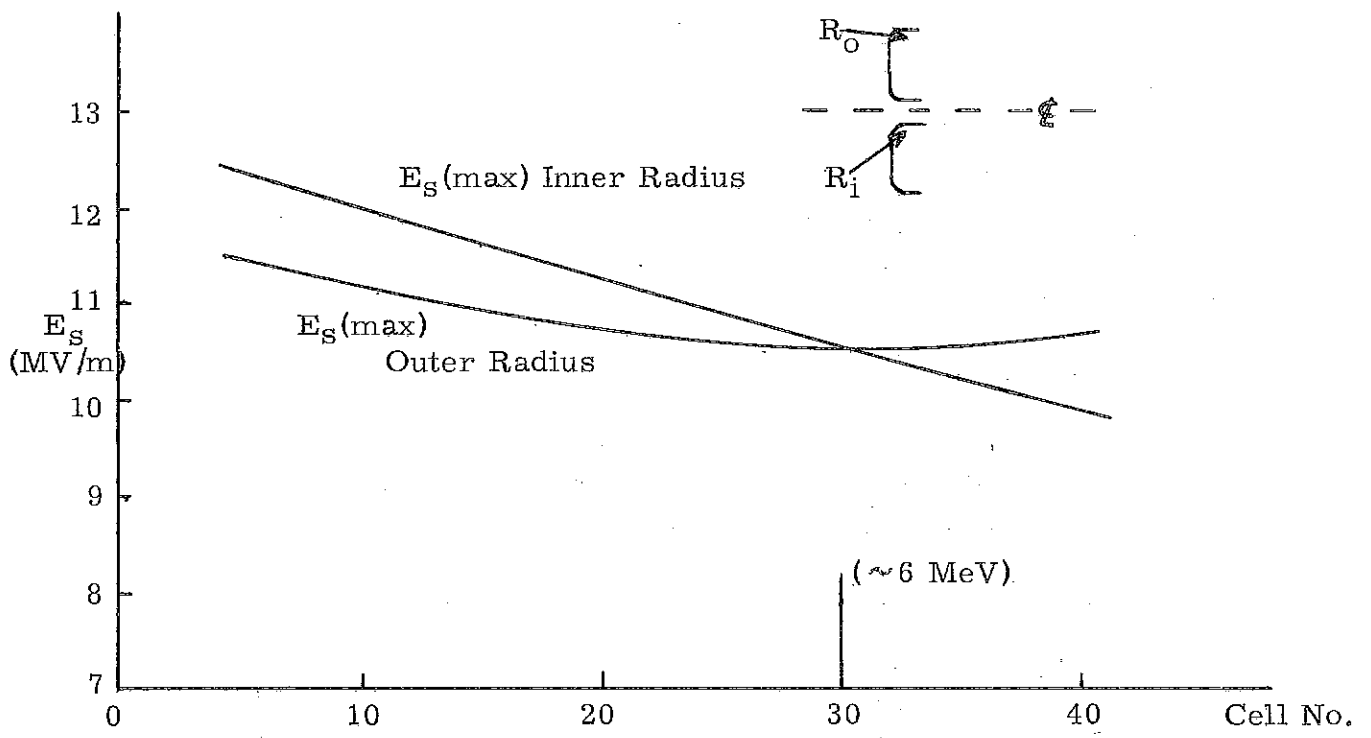

Plot of Maximum Surface E-Field Against Cell Number

HUBBARD: (On the new Bevatron injector.) It's not serious. I do not have any detailed information, but they do not lose any pulses in the machine. They do see evidence of sparks on the first few drift tubes but it does not interfere with the operation. They had trouble on the original Alvarez machine with sparking. Of course, this was with a poorly baffled oil pumping system. With regard to location of sparks, they were worse at the low energy end.

BLEWETT: I think what bothers everybody is that nobody seems to understand the mechanism.

SWENSON: That was my next question. Why are the sparks where they are rather than at some other place?

BLEWETT: Could I make some general comments? First of all, the story you get from the electrolytic tank is not the whole story. The rf magnetic fields are certainly playing a part in determining the electron trajectory. We found that whereas an electron may start off in the direction of the electric field, the magnetic field may very well turn it around. We know that electrons can get all the way across the gap. I want to propose, now that we have all the drift tube fields worked out on computers, that we ought to trace the trajectory of some ions and electrons across the gap and see what final energies and phases they have for a variety of starting phases.

HUBBARD: Are you going to insist that they get there in a half cycle?

BLEWETT: No, I think you should run the calculation for several cycles.

(At this point in the session about two-thirds of the people left to return to the regular afternoon session of the conference.)

CARNE: There is a theorem that says a nonuniform stationary rf field will have a dc force acting on any charge particle, directed toward the minimum in the field. We actually tried to use this force at one time to drive the electrons and ions towards the center of a resonant cavity. We were of course driving the electrons there much more easily and they were in fact sucking the ions in. If you look at the situation that you have across the face of the drift tube, you find, as I said earlier, a nonuniform distribution of field, with a minimum in the region of the face of the drift tube. So there can be this dc force acting on ions which will tend to drive the ions to the region of the flat face of the drift tube. If ions are indeed involved in the sparking process, this could explain the occurrence of sparks on the drift tube faces.

SWENSON: That would enhance the sparking on a flat face, would it not?

CARNE: Yes, certainly. Now the other point to observe is that as you go to higher energy drift tubes, the peak field near the bore radius decreases and the ions either tend to collect on the axis of the linac or tend to slide along the drift tube surface to the stem. If anyone has time to do the details of this calculation on a computer, I will certainly send him the details of the derivation.

PREIST: That is a very reasonable theory.

BLEWETT: It would be very interesting to take two cases, one at high energy and one at low energy and trace trajectories through the cell. The calculation ought to be run for several cycles, including both the electric and magnetic fields in the calculation.

FEATHERSTONE: I would like to point out another aspect of sparking, a question which has not been mentioned but may be significant in some cases. That is, when does sparking tend to clean up, as is usually observed, rather than produce progressive damage, as has been observed in a few notable accelerators? I have calculated that the energy stored in the Brookhaven tank is sufficient to vaporize several milligrams of copper, which is perhaps three orders of magnitude larger than any sparking damage that has been observed. So apparently only part of the energy in the cavity gets into the sparks.

BLEWETT: Yes, if you are watching the probes when the spark occurs, you can see the field drop to zero in the low energy end, and it is still there in the high energy end. With respect to the question made by Featherstone concerning the stored energy, there has been a criterion established by the beam separator people. They believe, if you store more than 50 joules in an electrostatic field, that the sparks will begin to be destructive.

HUBBARD: Yes, that is certainly a rough number, but the 50 joules is somewhere in the region where you might get damage from sparking.

BLEWETT: I think in the case of the Brookhaven linac, where we have about 100 joules, that the sparks detune the cavity and the power is dumped back into the amplifier.

PREIST: Have you come across this report by Little and Whitney at NRL?* People have suspected for years that what caused sparking to

*NRL Report #9544, dated 5/20/63, by R. P. Little and W. T. Whitney, entitled "Studies of the Inhibition of Electrical Breakdown in Vacuum." Astia Document #408298.

start in the dc case (that was all he was talking about) was the phenomenon of whiskers on the metallic surface. And he did a rather elegant experiment in which he saw the whiskers grow and actually measured them, and he computed the increase in the electric gradient that they caused and he found that they had a factor of 100 times the average gradient, and they found that no matter how well you polished the surfaces, that the whiskers were always there.

There is another paper, of which you might be aware, published in the Journal of Applied Physics in June of this year,* on gaps with dc fields in a vacuum. Their approach is to cover the cathode surface with a thin film of dielectric and they had remarkable success in two respects. One is that the ultimate breakdown voltage after conditioning is increased by a factor of two and the other is that (and they consider this most important) the pre-breakdown currents are decreased by three or four orders of magnitude, when you put this stuff on. They used some epoxies and fluorides and TiO_2. They point out you have to have a thin layer, and you have to have some electrical conduction. The whisker-growth idea may explain some of the area effects which were discussed in the main conference room. Of course, the bigger the area the more chance there is for whisker growth.

BLEWETT: This is probably quite true with dc, but I would be quite surprised at whisker growth in an rf field especially since the duty cycle is quite low.

CARNE: How large are the whiskers?

PREIST: I think they are typically a micron in diameter and some hundred microns long.

FEATHERSTONE: Is the presence of electric fields essential for the crystal growth or is it a chemical process?

BLEWETT: It must be an electrical process. I think the primary argument against this as an explanation of sparking in the rf case is that conditioning of the tank tends to get rid of sparking, whereas whisker growth should lend itself to a continuous process.

We have seen another funny effect. It was after a process of cleaning the drift tubes, in which we were using some sort of abrasive. We

---

*"Vacuum Insulation of High Voltages Utilizing Dielectric Coated Electrodes", by L. Jedynak, June 1964, JAP, p. 1727.

must have imbedded some sort of insulating particles in the drift tube walls. These did not result in any sort of disruptive breakdown, but if you peered into the cavity, you could see dozens of little stars on the drift tube faces at the lower energy end on every pulse.

SWENSON: Are there any other models which can help shed light on the sparking phenomena?

CARNE: Well, it seems that probably the rf pulse length is relevant. It would certainly be nice if someone would do some high power model studies (which I know you are going to do at MURA) at the actual pulse lengths for which you intend to run the machine.

HUBBARD: Isn't pulse length important because it affects the duty factor? Our experience suggests that you can convert from one duty factor to another just by taking the sparking rate proportional to the duty factor.

SWENSON: Have you seen anyevidence for beam dependent sparking?

LIVDAHL: We have seen beam dependent sparking at Argonne but only in the case where the operator had steered the injected beam off to one side so that a majority of the beam piles into one drift tube, but in situations where the beam is properly steered into the tank, I can't say that anybody has ever seen it.

BLEWETT: We have not seen beam dependent sparking in our linac.

SWENSON: Lamb reported that he had seen beam dependent sparking, but I guess that was on the MTA.

HUBBARD: Yes, that is true, but they had very high currents, a quarter of an ampere at times.

PREIST: Now, I would like to mention one more thing. Something that has not been important yet on 200 Mc machines, but may become important on the machines you are talking about. The effect I speak of is multipactoring on dielectric surfaces. I hear people talking about a megawatt or so that has to be put through some kind of window. We've found, and we've done a lot of work on this, that we do get a single surface multipactor in a strong enough field, where the E field is parallel to the dielectric surface; you can work out the critical field for this process. You find a minimum field strength at which it can occur, of about 1 V/cm/Mc/sec. The mechanism is that the electron leaves the surface with some initial velocity. It will then be carried parallel to the surface by the electric field, and if there is a restoring force, it

will come back, and if it comes back in the right place and with enough energy, you will find that the process can continue. Well, this has been found to occur at three frequencies: about 600 Mc, about 3000 Mc, and 9000 Mc. It can be eliminated completely by suitable coatings applied to the dielectric surface.

SUMMARY OF INFORMAL SESSION ON MECHANICAL ENGINEERING ASPECTS

John E. O'Meara
Midwestern Universities Research Association

There were a number of topics we did not discuss, such as architectural and engineering problems, water-cooling problems, or other topics specific to any site. Also, we limited our discussion to the Alvarez type of structure rather than the waveguide portion of the linac. The general ground rule that we operated under was that a number of linacs of this type have been built and have performed satisfactorily from a mechanical engineering point of view. Obviously, the same tanks could be built in the future, therefore, any design change should yield some reduction in cost. We prepared a drawing of a different approach to tank construction, shown in Fig. 1. This controversial drawing started our discussion. The Argonne and Brookhaven tanks were constructed with a set of rails to hold the drift tube stems. Figure 1 illustrates a support structure which is independent of the tank, the objective being to eliminate precision machining on the large tank weldment as had been done previously. Figure 1 shows this continuous tank, perhaps as long as 85 feet. This would eliminate the multiplicity of flanges that we see in the present tanks. This, of course, would have to be traded off against additional cost in handling and perhaps more difficult machining because of the larger piece. Conventional ion pumps would be used on this tank and, while a ball tuner is shown, there is a question as to whether or not ball tuners are best. We at MURA object to this drawing in that this additional drift tube support structure adds to material cost, and further, any temperature cycling within this support structure would lead to misalignment of the drift tube inasmuch as they are firmly anchored to it rather than to the tank itself. The discussion led to the conclusion that the tank should be used to provide the drift tube support structure but eliminate the precision machining activity that had previously taken place on the tank itself. This could be done by attaching an adjustable set of rails, for instance.

The problem of holding straightness in a long tank as shown in Fig. 1 was raised. Worstell of LASL pointed out that cylinders of 100-foot lengths have been held to approximately 1/16-inch straightness.

The other topic that we spent a good deal of time discussing was drift tube construction. The MURA computer program results in a cylindrical drift tube. This leads to some economies in fabrication,

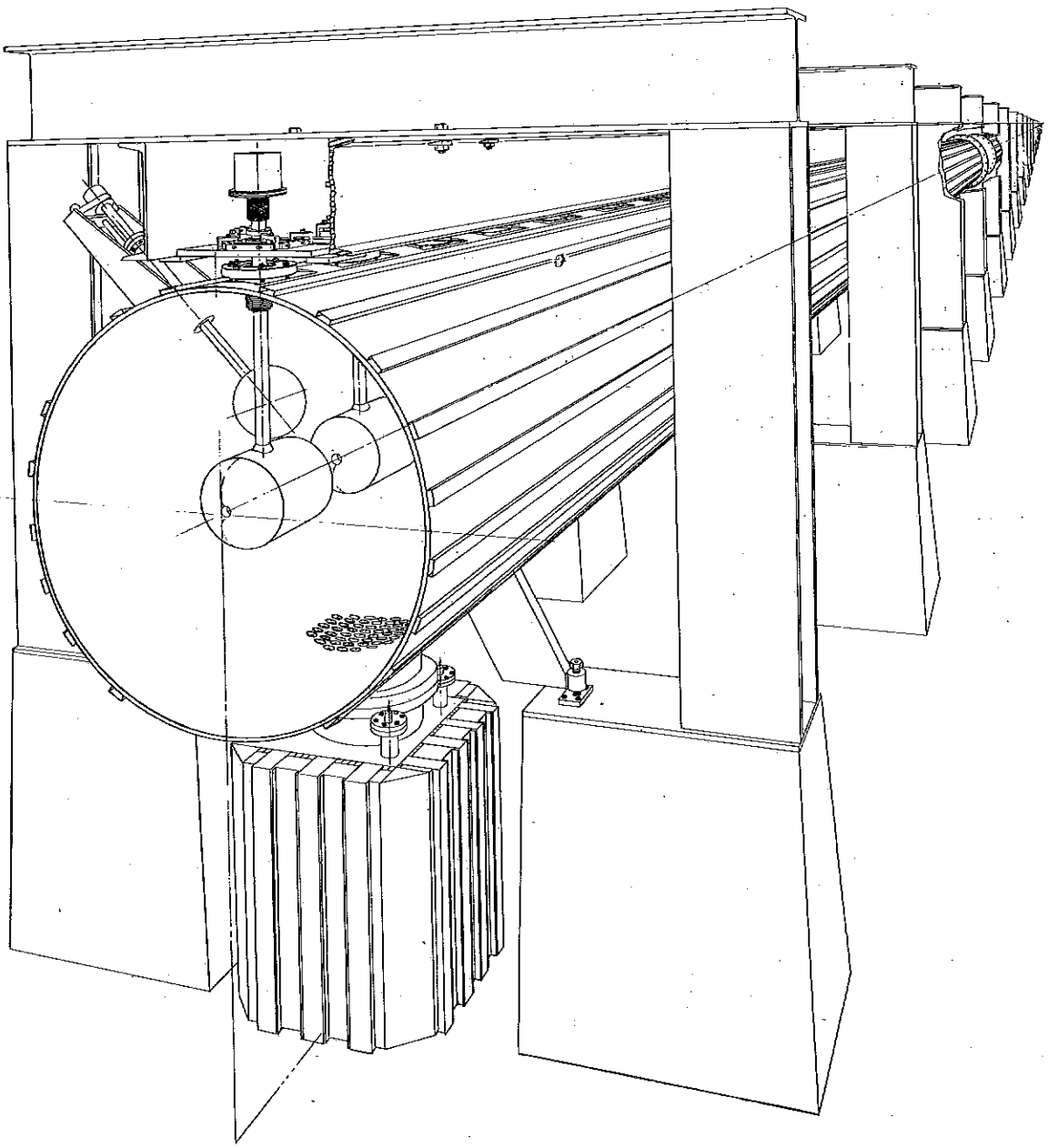

FIG 1 40 FOOT LINAC TANK WITH EXTERNAL DRIFT TUBE SUPPORT

especially when the drift tube diameter remains constant as it does from 50 MeV to the 200 MeV end of the linac. Figure 2 shows a proposed design of one of these drift tubes. Earlier designs required that the entire body be contoured. A cylindrical drift tube, of course, requires only contouring on the end and the center section can be fabricated from tubing. The drift tube in our Mark I tank in the MURA laboratory was fabricated from tubing with pressed end caps. The ends were made from flat sheet stock suggesting some savings over the previous method of construction. The quadrupole shown is constructed with laminations. Each lamination is split so that it may be stacked around a previously formed coil. Since the quadrupole cross section remains constant through a large number of drift tubes, it appears that a laminated magnet should be cheaper than a solid pole-piece magnet.

There was general agreement on tank construction that it should be of one-wall design rather than liner construction. There were some suggestions of alternate means of obtaining a copper surface on the inside. We also had some agreement on the total wall thickness. We feel that the tank could be constructed with a 1/2-inch total wall thickness with 1/8-inch copper. Hortonclad is available in any ratio of copper thickness to steel thickness so that it is possible to obtain this.

I think there is also a general agreement that ion pumps can be used on the tank proper, with some differences on what degree of rough vacuum is necessary and what type of pump should be used for roughing. While isolation valves over each pump may aid in starting, there is a difference of opinion on whether their cost is justified.

McGee of the AEC attended the mechanical engineering sessions and he is quite conscious of costs and the related topic of tolerances. One area of tight tolerances is the concentricity of the axis of the quadrupole magnetic fields with the geometric axis of the drift tube. In the past attempts have been made to hold the concentricity to within 2 mils. This puts rather stringent requirements on the fabrication of the quadrupole assembly plus the concentricity and fit of each piece as we build up the drift tube assembly. Rf resonance considerations require a tight tolerance on the over-all length of the drift tubes. An effort should be made to relax these tolerances or confirm that they are absolutely necessary.

Figure 2 also shows a stem illustrated which does not provide for any direct cooling of the stem proper; we all agreed that cooling must be done unless it can be demonstrated that elongation of the drift tube would not exceed a few tenths of a mil. In general, there are three